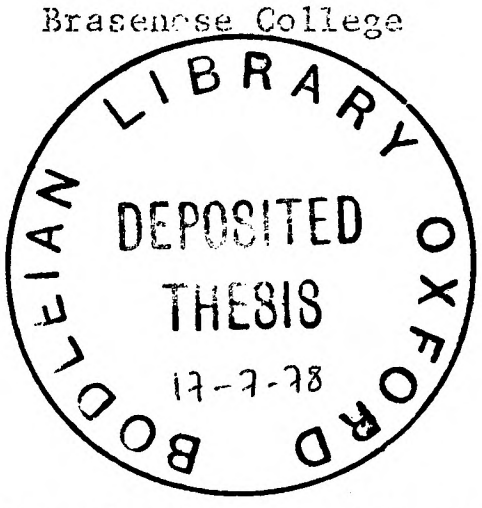
306467335.

The Thermal Accommodation of Helium and Argon on Hot Tungsten

Michael James Watts

Brasenose College



Thesis submitted for the degree of Doctor of Philosophy

University of Oxford

Michaelmas 1977

Dedication

To my father who taught me to disbelieve experimental
results until justified beyond all
reasonable doubt and then to consider
them only with extreme caution.

Abstract

Experiments are described in which the momentum flux of gas atoms, remitted normal to the surface of a hot clean tungsten ribbon immersed in a low pressure of helium or argon, is measured with a torsion balance and the thermal accommodation coefficient deduced. Data are presented in which the tungsten temperature range was 700 to 1900 K for helium and 1100 to 1700 K for argon.

If it is assumed that the normal remitted momentum flux is that expected on assumption of the cosine emission relation, accommodation coefficients much larger (and for argon physically impossible) than those found previously by other workers are implied. A model is proposed which assumes that atoms impinging on and remitted from the hot tungsten ribbon conserve momentum in directions parallel to the surface. This results in a remitted flux, in the direction of the normal, greater than the cosine relation would predict. The resulting accommodation coefficients are then of the same order as those found using the total heat loss method. The method here reported is believed to be novel. Its accuracy increases with the temperature of the hot solid. It permits the measurement of translational thermal accommodation without relying on the temperature coefficient of resistance of the solid and hence is applicable to alloys and to non-metals. For metals, which have a normal temperature coefficient of resistance, the method allows translational accommodation to be measured and internal energy accommodation to be deduced.

Acknowledgements

The author's thanks are due to:

Mr. W.N. Mair who was especially encouraging in those early stages of the work at the R.A.E. Farnborough.

Mr. L.G. Carpenter without whose experimental assistance and valuable discussion in the early hours experimental results could not have been obtained.

Professor F.O. Goodman for especially helpful discussions and assistance in the interpretation of the experimental results.

Professor H.Y. Wachman and Dr. R.G. Lord for valuable discussions.

Mr. D. Clark for X-ray and scanning electron microscope examination of the tungsten surface.

In addition to these acknowledgements in the text, thanks are also due to Mr. R.L. Bickerdike, Mr. B.F. Billing, Mr. A.B. Osborn, Dr. B.W. Viney and Mr. W. Watt of R.A.E. Farnborough who provided valuable advice. The Clarendon Laboratory glass blowers Mr. D.G. Saxton and Mr. S. Giles who were able to provide ingeneous solutions to almost any problem. The heads of the Engineering Department workshops Mr. R.J. Smurthwaite, Mr. J.T. Allen and Mr. G.N. Roger who, with their staff, performed miracles with difficult materials and "impossible" tolerances. Mr. P.H. Flint who did the photographic work, Mr. J. Gardner the most valuable asset to the stores. Mrs. Collins who didn't break anything.

The author's thanks are also due to the Procurement Executive, Ministry of Defence for financial support and the late Professor D.W. Holder for

his interest, support and provision of laboratory facilities.

Rosemary's skill as a typist is clearly evident.

Finally, to Valerie who was always there in those difficult and not so difficult times.

Contents

		page
Chapter 1	Introduction	
1.1	The Experiment Described in This Thesis	1
1.2	Presentation and Aims of This Work	2
Chapter 2	Origin and Development of Interest in Accommodation Coefficients	
2.1	Introduction	5
2.2	The First Experimental and Theoretical Work	6
2.3	Temperature Discontinuity at Gas-Solid Interface	7
2.4	Accommodation Coefficient	8
2.5	Early Microscopic Theory	9
2.6	Early Measurements of Accommodation Coefficient	10
Chapter 3	Essential Theoretical Consideration	
3.1	Definition of Accommodation Coefficient	14
3.2	The Current State of Theoretical Work on He/W and Ar/W	15
Chapter 4	Some Experimental Work on Thermal Accommodation	
4.1	Early Difficulties in Measurement of Accommodation Coefficient	17
4.2	The Importance of Clean Conditions	18
4.3	The Total Heat Loss Method	19
4.4	Values of Accommodation Coefficient for Helium-Tungsten	20
4.5	Values of Accommodation Coefficient for Argon-Tungsten	21
4.6	Investigation of Surfaces Using Molecular Beams	21

		page
Chapter 5	The Present Work	
5.1	Introduction	22
5.2	Requirements	
5.2.1	Development from Previous Apparatus	23
5.2.2	Cleanness	23
5.2.3	Temperature Range of Hot Solid	24
5.3	The Principle of the Experimental Method	
5.3.1	Gas Solid Interaction	24
5.3.2	Torsion Balance and Instrumentation	28
Chapter 6	Experimental Apparatus	
6.1	General Description	30
6.2	Design Philosophy of the Experiment	33
6.3	The Tungsten Solid Surface	
6.3.1	Introduction	34
6.3.2	The Tungsten Used in this Experiment	34
6.3.3	Assessment of Removal of Carbon Impurity	35
6.3.4	Design of Tungsten Ribbon Mount and Sub-Assembly	36
6.3.5	Vacuum Bake	38
6.3.6	Oxygen Treatment	38
6.3.7	Temperature Calibration	38
6.3.8	Surface Cleanness	42
6.3.9	Crystallographic Structure and Surface Topography	43
6.4	The Torsion Balance	
6.4.1	Introduction	47
6.4.2	The Torsion Balance Used in this Experiment	48
6.4.3	Mass Balancing and Pre-Baking the Torsion Balance	51
6.4.4	Calculation of Sensitivity	52
6.4.5	Electrostatic Damping	53

		page
6.5	The Isothermal Chamber and Aperture System	
6.5.1	General Description	53
6.5.2	Construction of the Isothermal Chamber	55
6.5.3	Temperature Control	55
6.5.4	The Aperture System	56
6.6	The Optical Amplifier	
6.6.1	Introduction	57
6.6.2	First Stage of Amplifier	58
6.6.3	Second Stage of Amplifier	63
6.6.4	Calibration of Optical Amplifier	63
6.6.5	Sensitivity of the Experimental Apparatus	66
6.7	The Vacuum Apparatus	
6.7.1	The Ultra High Vacuum Envelope and its Appendices Section A	66
6.7.2	Section B	75
6.7.3	Section C	76
6.7.4	Evacuation of the Vacuum Apparatus	77
Chapter 7	The Experimental Procedure	
7.1	Introduction	78
7.2	Cleaning Procedures	78
7.3	Procedure in the Argon Experiments	79
7.4	Procedure in the Helium Experiments	80
Chapter 8	Experimental Results and Analysis	
8.1	The Selection of Results for Analysis	82
8.2	The Net Force on the Torsion Balance	83
8.3	Analysis of Experimental Data	
8.3.1	Introduction	85
8.3.2	Calculation of Accommodation Coefficients (Cosine Remission)	88
8.3.3	Calculation of Accommodation Coefficients (Tangential Conservation)	90

		page
8.4	Accuracy of Results	93
Chapter 9	Discussion of Results and Development of Apparatus	
9.1	Introduction	94
9.2	Results Obtained Using the First Hypothesis	94
9.3	Results Obtained Using the Second Hypothesis	96
9.4	Dependence of Results on Conditions at Torsion Balance	96
9.5	Development of the Apparatus and Experimental Method	
9.5.1	Investigation of Remission from Hot Solid in Directions Other than Normal	97
9.5.2	Measurement of Remitted Number Flux	98
Chapter 10	Conclusions	99

Appendices

1	Details of Analytical Treatment of Experimental Data	101
2	Relation between F' and F	116
3	Relation between $\overline{C}$, $\overline{C^2}$, $\overline{Ce}$ and $\overline{Ce^2}$	118
4	Speed distribution of gas molecules Maxwell-Boltzmann	119
5	Characteristics of the surface of the copper torsion balance	120
6	Tabulated values of T' for a range of values of α and T_s	123
7	A tensioning spring for high temperature ribbon filaments	124
8	Pressure measurement of Argon and Helium	125
9	Titanium sublimation pump	132
10	Liquid Helium pump	140
11	Osmosis tubes	148
12	Auxilliary Apparatus	152
13	Vacuum Furnace	157
14	Evacuating the Vacuum Apparatus	165
15	Torsion balance measurements of the thermal accommodation of Helium and Argon on hot tungsten	167

Figures

Number		page
1.	Isothermal chamber, scale plan of contents	25
2.	Section A, schematic plan	27
3.	Vacuum apparatus: gauges, pumps and valves, schematic	32
4.	Temperature - current calibration of tungsten ribbon (graph)	40
5.	Tungsten ribbon, location of photographs	45
6.	Electrostatic damping circuit	54
7.	Optical amplifier, schematic plan	59
8.	Photo-voltaic cells, electrical connections	59
9.	Optical amplifier, calibration (graph)	65
10.	Experimental force-tungsten temperature (graph)	84
10a.	Experimental force, variation with time for argon (graph)	86
11.	Photodyne deflection-helium gas pressure (graph)	87
12.	Solution: accommodation coefficient, cosine remission, helium (graph)	105
13.	Solution: accommodation coefficient, cosine remission, argon (graph)	106
14.	Solution: accommodation coefficient, tangential conservation, helium (graph)	111
15.	Solution: accommodation coefficient, tangential conservation, argon (graph)	112
16.	Solution: accommodation coefficient, tangential conservation, helium. Various assumptions at torsion balance (graph)	113
17.	Solution: accommodation coefficient, tangential conservation, argon. Various conditions at torsion balance (graph)	114

Number		page
18.	Molecular remission geometry	116
19.	Circuit and operating voltages of IOG71 vacuum gauge	126
20.	Calibration of IOG71 for helium, $0 \rightarrow 11 \times 10^{-3}$ torr (graph)	128
21.	Calibration of IOG71 for helium, $0 \rightarrow 4 \times 10^{-3}$ torr (graph)	129
22.	Calibration of IOG71 for argon, $0 \rightarrow 15 \times 10^{-3}$ torr (graph)	130
23.	Calibration of IOG71 for argon, $0 \rightarrow 1 \times 10^{-3}$ torr (graph)	131
24.	Titanium sublimation pump, section	135
25.	Liquid helium cold finger pump	142
26.	Liquid helium dewar, section	145
27.	Auxilliary apparatus: gauges, pumps and valves	154
28.	Vacuum furnace, section	162

Tables

Number		page
1.	Accommodation coefficient values from Baule formula	10
2.	Tungsten ribbon impurities, typical analysis	34
3.	Tungsten ribbon, electrical parameters	41
4.	Argon impurities, typical analysis	76
5.	Accommodation coefficient results, helium and argon, cosine remission hypothesis	89
6.	Accommodation coefficient results, helium-tungsten, tangential conservation hypothesis	91
7.	Accommodation coefficient results, argon-tungsten, tangential conservation hypothesis	92
8.	Accommodation coefficient results, helium and argon, cosine remission extreme assumptions at torsion balance	95
9.	Maxwell-Boltzmann distribution	119
10.	Accommodation coefficient results, helium and argon, tangential conservation, various assumptions at torsion balance	122
11.	Values of remission temperature T' for a range of accommodation coefficient α and solid temperature T_s	123
12.	Helium impurities, typical analysis	151

Plates

		Page
1	The hot solid surface. Tungsten ribbon with molybdenum mounts, spring and tantalum frame. Side view.	37
2	The hot solid surface and sub-assembly. Oblique view. Normally mounted in a vertical plane with the end nearest the reader at the top.	37
3	Hot central portion of tungsten ribbon by scanning electron microscope (x 140)	44
4	- ditto - (x 700)	44
5	- ditto - (x 1400)	44
6	Cool end portion of tungsten ribbon by scanning electron microscope (x 700)	46
7	- ditto -	46
8	- ditto -	46
9	Torsion balance mount and component parts. (cm scale) Beam - 0.013 mm thick copper foil. Suspension - 10 mm diameter tungsten wire. Mount - Stainless steel with 0.5 mm diameter tungsten wire cantilever suspension spring.	49
10	Torsion Balance (approximately full size). Beam temporarily clamped. Mounted on stainless steel stand used during pre-baking and mass balancing.	50
11	Components of light source for optical amplifier (x 0.3 approx.).	61
12	Photo-voltaic cell receiver for optical amplifier (x 0.5 approx.).	61
13	Receiver and light source for optical amplifier (x 0.2 approx.).	61
14	Section A of experimental apparatus viewed from South West (x 0.25 approx.). See cover sheet for details. Note woven glass insulation on electrical leads which remain in place during baking.	68

Plates
(continued)

		Page
15	Section A of experimental apparatus viewed from South East (x 0.25 approx.). Note the two thermometers to measure temperature of water to internal isothermal chamber and also winch to lift baking oven.	69
16	Top flange of section A showing manifolds to vacuum pressure gauges and osmosis tubes (x 0.5 approx.). See cover sheet for details. Note foil covered port from which IOG71 has been removed.	72
17	Vacuum furnace component parts (x 0.5) Cylindrical nickel radiation shields. — Muffle with ceramic bead insulated nickel winding. Lower radiation shields in position. Top plate of muffle. — Top nickel radiation shields.	159
18	Vacuum furnace assembled (x 0.5). Fine wires within fused silica tubes are to thermocouples; thicker leads are to heating element.	160

Nomenclature

α Energy accommodation coefficient.

α_W^g Translational energy accommodation coefficient for gas g on tungsten in this experiment.

α_{Cu}^g Translational energy accommodation coefficient for gas g on copper torsion balance in this experiment.

α_W^{He}, α_W^{Ar}, α_{Cu}^{He}, α_{Cu}^{Ar} As above where gas is helium or argon.

$\bar{E}_g$ Mean energy of incident gas molecules.

$\bar{E}'$ Mean energy of remitted gas molecules.

E_s The value of $\bar{E}'$ if remitted gas molecules had come into equilibrium with solid surface temperature T_s.

C_v Specific heat of gas at constant volume.

k Boltzmanns constant.

$\bar{c}$ Mean speed of gas molecules.

$\bar{c}_e$ Mean speed of gas molecules arriving at a plane surface in the gas.

T_g Temperature of gas (helium or argon).

T_s Temperature of solid surface (tungsten).

T' Temperature of gas remitted from solid (assumed Maxwellian and cosine angular remission).

T^* Temperature of gas remitted from copper torsion balance (assumed Maxwellian)

T_n Temperature of gas remitted from tungsten, equivalent to the mean of the normal component of the velocities, $\bar{w}$.

T_t Temperature of gas remitted from the tungsten equivalent to the mean of the tangential component of the velocities $\bar{u}$ and $\bar{v}$.

τ Ratio T_n/T_t .

m_s Mass of atom in solid surface.

m_g Mass of gas molecule.

μ Ratio m_g/m_s .

ρ Ratio of normally remitted momentum flux for tangential conservation to cosine remission hypotheses.

D Potential well depth for gas-solid system.

a Inverse-length parameter.

θ Debye temperature

a Mean radius of apertures.

l Separation of aperture pair along axis.

b Moment arm of experimental force on torsion balance.

P_o Gas pressure

B Experimental force (normalized to 1 torr or 1.336×10^3 dynes cm^{-2}).

G Force from gas molecules remitted by hot tungsten, traversed aperture system, recoilless impingement on torsion balance (normalized).

G' Recoil force on torsion balance of molecules causing C. (normalized)

F Value of G when tungsten is at temperature of gas T_g (normalized)

F' Recoil force analogous to G' (normalized).

Chapter 1

Introduction.

1.1 The experiment described in this thesis

This thesis is, for the greater part, a description of some experimental work carried out to investigate the average energy exchange, or "thermal accommodation", at the interface between room temperature gas at low pressure [1] and a metallic solid at high temperature using a novel experimental method.

The average energy exchange may conveniently be expressed in terms of a dimensionless, abbreviated parameter called the thermal accommodation coefficient [2] or "α". Certain important assumptions and conditions are required and implied by the definition of α and these are considered later in general (see section 3) and for the particular circumstances of this experiment (see section 8).

This experimental data, when analysed in conjunction with one particular theoretical assumption, is shown to lead to values of thermal accommodation coefficient which are numerically of the same order as those obtained by careful experimenters using conventional [3] experimental methods. These results can be considered to increase confidence in the small number of previously obtained values for solids at high temperatures (>700K) and show that this method used is practicable and capable of providing valuable new information within the field of study.

---

(1) i.e. low molecular density. When the mean free path is large compared to the dimensions of the metallic solid. This is the situation hereafter unless specifically stated to the contrary

(2) For definition see section 3

(3) See e.g. total heat loss or low pressure methods by which the majority of measurements have been made. See section 4.

Two gas-solid systems were the subject of this investigation, helium-tungsten and argon-tungsten. In both cases the gas originated from a near isothermal low pressure source at room temperature and was allowed to impinge on the solid surface maintained at high temperature.

It was the particular intention in this work that both the gases and the solid should be of high purity and the solid surface should be free from contamination and well defined. From the care that was taken and the results obtained, which are fully described here, it will be evident that the intention has been achieved with some success.

This novel method, which is simple in essence, has many advantages over conventional methods and is potentially capable of providing a greater wealth of information for a wider variety of gas-solid systems than is currently otherwise possible. The primary detector consists of a sensitive torsion balance. Gas remitted from the hot solid surface impinges on one arm of this balance and the resulting momentum flux gives rise to a force and hence a deflection which is measured optically.

1.2 Presentation and aims of this work

The experimental and novel nature of the work necessitated a very large number and wide variety of experiments to be conducted. Some were preliminaries to the final results, others support or confirm the work or were calibrations. However, there was also the significantly large fraction of work in the invention and development of new techniques and in the design, building trials and calibration of auxil iary apparatus. In order to present the central novel part of the experimental work

concisely in the main text, descriptions of preliminary and auxiliary work are contained in a series of appendices near to the end of the thesis. These include, for example, technqiues, description and use of auxiliary apparatus and also calibration details, useful information and some analytical work not central to the main work. Details of the appendices are contained in the contents and fully cross referenced to and from the main text. The essential parts of this experiment are described in the numbered sections 6 and 7.

1.3 The importance and applications of the field of study

There are currently two journals[1,2] devoted to the study of surfaces and yet a further one[3] in which much work concerned with surfaces has appeared. Regular international conferences concerning the behaviour of gases at low pressure are held and their proceedings[4] contain evidence of a considerable amount of work in the field of gas-solid interaction. Within the last fifteen years there have certainly been published four review papers (Wachman 1962, Thomas 1967, Goodman 1971 and Goodman 1974) bearing directly on the subject of thermal accommodation the latter being an especially comprehensive account of both experimental and theoretical studies. The earliest work appears to be due to Maxwell in 1860.

Thus the general field of study is firmly established in addition to the particular investigations of gas solid systems under the conditions of low gas molecular density. Some indication of the importance of these studies and their applications are given below.

The nature of an interface requires the termination of one medium and the commencement of another. Thus the simplifications of infinite extent,

---

(1) Surface Science. North Holland Publishing Co., Amsterdam
(2) Progress in Surface Science. Pergamon Press, Oxford
(3) Journal of Chemical Physics. American Institute of Physics, New York
(4) Proceedings of Rarefied Gas Dynamics. Academic Press, New York

essential to many simple considerations of the behaviour of materials, are lost. Not only is it to be expected that the medium will exhibit different properties near to its boundary than within its bulk, but that the interactions at the boundary are with a medium different in state and commonly different in type. This latter, results in the necessity to consider, for example, the effects between gas and solid of energy exchange, relative atomic mass, adsorption, range of approach, surface migration and chemical reactivity.

Soddy and Berry (1910) believed that the macroscopic study of gas-solid interactions might be expected to throw some light on the nature of single impacts of gas molecules on a solid surface and thus further establish something of the nature of both the gas and the solid. It does now seem that their belief has been substantiated when the relatively recent publications of the authors Goodman, Logan, Manson and Trilling for example, are considered. The theoretical models and ideas developed by these authors must rest heavily on the results of experimental work in which it has been particularly difficult to ensure reliable knowledge of the interface.

However, the early work originated from essentially practical applications and a large portion of current work is derived from technological considerations. The first relevent work was concerned with viscosity and subsequently thermal conductivity of gases. The experimental work described in this thesis follows preliminary work[1] that coincided with the considerable interest in the problems of re-entry to the Earth's atmosphere of space vehicles and high altitude flight of military and commercial aircraft. The particular problems of concern were those of drag and thermal energy exchange.

---

(1) Carried out at the Royal Aircraft Establishment, Farnborough, England

Many industrial processes involve chemical reactions between gases and solids or heterogeneous catalysis. Here, the efficiency of the reactions is important for the best utilization of the reactants and the cost of the product. Detailed knowledge of the behaviour of gases at solid surfaces leads to the possibility of improvements in the processes. For example, optimizing the rates of reaction and gaseous diffusion or obtaining a variety of products from the same reactants.

Analytical tools for surface analysis are especially useful in for example the study of surface cracking. Whilst current techniques use electron bombardment of the surface this can induce desorption of surface material whcih affects crack propagation. Many authors from Blodgett and Langmuir in 1932 to Yamamoto and Stickney in 1970 have demonstrated the high sensitivity of energy accommodation (at thermal energies) to surface contamination. In addition Knudsen (1911) suggested that surface roughness could be investigated by this method.

Difficulties in instrument calibration are encountered where the details of the gas-surface interaction are not fully known. An example particularly relevent to the work in this thesis[1] is the Pirani Vacuum pressure gauge which relies on the transfer of thermal energy from a hot filament to a room temperature envelope by the gas. The instrument is simple, sensitive, reliable and most suitable to the pressure range 10^{-2} to 10^{-5} torr under normal operating conditions. However, by baking the instrument head, the filament becomes partially clean and its surface state may vary with time. Thus the calibration becomes unreliable and typically less sensitive.

Copious references to particular applications are given in the review papers cited above in section 1.2 and more recently by Bernasek and Samorjai in 1975.

---

(1) See appendix 8

Chapter 2

Origin and Development of Interest in Accommodation Coefficients

2.1 Introduction

The very earliest publications in the field and the origins of the experimental work referred to in this thesis[1] are similar in that both were concerned with the macroscopic interaction of gases and solid surfaces. However, the early experiments were not directed specifically at investigation of the gas-surface interface, but at practical applications involving viscous drag and thermal conductivity. Initially the work was conducted over a wide range of gas molecular densities but subsequently was concentrated on anomalies at low molecular densities. During the last century investigations and conclusions in this low density region involved some assumptions that were not easily justifiable. For example, that the gas remitted from the surface had come into thermal equilibrium with the surface and that within the gas there was a uniform temperature gradient.

Models of a gas and later of a solid were eventually combined in attempts at a theoretical description of their interaction at the interface where neither of these "bulk" models might be expected to be representative. There is the further complication that, except where the system is one of a vapour and its condensed solid, the molecular species of gas and solid are different. The comparison, between experimental results and predictions of potentially acceptable models describing the boundary conditions of various gas-solid systems, surely results inarigorous test of the models.

In an appendix to his paper of 1879 Maxwell, in connection with the gas surface interface said, "for I thought it very unlikely that any equations I could write down would be a satisfactory representation of the actual conditions". There is as yet no unified theory, rather a

(1) See later this section

set of models applicable to various systems and circumstances some of which are in surprising agreement with experiment.

Experimentally, although appreciated by Roberts as early as 1930, common recognition of the fundamental importance of purity and well defined surfaces of the experiment has only been achieved slowly (see e.g. Thomas and Brown 1950 , and also Thomas 1967).

2.2 The first experimental and theoretical work

The origins of the subject are important and interesting in that they show interaction between theory and experiment.

In 1860 a paper by Maxwell was published in which gaseous friction was the subject of consideration. He had deduced from kinetic theory that gaseous friction was independent of pressure, a result which he described as "startling" and the only experiment (1) which he had met did not confirm this. He had assumed that molecules, having impinged on a solid surface were remitted as if they had come into thermal equilibrium with that surface and independent of any possible consideration as to the variation of pressure. Subsequent experimentalists have shown beyond all reasonable doubt that, at least at low pressures, with certain gas-solid systems this assumption is very far from the truth.

The first possible reason for them to doubt Maxwell's assumption may have come from some experiments of Kundt and Warburg (1875). When investigating experimentally the variation of viscosity of gases with pressure they found that, in some experiments below a certain pressure, the

---

(1) Obscure, but possibly some early unpublished work by Kundt and Warburg - see later reference

viscosity decreased with pressure. This led them to propose that, unlike the behaviour at high pressure where there was no relative motion between the solid and the adjacent gas layer, at low pressure the gas somehow "slipped" over the surface.

Maxwell (1879) subsequently offered an explanation to the experimentally observed slip by introducing the concept of a fractional remission of gas molecules in thermal equilibrium with the solid, the remainder being "reflected": the surface being considered analogous to an optical mirror for the latter. Thus Maxwell's explanation, involving a fraction of asymmetric molecular remission, was introduced into his earlier kinetic theory to explain a phenomena concerned primarily with a transfer of momentum and only implied the non-equilibrium of energy of remitted gas molecules with respect to the surface. These details bear only obliquely on incomplete thermal accommodation but they are important in that they did result in Maxwell modifying his assumption and allowing the possibility of non-equilibrium remission to occur in gas-solid interactions.

2.3 Temperature discontinuity at gas-solid interface

Smoluchowski, in 1898, described his experimental investigations into the thermal conduction of gases at "very low" pressures [1] minimum of 1.3×10^{-3} torr) and found the first evidence of a temperature discontinuity between gas and solid under the conditions of thermal energy exchange. However, Kundt and Warburg had previously suspected a temperature analogy of slip and Smoluchowski's results also established some credit for Poisson who had based his heat flow theory on a

---

(1) A reference to Kundt and Warburg by Smoluchowski suggests that they too had, or were, conducting very similar work

special mechanism inferring a temperature discontinuity between two substances of different conductivity. This contrasted with Fourier's contemporary theory on the same subject, in which there was continuity of temperature. Smoluchowski clearly indicates considerable early appreciation of the temperature discontinuity and the gas-solid interaction, to say nothing here of his experimental ability [1]. In a particularly lucid paper he gives a microscopic account for the temperature discontinuity and quotes the magnitude of the difference in the discontinuity for different systems of gas-solid (air-glass and hydrogen-glass). He also makes the perceptive suggestion that the discontinuity depends on the ratio of molecular masses, gas to solid, μ [2]. ($\mu = {}^{m}g/m_s$). Having noticed that the greater value of μ corresponded to the greater temperature discontinuity Smoluchowski suggested further experiments with a wider variety of gas-solid systems - a suggestion echoed by Goodman (1974) almost eighty years later.

2.4 Accommodation coefficient

In 1911 Knudsen, when considering thermal conduction in gases at low pressure, first introduced the term "accommodation" to describe the ability of gas molecules to come into partial equilibrium with a solid surface. He also suggested the idea that gas molecules might be remitted from a solid surface as if they had reached equilibrium with a notional surface and corresponding to an effective temperature T'. The magnitude of T' being in between those of the impinging gas at T_g and the real surface at T_s. "Complete accommodation" would then correspond to the effective temperature T' being identical to that of

---

(1) See section 4
(2) Nomenclature here and elsewhere is consistent within this thesis

the real surface T_s. Knudsen also defined a coefficient of accommodation (α) as the ratio, in the limiting case where $T_g \to T_s$, of temperature difference between impinging and remitted gas to temperature difference between impinging gas and real solid surface [1].

$$\text{Thus} \quad \alpha = \frac{T' - T_g}{T_s - T_g} \qquad (2)$$

whilst the original α is in terms of gas temperatures the modern definition is of an <u>energy</u> accommodation coefficient defined in terms of mean molecular gas energies. In certain circumstances the definitions may be shown to be equivalent see section 3. In real cases where $T_s \approx T_g$, α is termed equilibrium accommodation coefficient [3].

2.5 Early microscopic theory

Baule (1914) was probably the first to produce a microscopic theory leading to an expression for α in terms of the gas-solid molecular mass ratio μ.

$$\alpha = \frac{2\mu}{(1+\mu)^2}$$

commonly known as the Baule formula [4].

The model, necessarily simple to allow analysis, was of a single collision between two isolated hard elastic spheres in which the solid atom was initially stationary, but it did include averaging for all possible angles of collision. Thus, this formula incorporated the Smoluchowski suggestion of mass ratio dependence. Even in this

---

(1) See section 3 later
(2) It cannot be expressed too strongly that great care must be exercised in interpretation of (experimental) data and its application to this apparently simple formula if the resultant values for α are to be meaningful
(3) Compare with non-equilibrium accommodation coefficient, section 4
(4) Compare similarity with Goodman's (1967) classical result, see section 4.

very simplified model the magnitudes obtained for α are close to α values from careful modern experimental workers. For example the Baule formula gives values of α for some gas-solid systems commonly studied experimentally in Table 1.

Gas Solid System	Baule formula prediction for α	Typical Experimental Result (Goodman 1974)
*Helium-Tungsten	0.042	0.017
Neon-Tungsten	0.18	0.04
*Argon-Tungsten	0.29	0.25
Krypton-Tungsten	0.43	0.40
Xenon-Tungsten	0.49	0.65

Table 1 Values for the accommodation coefficient α from the Baule formula (1914) compared with typical modern experimental work for gas and solid temperature of ∿ 300 K. (* Indicates the gas-solid systems of this thesis.)

It is immediately evident that there is reasonable agreement except for the case of Ne-W. It should be noted however that the Baule formula predicts a maximum α of 0.5, corresponding to μ = 1, whereas values of α close to 1 are all too commonly observed [1].

2.6 Early measurements of accommodation coefficient

In a large proportion of experimental accommodation coefficient measurements the solid surface has been of tungsten, indeed, it is so for the

---

(1) See section 4

subject of this thesis. There are important practical as well as theoretical reasons for this which are discussed later. See section 4. Thus Langmuir's work on accommodation coefficient measurements was especially appropriate considering his extensive experimentation with and intimate knowledge of the properties of tungsten. Like previous workers he had made measurements associated with the thermal conductivity of gases (see e.g. Langmuir, 1915) but in 1932 Blodgett and Langmuir published some accommodation coefficient results for the system hydrogen-tungsten. They admit that the interaction was probably not between hydrogen and tungsten believing that they never attained a clean tungsten surface with which to experiment, especially at the lower temperatures. However they do make an important objection to the Knudsen definition of α in terms of temperature which is relevant to this work. If the value of α is to have any meaning the temperatures T_s, T_g and T' must be represented by the corresponding Maxwellian distribution of velocities (1) for the gas molecules concerned. This is particularly relevant to the temperature T' for the gas molecules remitted from the surface.(2)

Soddy and Berry (1910 and 1911) made measurements on a very wide range of gases leading to values for α for the solid surface of platinum. The gases included helium, neon and argon but were otherwise more complex molecules ranging for example from hydrogen to ethane and nitrous oxide. They admitted that their work was not especially precise but some valuable points and experimental techniques are

---

(1) See Appendix 4

(2) See above. There is also the possibility that the spatial distribution of remitted molecules does not correspond to that of an isothermal molecular population. See section 8.

described which have been incorporated in relatively recent work including the subject of this thesis. They also spoke of energy exchange between gas and solid and noted the experimental dependence on molecular species, the "energy exchange" being near perfect for the "more dense" monatomic gases in contrast to that for helium where this was far from the case. Whilst the majority of their work was conducted near to 300K, some experiments were at the temperature of liquid air (about 82K [1]). This enabled Soddy and Berry (1911) to note that α was independent of the gas-solid temperature difference [2], a result largely confirmed by the extensive work of Kouptsidis and Menzel (1970) and at high temperature, by Watt, Moreton and Carpenter (1974). The last and almost certainly most important of the earlier workers was Roberts whose publication in 1930 clearly exhibited the fundamental importance of cleanness of the solid surface. A quote from this paper:- "Any attempt to develop a theory of the interaction between the gas and solid atoms necessarily involves a knowledge of the nature of the atoms which make up the solid surface. This means that the experimental data must be obtained from experiments carried out under such conditions that the surface of the solid is clean and free from films of adsorbed gas. The present experiments with helium and tungsten and nickel wires were carried out with this object in view.". He continues later by saying that a necessary condition for his object is that the gas also should be free from adsorbable gases. Recognition that α measurements were a sensitive function of surface condition was used in some surface adsorption investigations. (Roberts 1935a, 1935b, 1936). The criterion in this case was the value of α for the Ne-W system. Roberts' work profoundly influenced subsequent workers who, by paying

---

(1) For an interesting discussion see Dushman (1949) p. 788

(2) In cases where T_s and T_g are significantly different α is termed the non-equilibrium accommodation coefficient.

scrupulous attention to these matters, obtained values of α significantly lower than Roberts.

Chapter 3

Essential Theoretical Considerations

3.1 Definition of accommodation coefficient

When first used by Knudsen (1911) the terms accommodation and accommodation coefficient referred to ratios of temperatures in the study of gaseous thermal conduction. The present widely accepted definition, of accommodation coefficient (α) for the more general field of gas-solid interactions, is a ratio of energies:-

$$\alpha = \frac{\bar{E}' - \bar{E}_g}{E_s - \bar{E}_g}$$

where $\bar{E}_g$ and $\bar{E}'$ are the average energies of the incident and remitted molecules and E_s is the value of $\bar{E}'$ if the remitted molecules had come into thermal equilibrium with the solid at temperatures T_s before remission. This is the EAC (energy accommodation coefficient) of Goodman but it is referred to in this thesis as the thermal accommodation coefficient for historical reasons and it is useful in that it indicates the energy range concerned.

E_s may be written as:

$$E_s = (C_v + \tfrac{1}{2}k)T_s \quad (1)$$

where C_v is the molecular heat capacity of the gas.

This expression may now be re-written (for a monotomic gas)

$$\alpha = \frac{T' - T_g}{T_s - T_g}$$

---

(1) The additional term $\frac{1}{2}k$ arises from the fact that we are concerned here with the bombardment of molecules on a surface. Allowance must be made for an enhanced proportion of the faster molecules which because of their greater speed arrive at the surface more frequently than do the slower ones.

However this assumes that the mean energy gas molecules may be justifiably described by a temperature and implies a Maxwellian distribution and isothermal conditions.

Strictly

$$\alpha = \underset{T_g \to T_s}{\text{Limit}} \left(\frac{T' - T_g}{T_s - T_g} \right)$$

This is commonly known as the equilibrium accommodation coefficient.

However, experimentally it is quite usual for $T_s > T_g$ and frequently α is found to be almost independent of $T_s - T_g$. This does appear to be the case for both helium and argon on tungsten for ... $T_g \gtrsim 300$ K.

It must be emphasized though that under these non-isothermal conditions there is no justification for assuming that the remitted gas has a Maxwellian speed distribution for its constituent molecules or that it can be represented by a unique single temperature T'.

3.2 The current state of theoretical work on He/W and Ar/W

A complete review of the thermal accommodation coefficient from both a theoretical and an experimental point of view, has been given recently by Goodman (1974). Very briefly, the current status of the theoretical work on He/W and Ar/W is as follows. The work falls naturally into two separate groups (classical-mechanical and quantum-mechanical). Classical calculations exist for both He/W and Ar/W, and the most reliable of these calculations are those from the 'lattice theory' (Goodman 1966, 1969, Goodman and Wachman 1967) and those from the 'soft cubes theory' (Logan 1969). Usually, a Morse gas/surface interaction potential (with the

usual parameters a and D) is assumed, and the dynamics of the solid are treated via a characteristic (Debye) temperature either of bulk vibrations (θ_b in the lattice theory) or of surface vibrations (θ_s in the soft cubes theory). The comparisons made are generally satisfactory to good; and, although the actual values of the theoretical parameters differ from paper to paper, typical (Goodman and Wachman 1967) values are θ_b = 380 K, a = 1.3 A^{-1} for He/W and 1.5 A^{-1} for Ar/W, D = 210 cal $mole^{-1}$ for He/W and 2400 cal $mole^{-1}$ for Ar/W; also a ratio $\theta_b/\theta_s \underline{\sim} 2$ is typical (Logan 1969). Reliable quantum calculations (Goodman 1972b, Manson 1972) exist for He/W. The comparisons made are satisfactory at higher temperatures T, but not at lower T, the reasons for this being under discussion (Goodman 1972b). Typical (Goodman 1972b, Manson 1972) theoretical parameters are θ_b = 325 K, θ_s = 235 K, a = 1.5 A^{-1} and D =0. (The earlier quantum treatments using one-dimensional models, such as the Devonshire (1937) theory, have been rejected (Goodman and Gillerlain 1972), and are not considered here.) Readers are referred to Goodman (1974) for further discussion.

Chapter 4

Some experimental work on Thermal Accommodation

4.1 Early difficulties in Measurement of Accommodation Coefficient

The early experimental work referred to in Section 2 was concerned initially with gaseous friction and subsequently with thermal conduction in gases both of which led to fascinating results in the region of low pressures. Considerable enthusiasm is evident in publications of the experimental work and Maxwell (1860a) described the results as startling. Maxwell (1860b) also noted that
"It would be almost impossible to establish the value of conductivity of a gas by direct measurement, as the heat radiated from the sides of the vessel would be far greater than the heat conducted through the air, even if air currents could be entirely prevented."

It is just this effect which limits the maximum temperature at which accommodation coefficients may be investigated on the surface of a hot solid. He also noted the importance of the value of the mean free path of the gas with respect to the dimensions of the apparatus.

Some of the early workers showed considerable experimental and perceptive ability. Smoluchowski (1898) is outstanding here and gives a beautiful account of the gas surface temperature discontimuity when there is a net transfer of thermal energy.

However, whilst experimental techniques improved and reliable methods were developed for measuring thermal conductivity and later accommodation coefficients (Knudsen 1911), it is not evident that

proper consideration was given to cleanness of either the gas or the surfaces being investigated.

4.2 The importance of Clean Conditions

Roberts (1930) was the first to realise the requirement for a high degree of purity of both gas (helium), which was carefully and continuously processed and the solid surface (nickel and tungsten) which was cleaned by outgassing and desorbing impurities at high temperature ($>2000^{\circ}C$ in the case of tungsten). He noted that the accommodation coefficient increased with time after the surface had been cleaned and attributed this to the build up of adsorbed films of the residual impurities in the gas.

The values of α he obtained for helium-tungsten were between 0.05 and 0.07. The temperature of the gas was about 300K and that of the tungsten about 10 to 30K above this.

Later, Thomas obtained significantly lower values of α and this work is characterised by his paying scrupulous attention to the degree of cleanness of the solid surface.

Most of the studies of accommodation coefficient have been carried out on metals of high melting point (such as tungsten or platinum) so that they could be cleaned of the adsorbable gases (for example oxygen) using high temperature treatments in high vacuum. The gases used have typically been of simple monatomic structure with no internal degree of freedom and low heats of adsorption (ie the noble gases especially helium and argon).

4.3 The Total Heat Loss Method

Most of the experiments which have been done to measure accommodation coefficient have used the total heat loss method. The typical apparatus used consists of a long vertical glass tube held at a uniform constant temperature. A small diameter pure metal filament is mounted along its axis and the filament is ohmically heated. The temperature of the central section of the filament, defined by a pair of electrical potential leads, is deduced from its electrical resistance. Usually the filament forms one arm of a Wheatstone bridge circuit. The difference in electrical power required by the filament to maintain a given temperature with and without gas in the tube allows the accommodation coefficient to be calculated if the specific heat of the gas and the geometry of the apparatus is known. A major difficulty with this method is that at high temperatures (> 1000 K) the thermal radiation loss is large compared to that loss caused by conduction in the gas. Also temperature measurement relies on the temperature coefficient of resistance which has usefully large values only for the pure metals.

Usually the mean free path of the gas is large compared to the dimensions of the apparatus (the low pressure method) but some work has been done where this condition does not apply (temperature jump method) and the pressure is considerably greater. This method has been criticised for the assumptions which need to be made although it gives values of accommodation coefficients comparable with the low pressure method. An improved analysis for these "high pressure" conditions is now available, (Wachman 1965).

There is an excellent review by Wachman (1962) of the earlier work and more recently a most comprehensive review of the whole subject of thermal

accommodation by Goodman (1974)

4.4 Values of accommodation coefficient for helium-tungsten (1)

The only high temperature data published for the accommodation coefficient of the tungsten-helium system are those of Carpenter, Humphries and Mair (1963a) and Watt, Moreton and Carpenter (1974). The Carpenter et al work was a preliminary trial of the torsion balance method. The results are reported for T_s = 2800 K at which temperature the tungsten surface was likely to be clean. The values for accommodation coefficient were given as 0.07 to 0.12 depending on the assumption made about accommodation on the torsion balance. As it was assumed that the normal (to the surface) remission for the hot tungsten was cosine-wise, while it is now believed to be greater than cosine-wise in the normal direction, the quoted results are likely to be too high.

Watt et al (1974) report a constant value of 0.018 for the temperature range 1073 to 1785 K. In the lower temperature range there is the work of Kouptsidis and Menzel (1970) working with $T_s - T_g \nmid 100$ and $T_s \nmid 400$ K. They took great care to obtain clean surfaces and report values of order 10^{-2} increasing with temperature.

Wachman (1966) measured accommodation coefficients between 324 and 473 K and obtained values ranging from 0.0192 to 0.0228.

---

(1) These values may be compared to the values resulting from this work which are within the range 0.023 to 0.028 for the temperature range of 700 to 1900 K

4.5 Values of accommodation coefficient for argon tungsten (1)

For argon, Carpenter et al (1963a) report values of accommodation coefficient at 2800 K ranging from 0.23 to 0.50 depending on what assumption was made about accommodation on the torsion balance. Again these values, like the helium ones, are probably too high because of the adopted hypothesis of cosine remission from the hot tungsten. For argon Watt et al (1974) report values for accommodation coefficient of 0.25 to 0.23 over the range 1073 K to 1785 K while the values of Kouptsidis and Menzel (1970) decrease with increase of T_s and appear to asymptote to about 0.26 at 400 K.

4.6 Investigation of surfaces using molecular beams

More recent investigations of the interaction of helium and argon with tungsten have tended towards examination of remission phenomena, as a function of angles of incidence and remission, of beams of gas molecules. Typical recent studies are those of Moran, Wachman and Trilling (1969) Yamamoto and Stickney (1970) and West, Kozak and Somorjai (1971). However there has been a recent review of the past ten years work on molecular beam scattering by Bernasek and Somorjai (1975). To the author's knowledge sufficiently detailed and calibrated data is not available from "beam" work to deduce values of accommodation coefficient, though it does clearly indicate cleanness of surfaces (Yamamoto and Stickney 1970).

---

(1) These values may be compared to the values resulting from this work which are within the range 0.17 to 0.10 for the temperature 1100 to 1700 K.

Chapter 5

The Present Work

5.1 Introduction

The experimental method described here was originally devised by Carpenter, Humphries and Mair (1963a) and full details of the first experiments have been published by the same authors (1963b).

The disadvantages of other methods of measuring accommodation coefficients have already been discussed in the previous section 4. The advantages of this method are that

(a) The momentum flux of gas molecules remitted from the solid surface (within a small solid angle) in a particular direction is measured directly by the deflection of a torsion balance.

(b) The sensitivity of this method increases with the temperature of solid surface in contrast to total heat loss methods whose sensitivity decreases with temperature.

(c) This method is applicable to insulators and metal alloys. The total heat loss methods rely on the temperature coefficients of resistance of pure metal solids to measure the change in the solid temperature caused by the additional loss of energy due to the introduction of the sample gas.

Further more detailed advantages that would result from modification to the existing apparatus are described in section 9.

5.2 Requirements

5.2.1 Development from previous apparatus

This apparatus is essentially the same as that described by Carpenter et al (1963a) in that it uses a torsion balance as a detector to measure the momentum flux of gas molecules remitted from the hot solid surface but the geometrical arrangementsare more simple. This reduces the necessary assumptions required to interpret the results and simplifies the calculation of the momentum flux within the solid angle around the remitted direction investigated. The torsion balance is now arranged symmetrically about two similar but independent solid surfaces to provide increased reliability and the possibility of confirming reproducibility of the results.

5.2.2 Cleanness

The present apparatus was especially designed with intention that both the gases and the solid should be of high purity, the solid surface should be free from contamination and well defined and that these stringent conditions would be maintained throughout the duration of the experiment. It was fully appreciated that without strict adherence to this essential requirement of cleanness this work, like so much previous work that has been criticised, would be of little value as additional evidence to further the investigation of gas-solid interactions.

Thus the apparatus was designed and built to those standards normally accepted for ultra high vacuum and each component part subject to scrupulous attention in maintaining the required standard. These details are given in sections 6, 7 and the appendices.

Cleanness is thus the crucial part of this work in order that this novel method might be evaluated and the results compared with those of other methods where similar conditions were maintained. This, together with previously discussed reasons (1), was important in the decision to investigate the gas-solid systems helium-tungsten and argon tungsten.

5.2.3 Temperature range of hot solid

The temperature range of this investigation was approximately 700 - 1900K for He - W and 1100 - 1700K for Ar - W.

There is, to the author's knowledge, only one other set of measurements of accommodation coefficient over a similar temperature range to this work using other methods but with the same gas-solid systems and that is the work of Watt and Moreton (1964) subsequently published by Watt, Moreton and Carpenter in 1974.

5.3 The Principle of the Experimental Method

5.3.1 Gas-Solid interaction

Gas (2) molecules originating from a near isothermal chamber at room temperature are allowed to impinge on a small solid (2) surface maintained at known high temperature within that chamber. A simple aperture system allows only those gas molecules which have been remitted from the solid in a particular direction (3) to impinge on one arm of a

---

(1) see sections 3 and 4
(2) Gas and solid here refer to those substances of the gas-solid system that is the subject of investigation
(3) In this experiment the direction investigated was that normal to the hot solid, see also section 9 where the feasibility of other directions is discussed

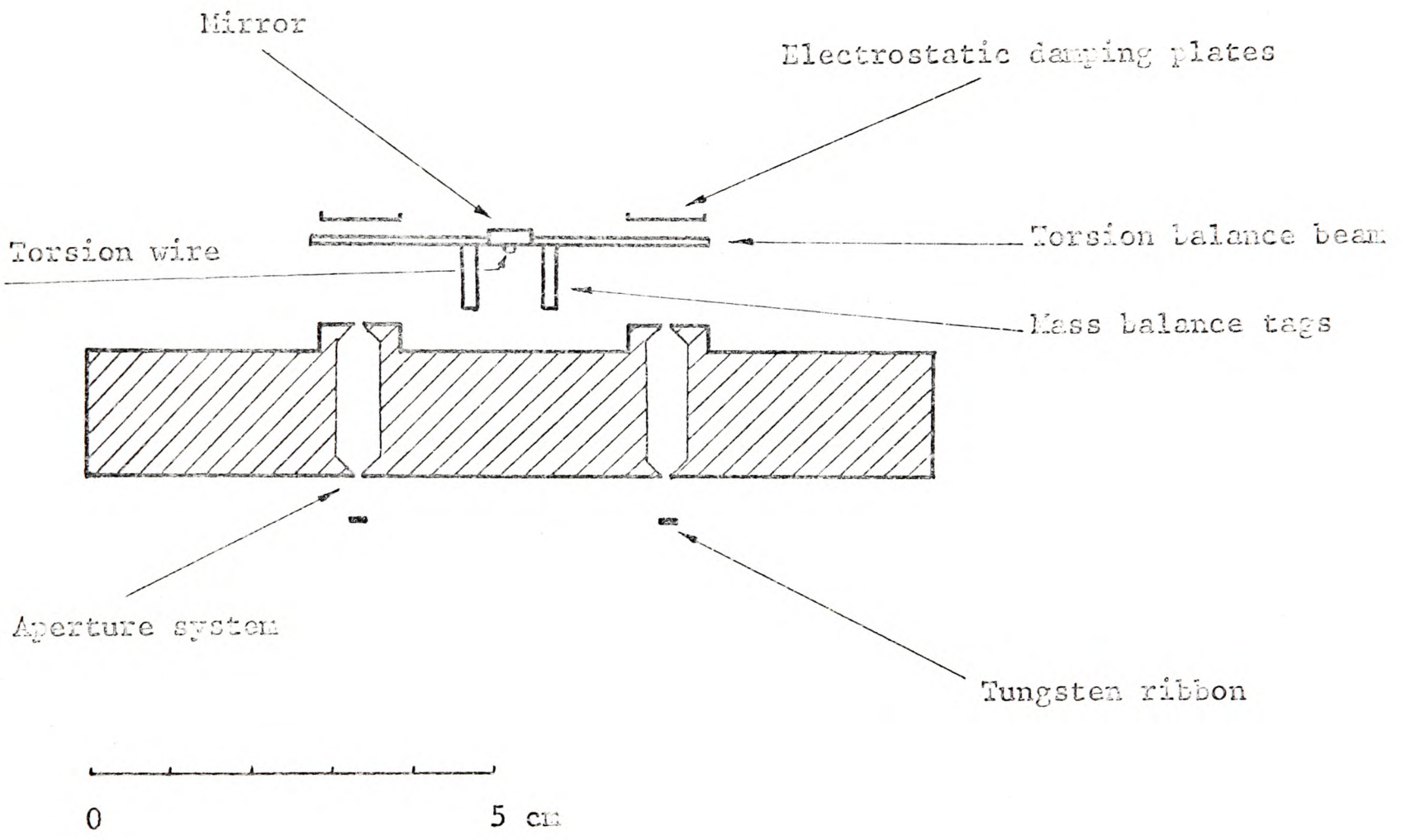


Figure 1 Plan of contents of isothermal chamber

Key to Figure 2.

Schematic plan view of section A.

1. Stainless steel vacuum envelope
2. Copper isothermal shield and septum
3. Apertures
4. Tungsten ribbon
5. Torsion balance beam
6. Sputter ion pump
7. Titanium sublimation pump
8. Liquid helium cold finger
9. Metal valve
10. Metal valve, section A → B
11. Torsion balance mirror
12. Electrostatic damping plates
13. Window
14. Bayard-Alpert ion gauge
15. IOG 71 ion gauge
16. Pirani gauge
17. Silver osmosis tube
18. Fused silica osmosis tube
19. Extent of bake out oven
20. Tungsten suspension
21. Copper septum

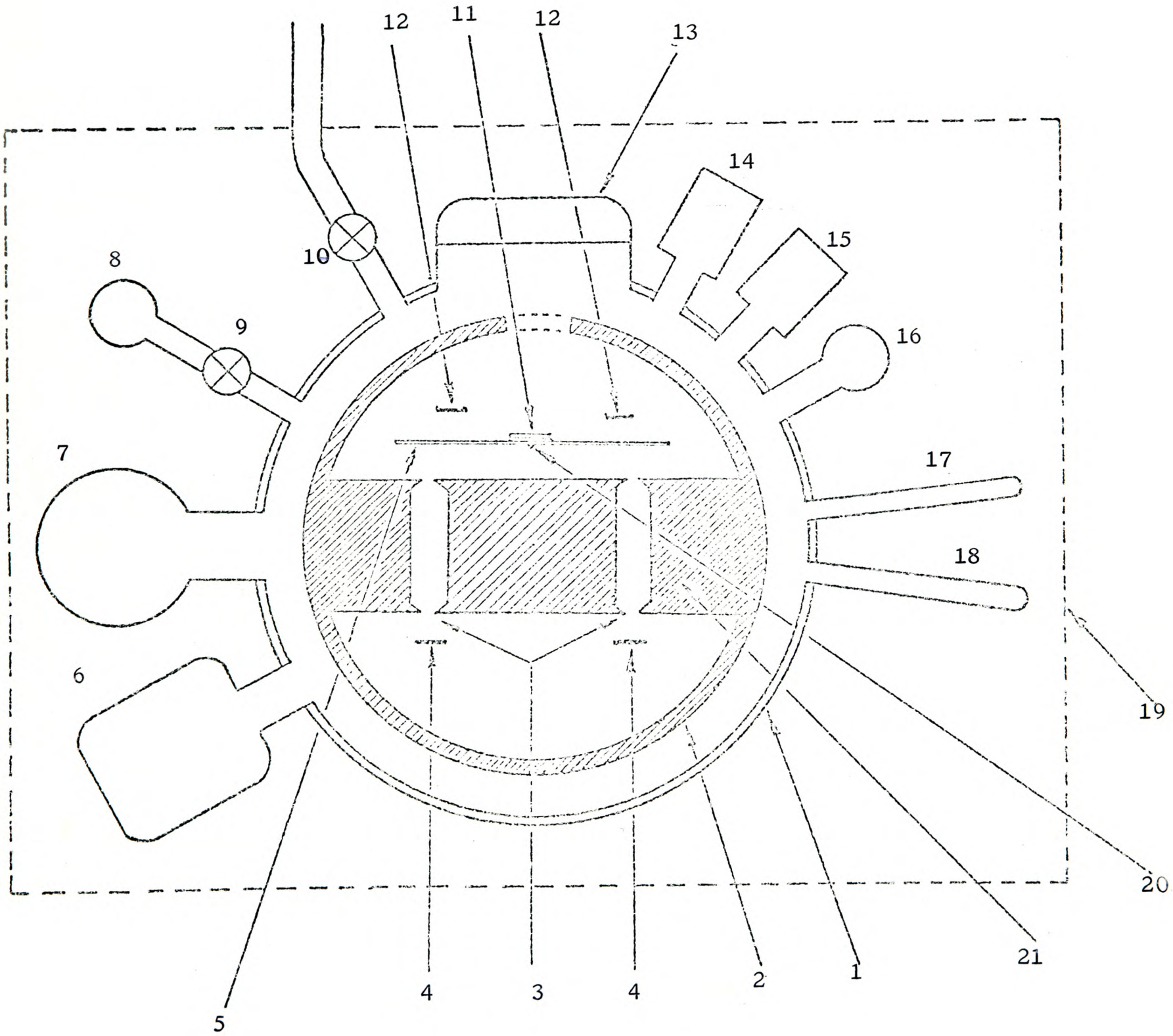


Figure 2 Schematic plan view of Section A (see key on previous page)

torsion balance also within the chamber.

The gas is at a sufficiently low pressure so that its mean free path is large when compared to the distance traversed between the hot solid via the aperture to the torsion balance.

The resulting momentum flux of the "hot" gas molecules remitted from the solid onto the torsion balance gives rise to a force and hence a deflection which is measured optically .

A scale plan of the septum, apertures, hot solid and torsion balance (vertical axis) is shown in fig. 1 and a more general schematic plan is shown in fig. 2 . The hot solid and aperture is duplicated as mentioned above. The isothermal chamber is divided into two parts by a septum, penetrated only by the aperture system, separating the hot solid from the torsion balance. The chamber is within a vacuum envelope which contains the sample of gas at low pressure. The gas may communicate easily but only indirectly between the envelope and each part of the chamber via the top and bottom of that chamber

5.3.2 The torsion balance and instrumentation

From the experiment a value for the deflection of the torsion balance is related to the average translational energy of the gas molecules and hence to a value of translational thermal accommodation coefficient. This was one of the reasons for choosing the inert gases helium and argon with their relatively simple molecular structure of single atoms.

Certain assumptions must be made about the interaction of the gas molecules

at the torsion balance arm, see section 8. However, it has already been shown feasible to modify the torsion balance so as to reduce the ambiguity of the interaction. This modification would also render possible the distinction between and measurement of total and partial accommodation coefficients of the more complex gas molecules, see section 9.

The deflection of the torsion balance was observed by means of an attached mirror and reflected light beam via a window in the vacuum envelope and hole in the isothermal chamber. The displacement of the reflected beam was monitored by a photoelectric amplifier and recorder.

Chapter 6

Experimental Apparatus

6.1 General Description

A suitable environment in which to conduct the experiments was provided by a system, part of which was capable of being evacuated to ultra high vacuum conditions. It is conveniently considered as three sections, A, B and C, shown schematically in figure 3 .

Section A is the ultra high vacuum envelope constructed of stainless steel and also shown in figure 2 . This contains the isothermal chamber, gas-solid system under investigation and the torsion balance detector.

Section B is connected via a metal isolating valve to section A and constructed mainly of Pyrex and used for preliminary evacuation of section A and also for the introduction of the gas argon into section A. Helium gas was introduced directly into section A via a silica osmosis tube.

A third section, C, is connected to B via a metal isolating valve and is interposed between section B and the atmosphere. It was the rough pump for A and B and acted as a guerd vacuum for B.

Section A was baked by an oven and section B by heater tapes. All three sections were provided with vacuum pressure gauges to monitor the pump-down and integrity of the system.

CF_1 CF_2	Liquid Helium cold finger pumps
CF_3	Liquid Nitrogen cold finger
IP_1 IP_2	Sputter ion pumps
S_1 S_2	Sorption pumps
S	Titanium sublimation pump
W	Water jet pump
D	Mechanical dial gauge
I_a I_b	Bayard-Alpert ionization vacuum gauges
P_a P_b	Pirani Vacuum gauges
P_c	
VT_1 VT_2	Liquid nitrogen cooled vapour traps

Figure 3 Key for Vacuum apparatus. Gauges, pumps and valves.

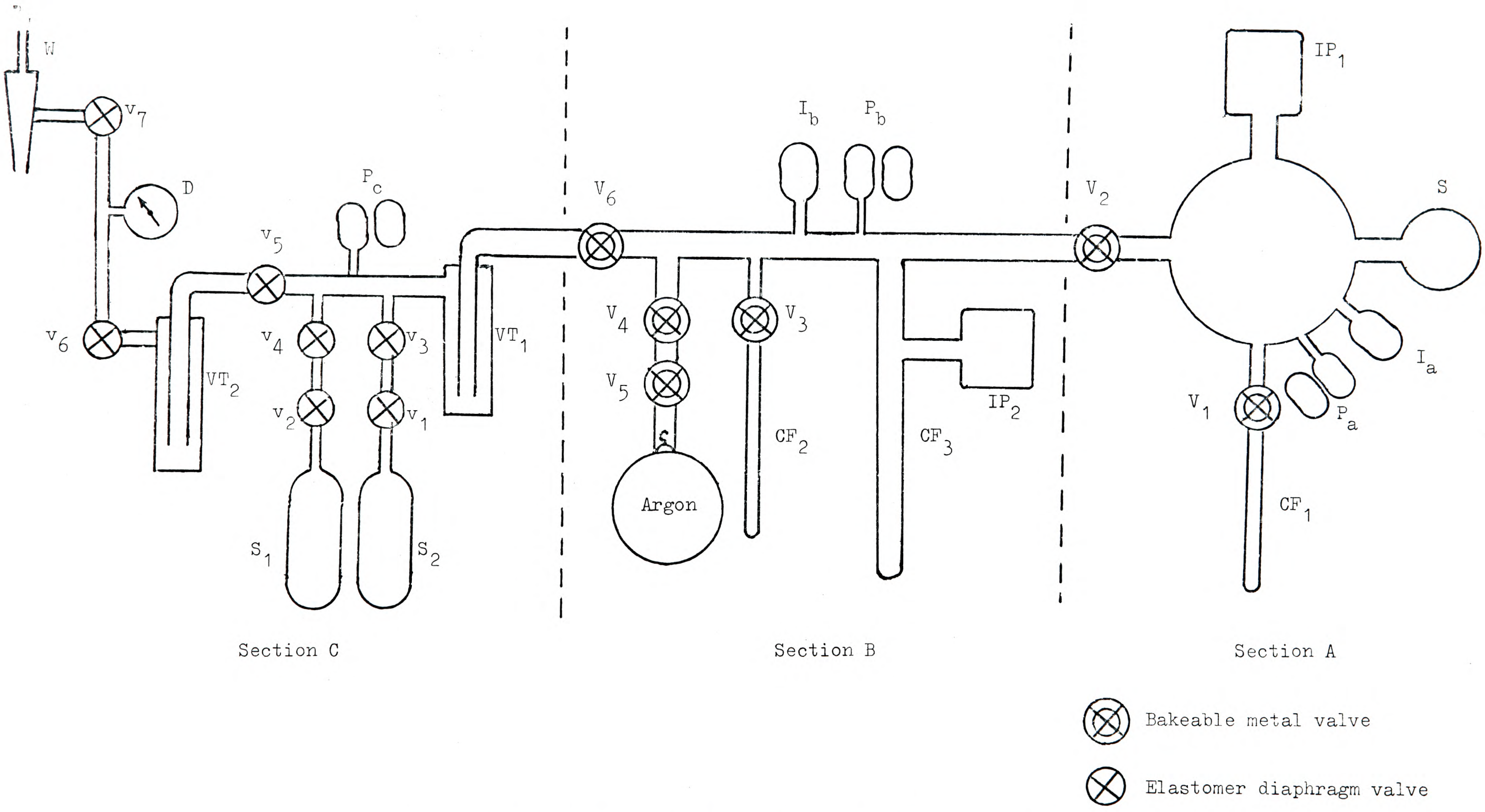


Figure 3 Vacuum apparatus showing gauges, pumps and valves (schematic)

6.2 Design philsophy of the experiment

The general philosophy by which preparations were planned and the experiments conducted was as follows:-

(a) Carefully prepare every item that is to be within or form part of section A and do not use any organic material in sections A or B.

(b) Use the purest available tungsten ribbon for the hot solid surface and purify it further by high temperature treatments in vacuo and in a low pressure of oxygen before and after installation in section A.

(c) Ensure that the only effect on the torsion balance of the hot solid tungsten surface was due to remission from it of hot gas molecules via the well defined aperture system.

(d) Reduce the pressure in section A to order 10^{-10} torr (1) before introducing pure helium or argon and thereafter maintain the low background pressure and purity of the gas by selective gettering and cryopumping of all other gases.

(e) Examine the solid tungsten surface at the conclusion of the experiments by X-ray diffraction , scanning electron microscopy and Auger surface analysis.

---

(1) All pressures quoted are "nitrogen equivalent" unless specifically stated otherwise

6.3 The tungsten solid surface

6.3.1 Introduction

The solid surface consisted of a ribbon of tungsten heated electrically[2] by passing a direct current along its length. Temperature calibration and the major part of the pre-treatment was conducted in the bell jar of the auxilliary apparatus (see appendix 12). Two tungsten ribbons were prepared in the same way and installed in the apparatus as shown in figure 1.

6.3.2 The tungsten used in this experiment

The tungsten was the purest [1] available and a typical analysis from the suppliers (Messrs. Metallwork Planse) is given below in table 2.

Impurity	by weight %
Oxygen	0.005
Hydrogen	0.001
Nitrogen	0.005
Carbon	0.008
Iron	0.005

Table 2. Typical Analysis of the major impurities (by weight per cent) of the tungsten ribbon used for the hot solid surface.

---

(1) The tungsten commonly available frequently has two major impurities, thoria (approximately 0.7%) which is added to inhibit crystal growth at high temperatures and carbon which originates from the dies and rollers used in fabrication

(2) Direct current was used. Alternating current may have induced vibration by interaction with nearby sputter ion pump magnets

However, the average amount of carbon in the batch of strip from which these particular ribbons were cut was given as 0.002 to 0.003 by weight per cent.

Carbon is an especially difficult impurity to remove but it was essential that it should not exist on the tungsten surface since with its low atomic mass, compared to that of tungsten, the effect on accommodation coefficient measurement would be considerable. The above carbon concentration was estimated to be equivalent to 30 to 40 monolayers of carbon on the surface of the tungsten ribbon used.

6.3.3 Assessment of removal of carbon impurity

In a preliminary experiment 120 mm of the same batch of tungsten ribbon was subject to a treatment routine suggested by Becker, Becker and Brandes (1961) for removal of carbon, hereafter referred to as the oxygen treatment. This consisted of maintaining the tungsten at a temperature of 2240K in a vacuum with a background oxygen pressure [1] of 1×10^{-6} torr. This treatment was continued for a total of 12 hours.

The oxygen treated sample was then chemically analysed [2] and compared with a similar but untreated sample of the same batch of tungsten ribbon. The results of the analysis showed that the carbon content had been reduced by a factor between 2 and 10, the accuracy of the analysis being limited by the small size of the available samples.

---

(1) The oxygen was admitted to the bell jar of the auxilliary apparatus by means of a silver osmosis tube, whilst the vacuum pump was in action. See appendices 11 and 12

(2) The author is grateful to Mr. F.W. Dodgson of Murex Ltd.

6.3.4 Design of tungsten ribbon mount and sub-assembly

The ribbons used were from the batch of tungsten strip 2 mm wide and 0.03 mm thick each cut to a length of 20 mm, but the actual free length when mounted was approximately 16 mm.

The ribbons were attached at each end to 0.26 mm thick molybdenum (1) mounts. The joint was made by electrical spot welding without any intermediary metal or chemicals. Thermal expansion of the tungsten ribbon was taken up by means of a cylindrical molybdenum (1) spring (2) especially designed (see Watts 1972 or Appendix 7). The spring and ribbon with its end mounts was held by stainless steel bolts to a frame fabricated from 0.26 mm thick tantalum (1). The whole sub-assembly shown in plates 1 and 2.

Electrical potential leads were attached to each end of the ribbon. Necessary electrical insulation of the main current and potential leads was provided by ceramic washers and fused silica tubes.

A small silver foil radiation screen was secured with tantalum clips in between the tungsten ribbon and the tantalum frame to reduce the radiant energy absorbed by the frame from the hot tungsten ribbon.

In an earlier design of this sub-assembly the tungsten ribbon was welded to nickel mounts and no provision was made for thermal expansion. Following considerable thermal cycling the ribbon failed near to one end. It was subsequently discovered (Bickerdike 1969) that when nickel

---

(1) The molybdenum and tantalum used was of high quality and 99.99% pure
(2) It is interesting to note that Roberts used a molybdenum spring in his experiments with a tungsten surface in 1930

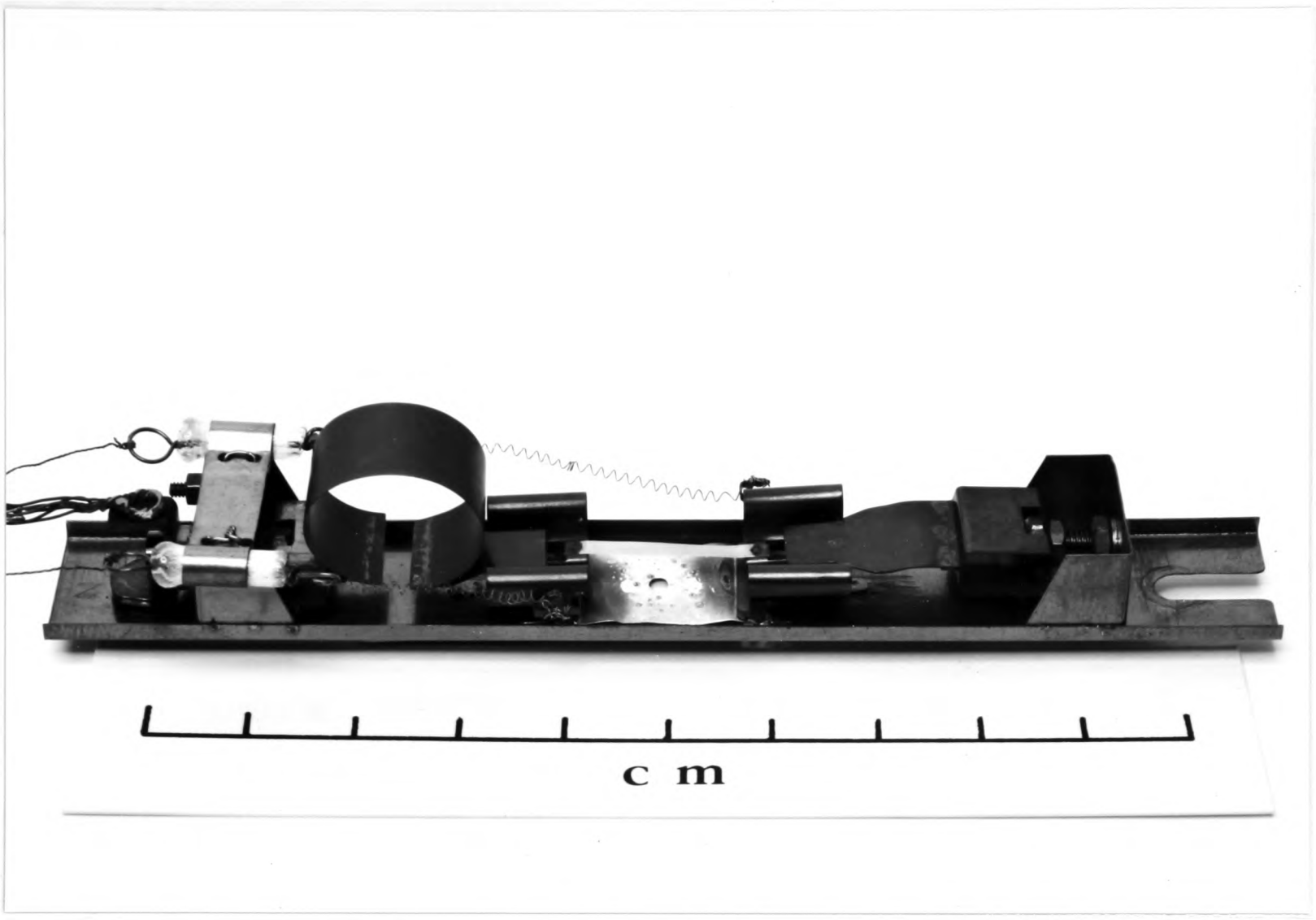


Plate 1. The hot solid surface. Tungsten ribbon with molybdenum mounts, spring and tantalum frame. Side view.

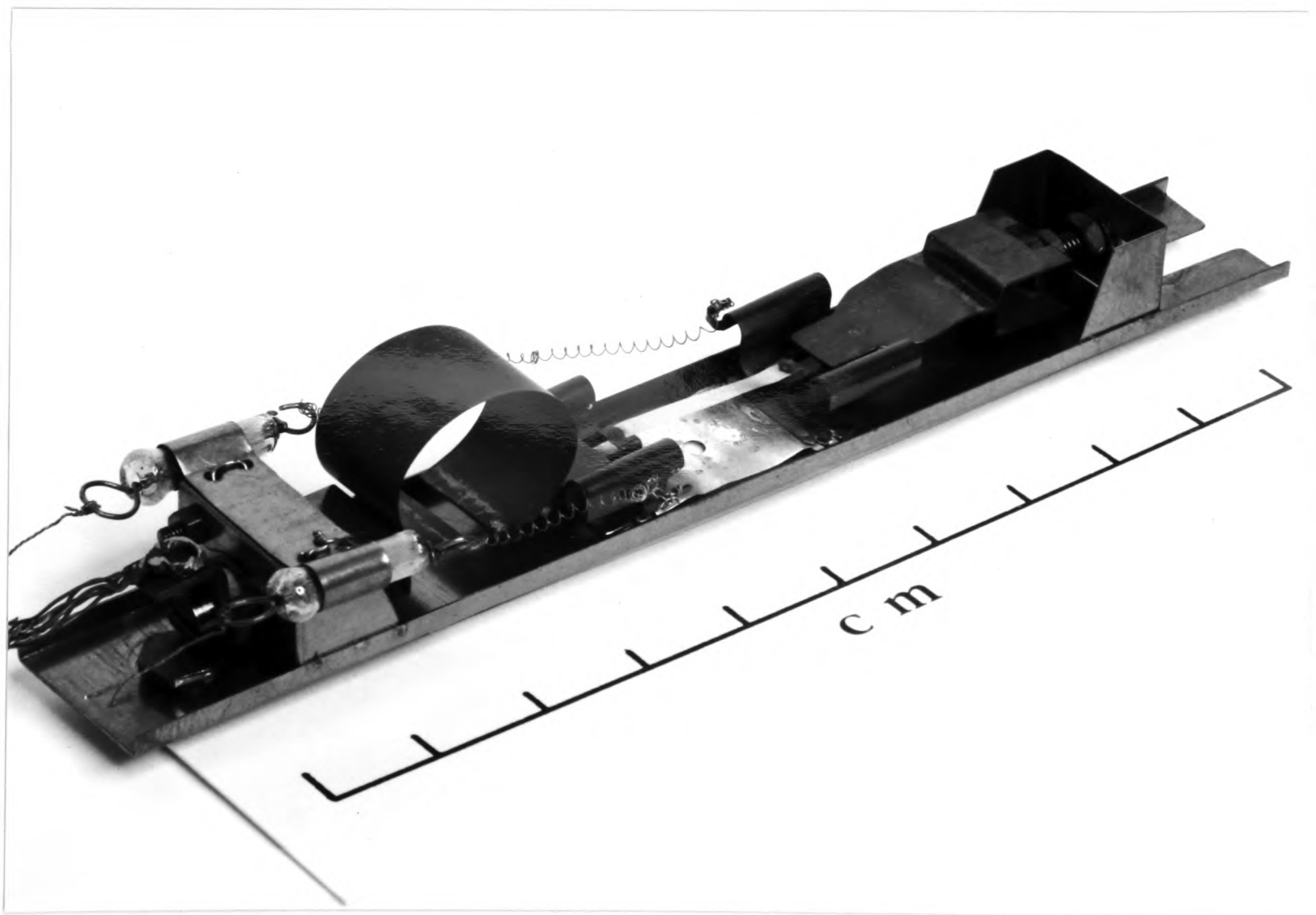


Plate 2. The hot solid surface and sub-assembly. Oblique view. Normally mounted in a vertical plane with the end nearest the heater at the top.

and tungsten are in contact at temperatures in excess of 1240K they form intermetallic compounds with several possible phase changes. Thus this part of the ribbon was probably unable to withstand the strain imposed as the ribbon took up a bowed shape when heated. A further disadvantage of this arrangement was that movement of the tungsten surface altered the geometry important to the final analysis.

6.3.5 Vacuum bake

The two completed sub-assemblies together with their stranded copper wire electrical leads were then baked in the vacuum furnace (appendix 13) for preliminary outgassing as follows: Total time at 500°C or greater, 14 hours. Maximum temperature 590°C. Typical pressure whilst at 500°C was 1×10^{-5} torr.

6.3.6 Oxygen treatment

Both tungsten ribbon sub-assemblies were mounted on a jig in a vertical plane in the auxil iary apparatus bell jar. They were subjected to the oxygen treatment already described above. The treatment was continued in this case for 35 hours. Additional oxygen treatments were conducted inside section A before experiments (see section 7) and followed by high temperature "flashes" to desorb impurities from the surface (see later this section and section 7).

6.3.7 Temperature calibration

The relationship between the temperature of the tungsten ribbons and their heating current was determined by optical pyrometry [1]. This

---

(1) In fact two different pyrometers were used and found to give consistent and reproduceable results to ± 10K or better

was conducted in the bell jar of the auxil iary apparatus with a typical pressure of 4×10^{-6} torr. The pyrometer was focused on the central portion of the ribbon (approximately 1.7 mm diameter) that would be "seen" by the torsion balance via the aperture system.

Corrections were made to the observed temperature for the effect of the Pyrex wall of the bell jar and the spectral emissivity of a tungsten surface at the wavelength of the pyrometer filter (650 nm). The Pyrex correction was found by means of introducing a further sample of Pyrex glass into the light path. The spectral emissivity data and its variation with temperature was obtained from Kaye and Laby (1973) and Thorn and Winslow (1962). The corrected temperature-current relation is shown for one of the tungsten ribbons in the graph at figure 4.

The temperature along the tungsten ribbon was not uniform because it was short and the end losses due to thermal conduction were large. The greatest non-uniformity would be expected at the lower end of temperature range where thermal radiation losses were relatively small. Thus a temperature profile was taken at a corrected central temperature of approximately 1100K. It was found that the central 4.5 mm of ribbon was at the same temperature as the centre to within ± 10K which was considered as satisfactory (1).

The accuracy of the temperature current relation obtained was considered satisfactory in relation to the slope of the graph of the experimental force B against tungsten temperature T_s shown at figure 10 , see section 8.

---

(1) The free ends of the ribbon however were not emitting radiation that was visible in a darkened room; central temperature 1100K.

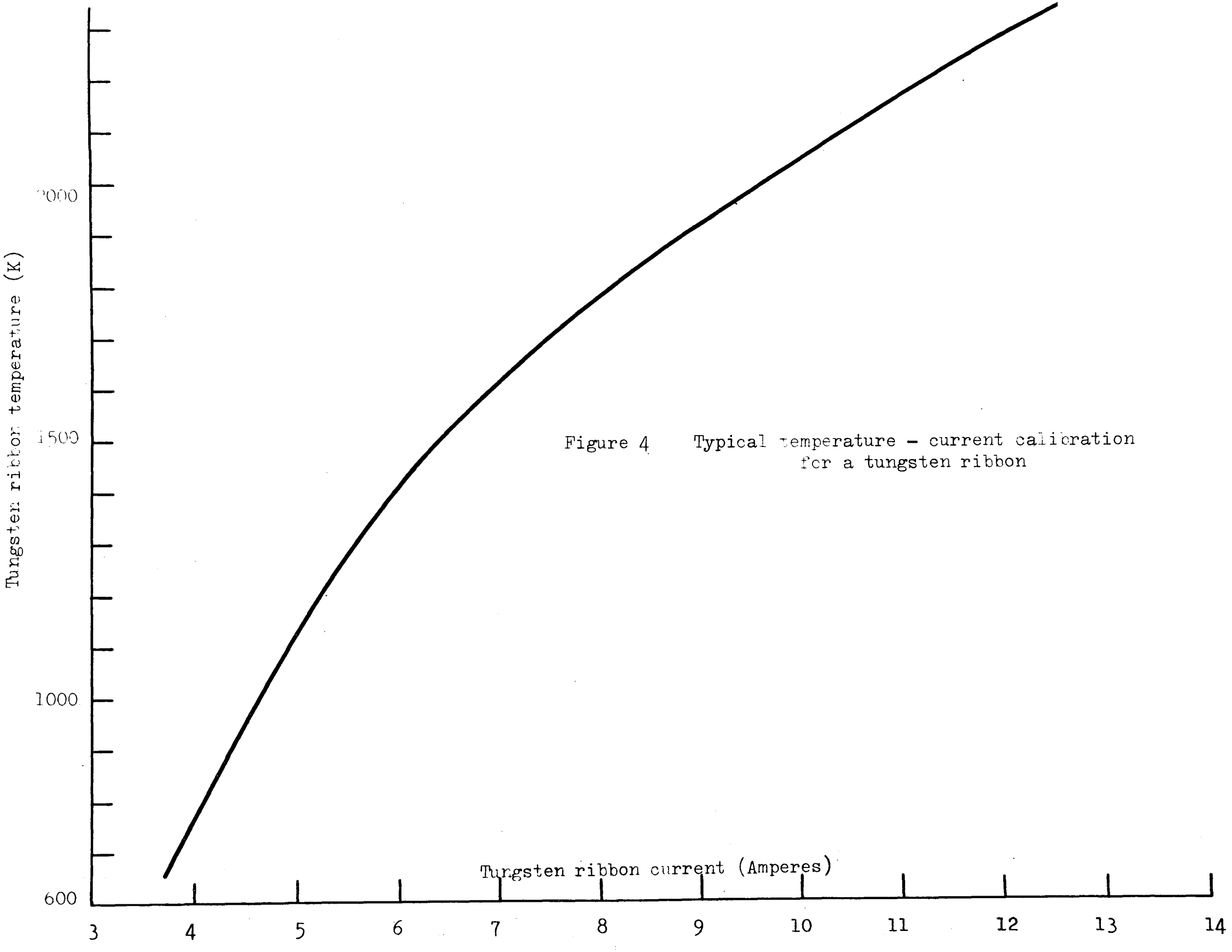


Figure 4 Typical temperature - current calibration for a tungsten ribbon

It was the original intention to use the electrical resistance of the tungsten ribbon as a measure of its surface temperature and it was for this reason that electrical potential leads were provided at each end of the ribbon. During temperature calibration and use of the ribbon in section A readings of electrical current and potential were recorded. However it was discovered that the resistance at a given current remained unchanged throughout the duration of all the experiments so that the more simple current-temperature relation was used. Typical values are quoted in table 3.

Current I (Amperes)	Potential Difference V (volts)	Resistance $\frac{V}{I}$ (Ohms)	Corrected Temperature (centre position) K
5.00	0.436	0.0872	1170
12.00	2.584	0.2155	2323

Table 3. Typical temperature and electrical parameter relation for hot tungsten ribbon

Analysis of the tungsten surface

Following completion of experiments the tungsten ribbon sub-assemblies were removed from the isothermal chamber for analysis.

6.3.8 Surface Cleanness

It was desired to look for surface impurities, especially carbon and oxygen, by Auger analysis (see for example Riviere 1969). It was not possible to conduct the procedure within section A of the apparatus. One of the tungsten ribbons with its sub assembly was taken to the AERE, Harwell where there was an Auger apparatus (1) large enough to accept the whole sub-assembly and equipped with current leads of sufficient capacity for giving the tungsten a thermal treatment similar to that given within section A immediately before an experimental measurement.

Following installation and a 250°C bake the pressure within the Auger apparatus was about 4×10^{-10} torr. The area examined in each case was the full width (2 mm) of the central portion of the ribbon and 0.75 mm in length, i.e. almost the whole of the tungsten surface "seen" by the torsion balance.

Since exposure to atmosphere must have inevitably contaminated the surface this was examined before any pre-treatment and found to consist of thefollowing: 46.4% Oxygen, 24.3% Carbon, 29.3% tungsten. The oxygen treatment was then given (i.e. heating to 2240K in 1×10^{-6} torr of oxygen) to remove the carbon. It was found that only 1.5 minutes (2) of this treatment removed the carbon completely and that subsequent flashes to 2500K removed the oxygen without bringing back the carbon (3).

---

(1) The apparatus and analytical work was directly supervised by Dr. J.C. Riviere
(2) This was considerably less than that used before an experiment
(3) It was previously suspected that at high temperature any remaining carbon within the bulk of the tungsten might well diffuse out to the surface

The conclusion of the Harwell analysis (Riviere 1971) was that the standard procedure adopted, viz a preliminary oxygen treatment followed by 2500K flashes in ultra high vacuum (pressure approximately 4×10^{-10} torr) before a set of experimental results produced a tungsten surface on which the impurity did not exceed 1% of a monolayer and may have been very much less.

6.3.9 Crystallographic structure and surface topography

An X-ray diffraction study and scanning electron microscope pictures were made from one of the tungsten ribbons (1).

It was found that, for the central position of a ribbon, there was a preferred orientation which was common rolling texture in b.c.c. metals. The (100) planes lay in the plane of the ribbon with a certain amount of spread about the rolling direction as axis and a ⟨110⟩ direction in the direction of rolling.

Scanning electron microscopic pictures of the central portion of the ribbon Plates 3, 4 and 5, showed that the surface was relatively smooth, apart from thermal etching of the grain boundaries. There was a "basket weave" structure of low relief which correlated roughly with ⟨110⟩ directions in the surface, but the origin was obscure. It is not clear whether it is an incompletion of the smoothing process of a thermal etching effect. No fine detail such as facetting was observed.

Plates 6, 7 and 8 are from the cooler portion near to the end of the ribbon (figure 5 gives a location key) and are for comparison with plate

---

(1) This work was kindly done by Mr. D. Clark (1971) of R.A.E. Farnborough



Plate 3.

Hot central portion of tungsten ribbon by scanning electron microscope (x 140)

0 100 µm

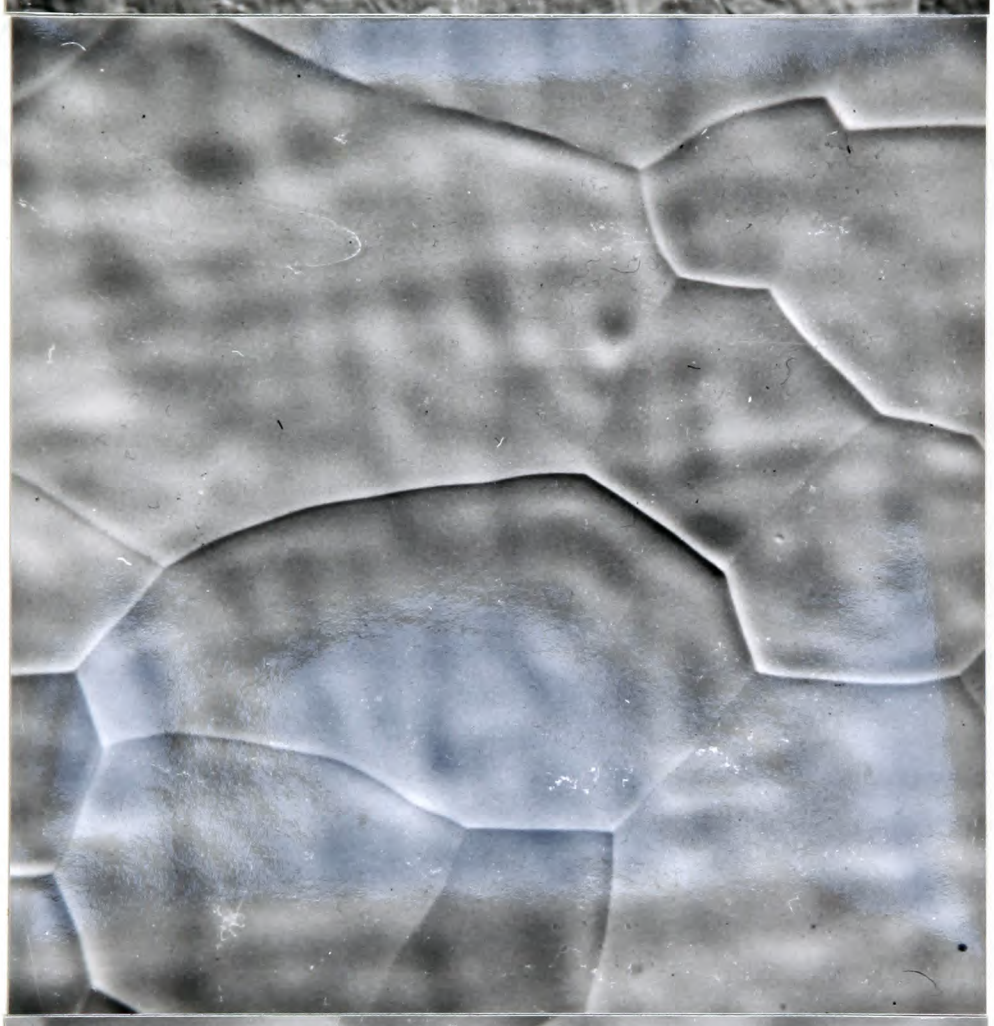


Plate 4.

(x 700)

0 50 µm

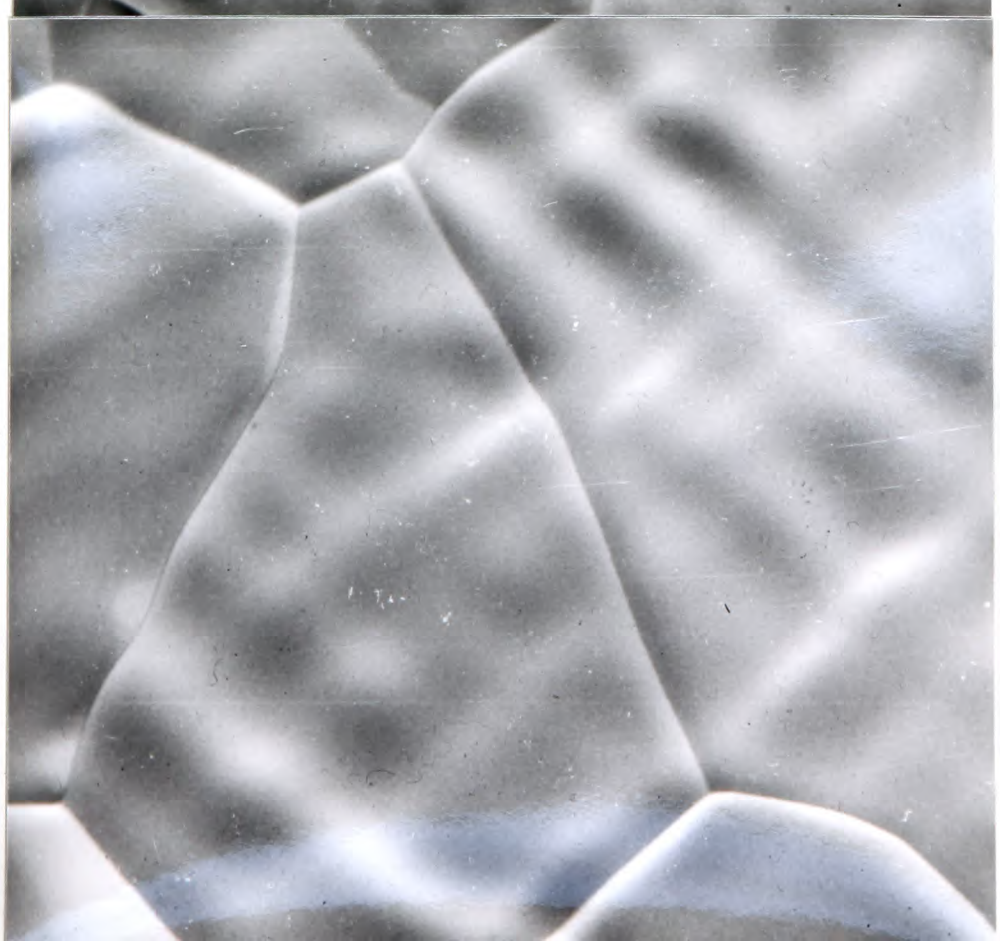


Plate 5.

(x 1400)

0 10 µm

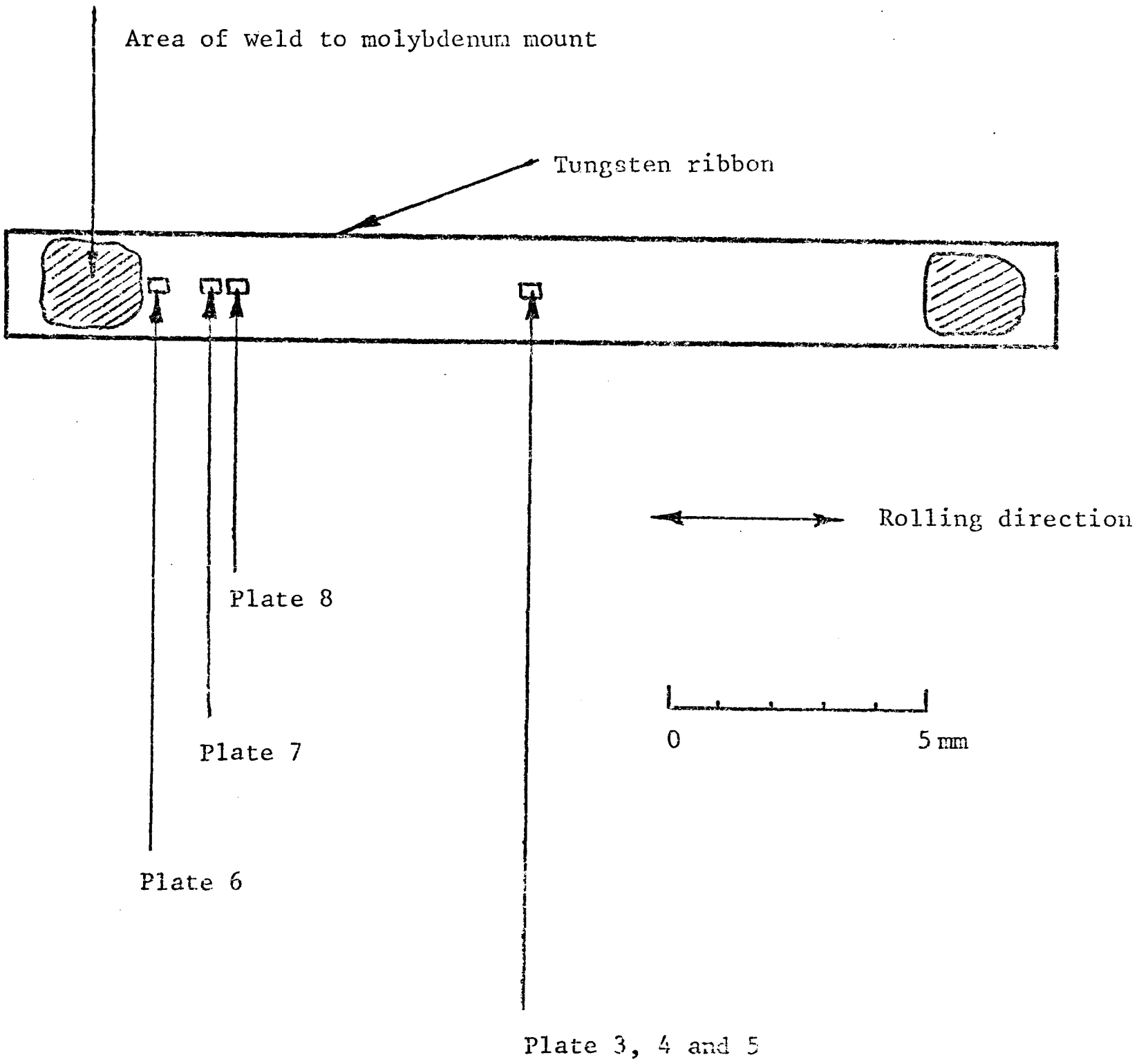


Figure 5 Location key for scanning electron microscope photographs of tungsten ribbon.

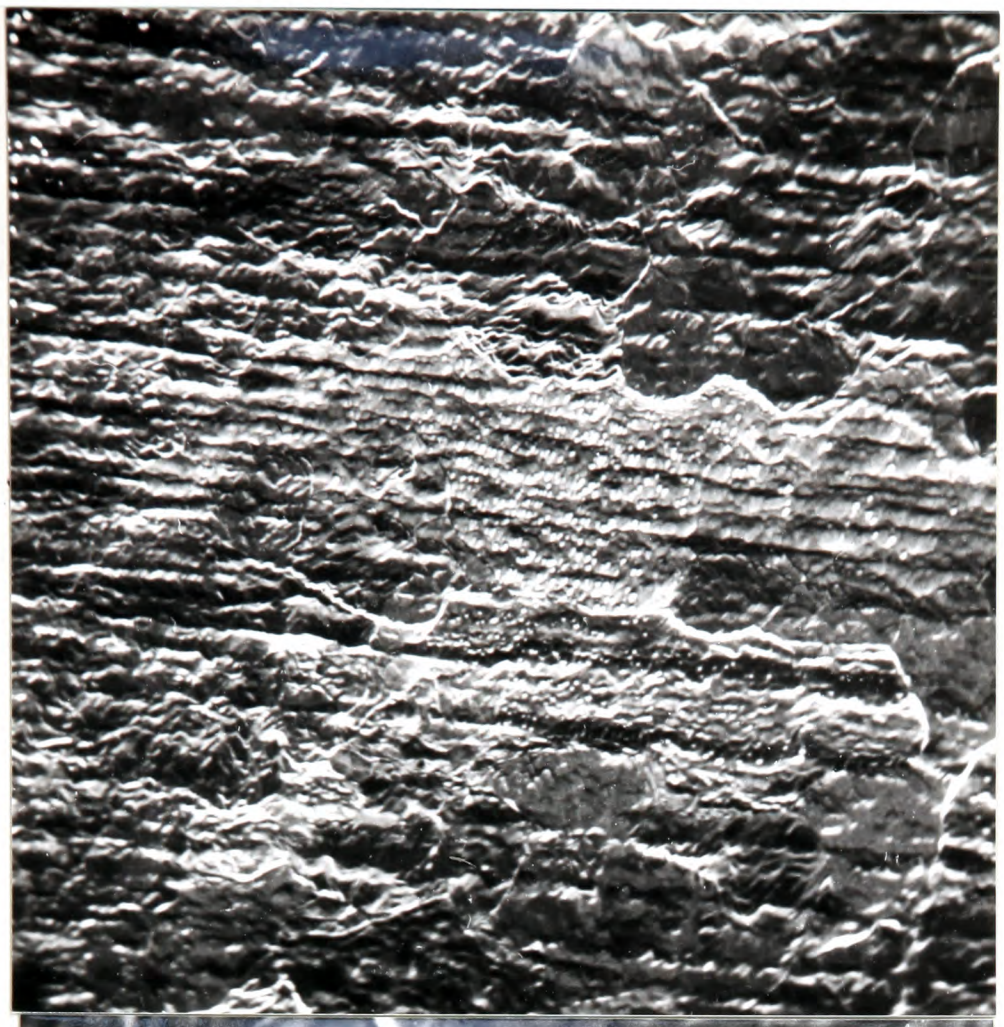


Plate 6.

Cool end portion of tungsten ribbon by scanning electron microscope (x 700).

See figure 5 for location.

0 50 µm

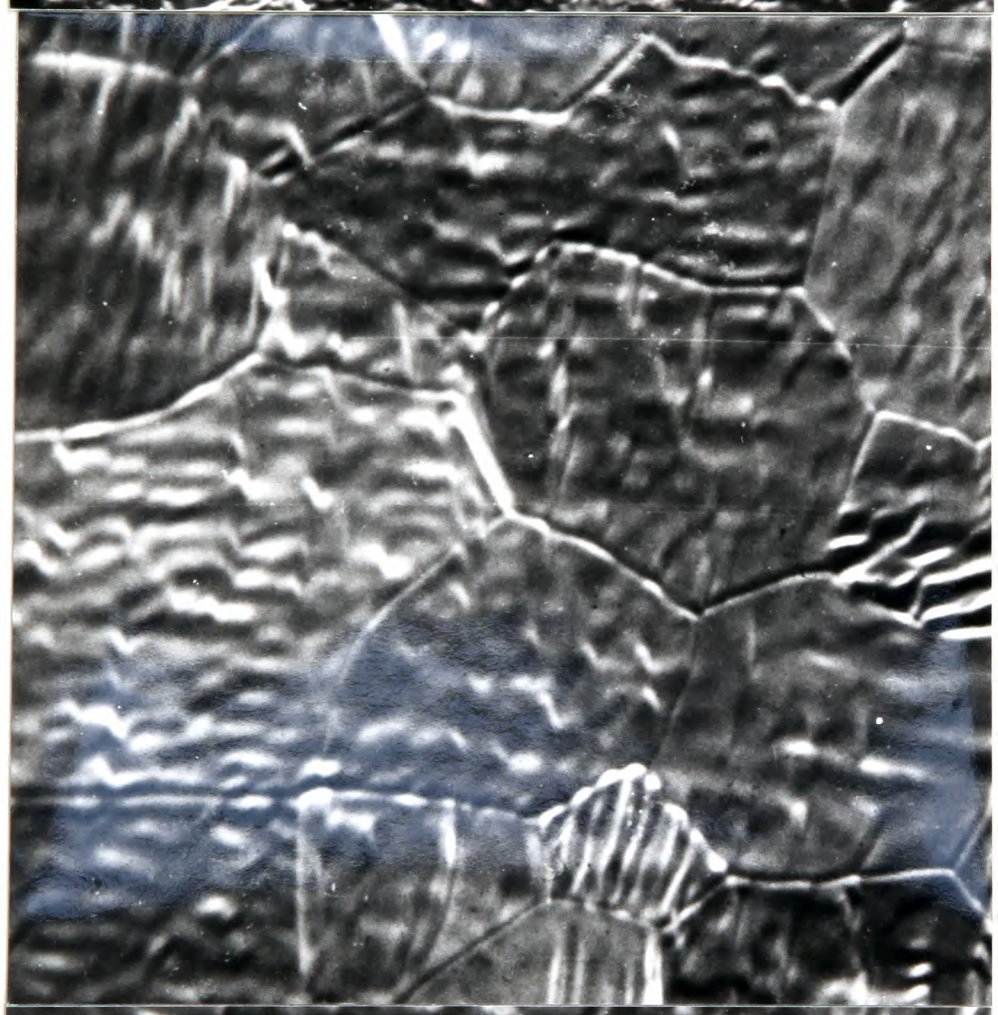


Plate 7.

(x 700)

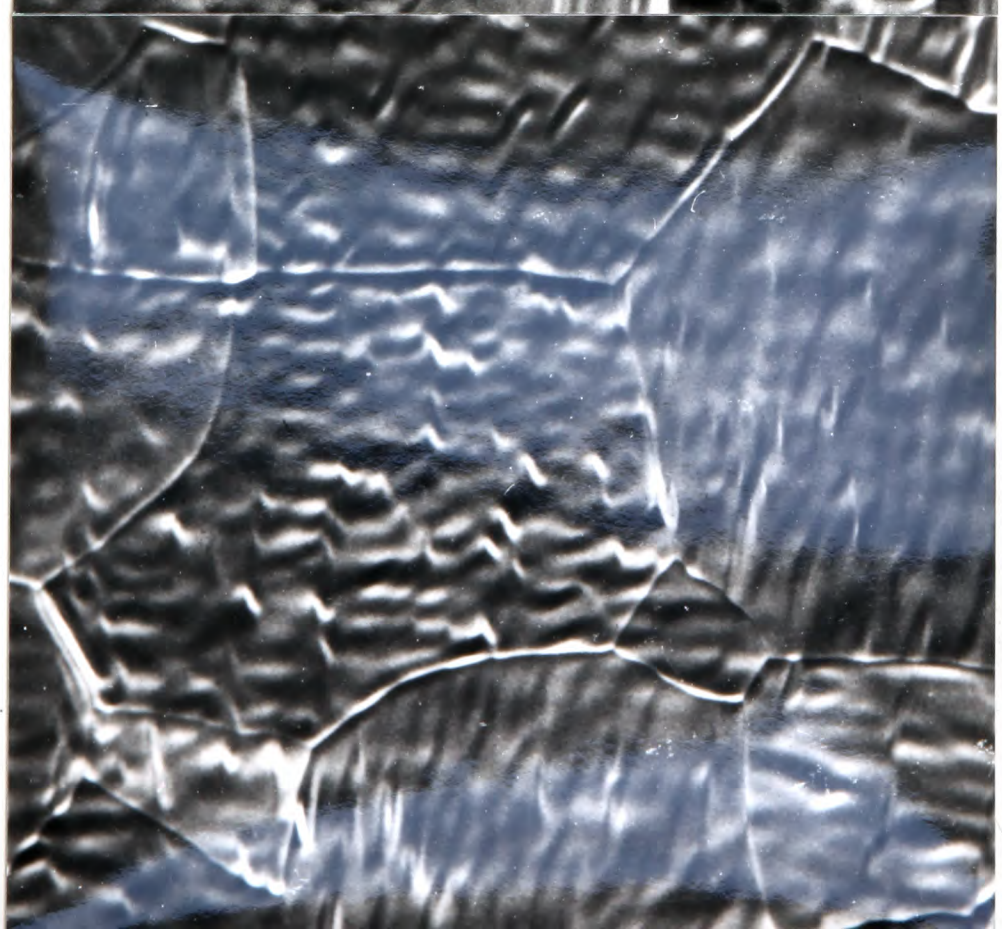


Plate 8.

(x 700)

4, of the hottest central portion and of the same magnification.

Examination of a sample of untreated ribbon of the same batch showed a rougher surface on which rolling marks were evident. This was confirmed by visible light microscopy.

6.4 The torsion balance

6.4.1 Introduction

This torsion balance is the primary detector of the experimental apparatus and is the essential part of this novel method of measuring accommodation coefficients.

It consists of a horizontal beam fixed symmetrically to the centre of a fine torsion wire clamped at each end. The torsion wire is vertical and the beam, which is statically mass balanced, can swing in a horizontal plane. The balance is mounted inside the isothermal chamber in section A in the symmetrical relationship to the two aperture systems and hot tungsten ribbons shown in the plan view of figure 1.

Atoms remitted from the hot tungsten surface that pass through the aperture system impinge on a small area of the beam at a known distance from the torsion wire. The deflection of the beam can be measured by means of a light beam reflected in a mirror mounted on the beam. The sensitivity was calculated from measurements giving its moment of inertia and its time period of oscillation.

6.4.2 The torsion balance used in this experiment

Earlier torsion balances, from which this design was developed, were described by Pearson and Wadsworth in 1963. The various designs included a very sensitive version in which a very fine suspension wire (approximately 3 μm diameter) was clamped only at the top, the beam hanging freely at the lower end. A less sensitive design, with a suspension wire of greater diameter and clamped at both ends, was used in these experiments. This was more robust, had a satisfactorily short period of oscillation and did not vibrate in any other mode.

The suspension consisted of a nominally 10 μm diameter tungsten wire with a mounted length of approximately 100 mm. See plate 9. Each end was clamped and spot welded via the intermediary of 0.25 mm diameter nickel wire. At the top the nickel was welded to the tip of a small stainless steel screw which could be rotated (and clamped) to provide a rotational adjustment. The bottom was attached to 0.5 mm diameter tungsten wire cantilever spring with an effective length of 35 mm. The tension in the suspension was equivalent to the end of the cantilever being displaced by about 2 mm [1]. The frame supporting the suspension was entirely of stainless steel. The beam consisted of a strip of 0.013 mm thick copper foil stiffened by bending so that its cross-section was in the form of a very shallow rectangular U of overall dimensions 52 mm long and 6 mm high. The component parts and completed torsion balance are shown in plates 9 and 10. The mirror "claw" [2] and two mass balancing strips, made from the same copper foil as the beam, were attached to the beam by spot welding using carbon electrodes [3].

---

(1) Equivalent to the weight of a 10 g mass
(2) Similar to those used by jewellers for securing precious stones
(3) The South London Electrical Equipment Co. Ltd., (S.L.E.E.) kindly carried out trials to discover suitable electrode material and the results were very satisfactory. Note also the more recent publication by Dance and Duncan in 1972.

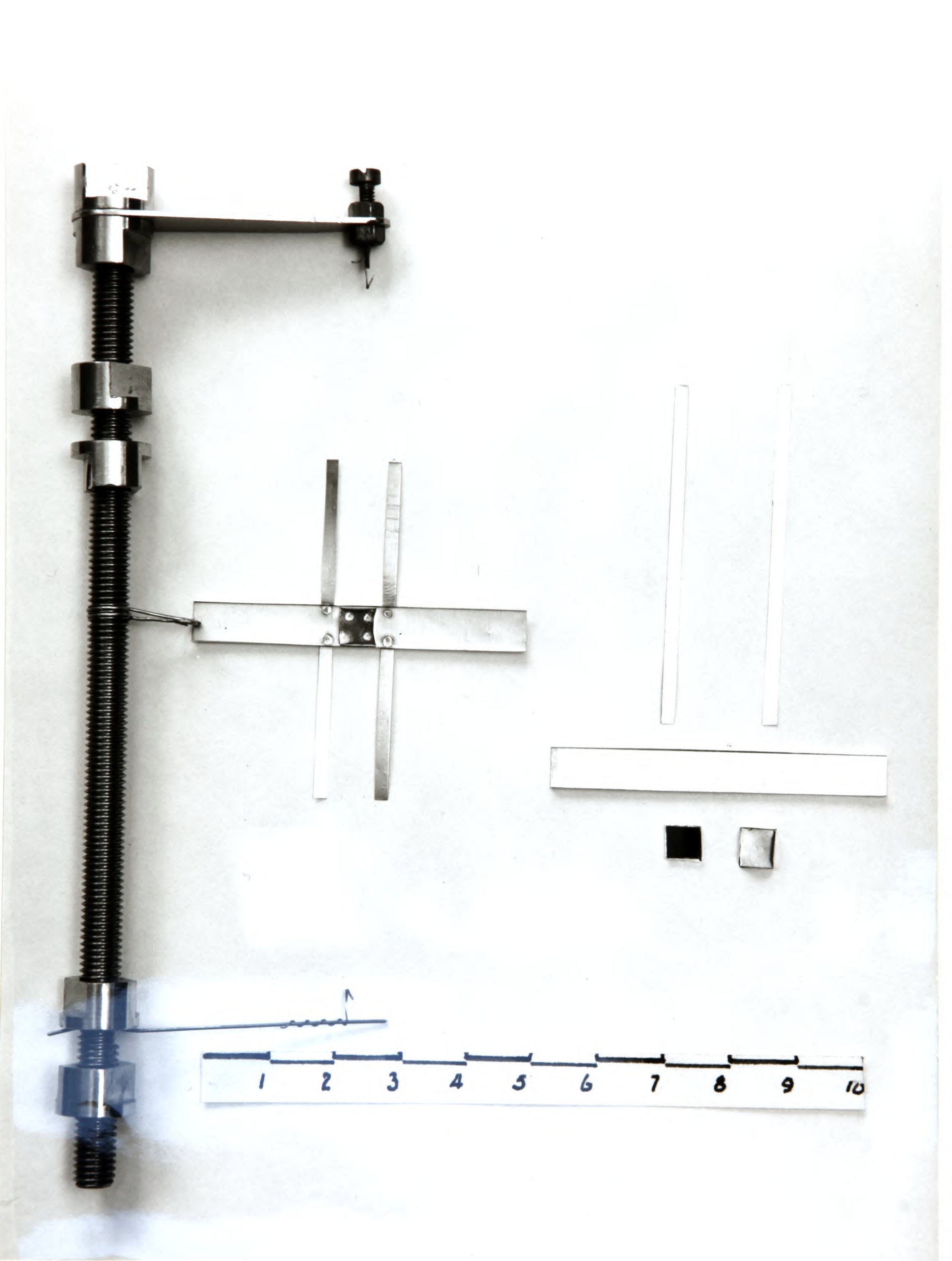


Plate 9. Torsion balance mount and component parts. (cm scale)
Beam - 0.013 mm thick copper foil.
Suspension - 10 μm diameter tungsten wire.
Mount - Stainless steel with 0.5 mm diameter tungsten wire cantilever suspension spring.



Plate 10. Torsion Balance (approximately full size). Beam temporarily clamped. Mounted on stainless steel stand used during pre-baking and mass balancing.

The beam was attached symmetrically to approximately the mid point of the suspension wire by electro depositing two small areas of copper (about 1 mm diameter) over the suspension onto the beam. For details of the method see Bassett and Robertson (1959). The mechanical strength of the joint was improved by preparing the tungsten wire suspension in the region of the intended attachment by electrolytic etching. The tungsten is made the anode in a solution of sodium hydroxide as suggested by Espe (1966).

A 5 mm square mirror of front aluminized optically flat crown glass was fastened securely to the beam by the claws.

6.4.3 Mass balancing and pre-baking the torsion balance

The mass balancing strips were each bent into a horizontal plane and the whole torsion balance mounted vertically on a table that could be tilted through known angles about two horizontal axes at right angles. The lengths of the balancing strips were shortened until, typically, a tilt of the torsion balance about either horizontal axis of 13×10^{-3} radians, produced an approximate rotation of 7×10^{-3} radians of the balance beam about its vertical torsion axis. It was found not possible to improve on this significantly.

An initial pre-bake (in the bell jar of the auxilliary apparatus) of the torsion balance for 3 hours at 450°C caused an out of balance which was corrected. A further bake of 10 hours at 450°C and maximum temperature of 590°C, produced no further change and the out of balance was within those limits originally obtained above.

A method was devised for checking the mass balance even when the torsion

balance was installed within section A. This was pulled to one side with a known force and through an angle indicated by a very sensitive spirit level. The resultant rotation of the torsion balance was measured with the optical amplifier. The mass balance did not measurably change throughout the whole series of experiments.

6.4.4 Calculation of Sensitivity

During the assembly of the torsion balance the mass and dimension of each component part was carefully measured [1]. From this data the moment of inertia of the beam and its attachments was calculated as $117.9 \pm 0.7 \times 10^{-3}$ g cm^2. The time period of oscillation was measured several times under the conditions of the experiment with either helium or argon in section A. It was found to be 8.4±0.1 seconds. There was a slight decrease with the increase of gas pressure over the range used [2] but this was small when compared with experimental error. (The period at very low pressures, 2×10^{-9} torr, was 8.5 seconds[3]).

This results in a torsional sensitivity of $66.0 \pm 1 \times 10^{-3}$ dyne cm radian^{-1} which can be alternatively expressed in terms of the force sensitivity at the beam on the axis of the aperture system (19 mm from the torsion axis). 34.5×10^{-3} dynes radian^{-1}.

These results agree well with a value of 33.8×10^{-3} dynes radian^{-1} estimated from the measured dimensions of the torsion wire and a value for the rigidity modulus for tungsten of 16.06×10^{11} dynes cm^{-2} (Smithalls 1952).

---

(1) All possible dimensional measurements were repeated after the final pre-bake described above. It was discovered that, for example, the length of the beam had permanently increased from 50.90 to 52.31 mm (+ 3%) as a result of the bake.

(2) See for example Mair (1967), On the theory of oscillation vane vacuum gauges

(3) This surprising sense of variation has been verified.

6.4.5 Electrostatic damping

Electrostatic deflection plates were used to damp out any unwanted large amplitude oscillations of the torsion balance. Their position is shown in figure 1 and the electrical circuit diagram in figure 6.

The plates were of stainless steel covered with 0.025 mm thick, 99.99% pure gold [1]. They had an effective size of 15x10 mm and were parallel to and 4 mm from the beam, one on each axis of the two aperture systems. They were mechanically connected to the balance frame but electrically insulated from it with ceramic washers. When the oscillations had been satisfactorily reduced as described in section 7, using the circuit shown in figure 6 , the plates were connected electrically to the balance. This prevented any change in the sensitivity due to an effective change in the stiffness of the suspension under damping conditions.

6.5 The isothermal chamber and aperture system

6.5.1 General description

The essential parts of the apparatus, the hot tungsten surfaces and the torsion balance, were surrounded by a cylinder with axis vertical and separated by an internal vertical diametrical septum in which there were two aperture systems. The purpose of the chamber was to maintain a gas source of uniform and constant temperature at about 300K from which molecules would impinge on the surface of the hot tungsten ribbon and to provide a similar environment for the torsion balance. Small spurious variations in gas temperature would cause large deflections of the torsion

---

(1) To reduce any spurious electrostatic effects due to oxide layers on the stainless steel

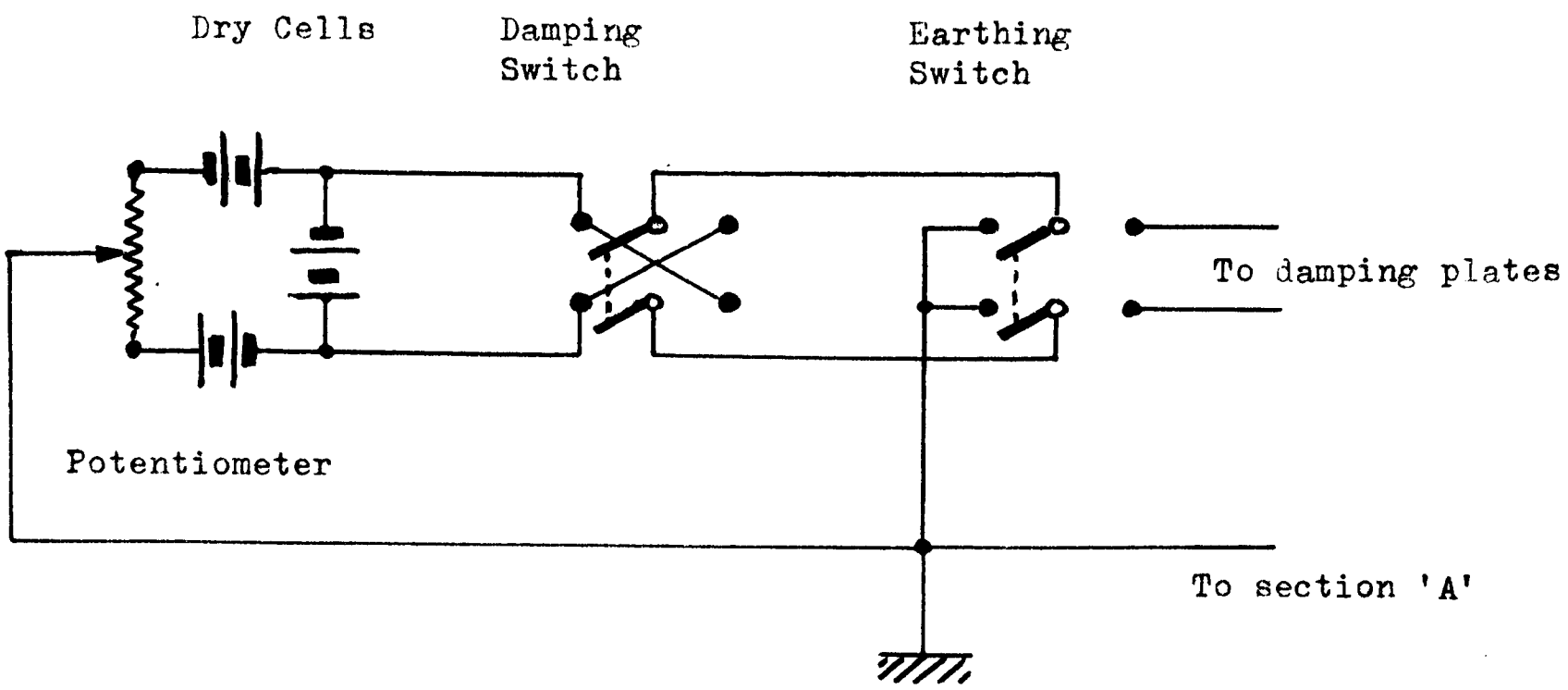


Figure 6 Electrostatic damping plate circuit.

balance and a continual drift of the mean or zero position. Molecules remitted from the hot tungsten in a normal direction would pass through the apertures and impinge on the arm of the torsion balance. Several collisions with the chamber were then required before a further impingement on the hot tungsten. Water at a controlled temperature (the same as that of laboratory) was circulated in the septum to maintain the temperature constant. The chamber was closely surrounded by the coaxial stainless steel vacuum envelope, section A. A general plan view is shown in figure 2, see section 5.

6.5.2 Construction of the isothermal chamber

The isothermal chamber consists of a high conductivity copper cylinder 105 mm OD, 127 mm tall and 1.5 mm wall thickness. The copper septum, which was of the same height and 15 mm thick was vacuum brazed diametrically within the cylinder. The chamber was mounted on a stainless steel ring provided with three legs, each terminating in a small contact area to stand on the base of the vacuum envelope. The torsion balance frame was bolted to the stainless steel ring and the tungsten ribbon frames bolted direct to the face of the septum remote from the torsion balance. Electrical leads were led through the open top of the chamber and down to the lead throughs between the chamber and vacuum envelope. The electrical insulation was fused silica tube.

6.5.3 Temperature control

The septum was provided with a simple system of internal channels for water (approximately 6 mm diameter). The inlet and outlet at the septum base were connected to and through the vacuum envelope via flexible

corrugated tubes arranged to be under tension so that they also retained the relative position of chamber and vacuum envelope. Two helixes of 1 mm diameter wire in the channels increased turbulence and thus the efficiency of thermal exchange between water and septum. The temperature of mains water was typically 10°C. This was taken via a constant head device to provide an adjustable constant flow rate. It was pre-heated to laboratory temperature (20°C) immediately before entry to the septum by a small heat exchanger (1). Adjustment of the flow rate (typically 5 cm^3 s^{-1}) and the input power allowed temperature of input and output water and vacuum envelope to be matched to within ± 0.1°C as indicated by three previously calibrated thermometers.

6.5.4 The aperture systems

Each aperture system consists of two circular holes in the septum, one immediately behind the tungsten ribbon and the other in a protruding copper plug screwed into the septum on the same side as the torsion balance, see figure 1 . The position of each of the components was such that all molecules remitted by the hot tungsten which traverse the aperture system must impinge on the torsion balance and molecules from no other source can achieve this via the aperture system (2). The tungsten ribbons were arranged to be normal to the apertureaxes but those atoms reaching the torsion balance would be included in an angular spread of approximately 2.5° around that normal. The important remission area of the tungsten was a circle about 1.7 mm diameter and the impinging area on the torsion balance was a circle about 2.2 mm diameter.

---

(1) This comprised a 20 cm long, 12 mm diameter copper tube with internal vanes to cause turbulence and an insulated (70 Ω) nichrome winding heated electrically, maximum power 300 Watts.

(2) i.e.: the torsion balance and the tungsten ribbon each fill the field of view via the apertures when viewed from the alternative side of the septum.

Mean diameter of apertures (2a) = 1.17 mm

Separation of aperture pair (1) = 19.15 mm

Distance between axes of each

aperture system (2b) = 38.1 mm

where a = mean radius of apertures

and b = moment arm of torsion balance

The ratio of molecules transmitted through the system to those arriving at the aperture nearest to the tungsten ribbon may be determined by using a formula due to Milne (1929). The full analytical details are given in section 8.

6.6 The Optical Amplifier

6.6.1 Introduction

The small deflections of the torsion balance were amplified in two separate stages. The final stage automatically produced a permanent record with respect to time on a special pen recorder. Apart from the light beam, which passed through the window in the vacuum envelope of section A and the hole in the wall of the isothermal chamber, the whole amplifier and recorder system was outside the main apparatus.

In the first stage a light beam, directed onto the torsion balance mirror, was reflected back onto a photoelectric device. The electrical output was connected to a sensitive mirror galvanometer in the second stage. The deflection of the reflected light beam from the galvanometer was sensed by a photoelectric "eye" attached to the pen carriage of the recorder which was driven by a servo motor. (A Photodyne recorder).

The amplifier was calibrated by two different means each of which produced a known shift of the reflected light beam relative to the photoelectric device in the first stage.

The relative positions of the main components are shown in figure 7.

6.6.2 First stage of amplifier

Photo Cells

The photoelectric device [1] in the first stage consisted of a pair of photo-voltaic cells [2] each of size 6.3x5.1 mm. The shorter sides were placed adjacent to each other in a vertical plane normal to the direction of the incident light beam. They were mounted on a slide so that they could be moved horizontally in their own plane by a fine screw thread to adjust the zero position and provide one means of calibration. The cells are shown mounted in plate 12. The electrical circuit for the cells and galvonometer is shown in figure 8.

The incident light beam produced a bright rectangular image taller than the cells and 5 mm wide. When this was symmetrically placed on the cells the electrical output was zero. Displacement of the image produced an output proportional to displacement providing the electrical load was suitably matched [3]. The output was also proportional to the luminance of the image. Thus a large output was to be obtained from a large mirror to cell separation and a bright image. The cells were placed as far from

---

(1) Cadmium selenide photo-conductive cells previously used were found to suffer from "fatigue", but no such effect was detectable with silicon photo-voltaic cells

(2) Made by Ferranti, type number MS4B

(3) In this case the resistance of galvonometer was chosen following reference to data supplied by Ferranti

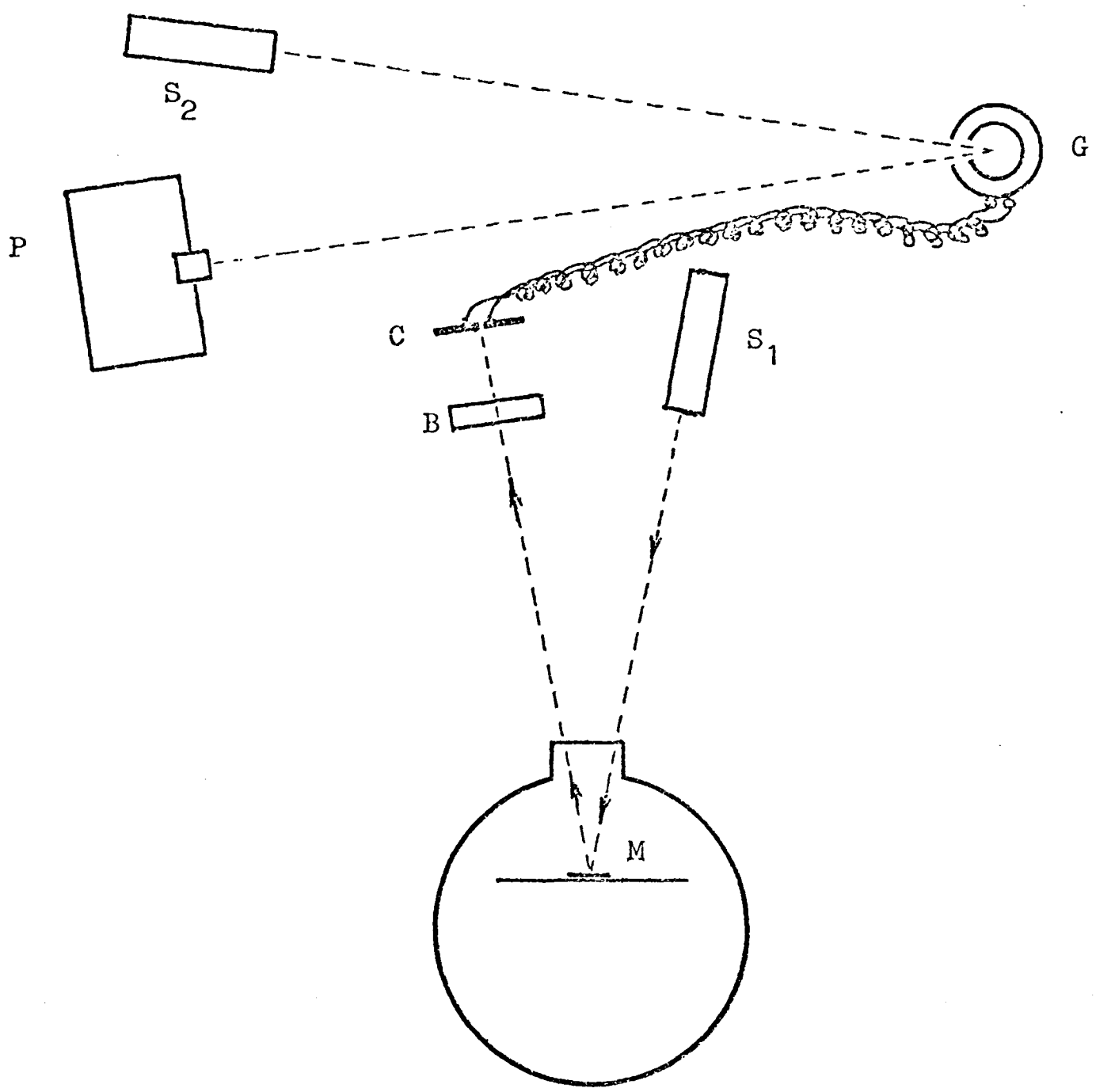


Figure 7 Schematic plan view of optical amplifier

B. Calibrating glass

C. Pair of Ferranti photo voltaic cells

G. Mirror galvanometer

M. Torsion balance mirror

P. Photodyne pen recorder

S_1 Light source to photo-cells

S_2 Light source to pen recorder

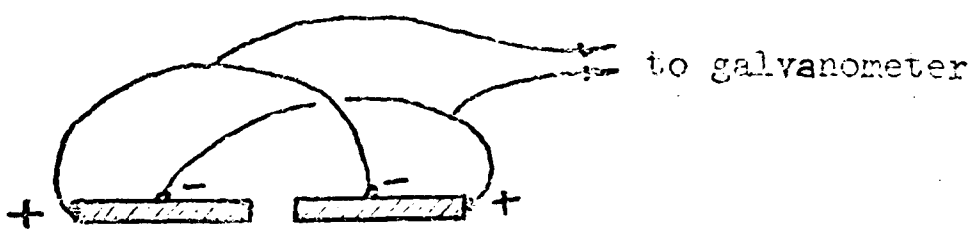


Figure 8 Electrical connections to photo-voltaic cells

Plate 11.

Components of light source for optical amplifier (x 0.3 approx.). Left to right: adjustable slit, lens and water filter tube, adjustable bulb mounting. (cm scale)

Plate 12.

Photo-voltaic cell receiver for optical amplifier (x 0.5 approx.). Left to right: photocell pair on transversely adjustable mounting, calibration glass on rotatable head with Vernier scale.

Plate 13.

Receiver and light source for optical amplifier (x 0.2 approx.). Note stray light screen over cells and alignment mount for light source.

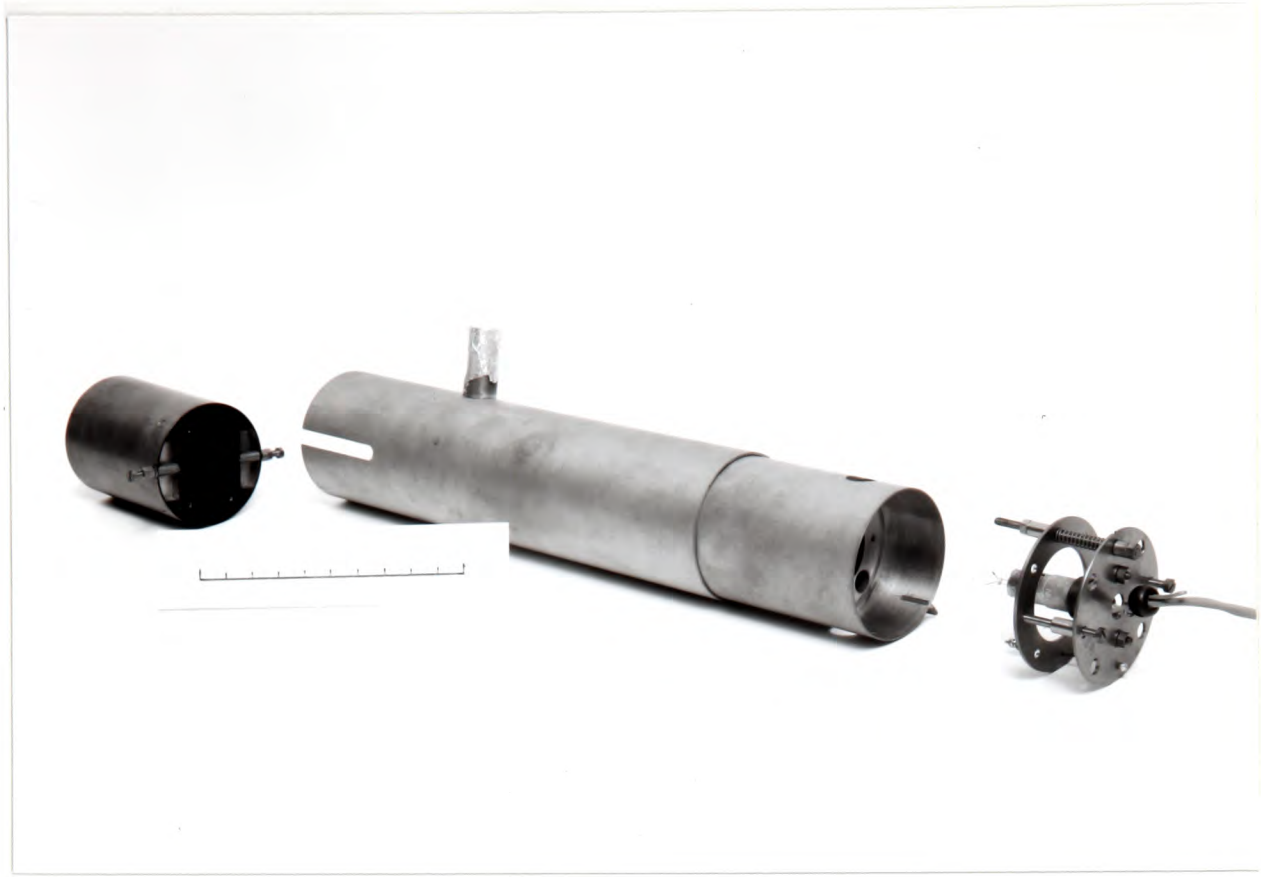


Plate 11.

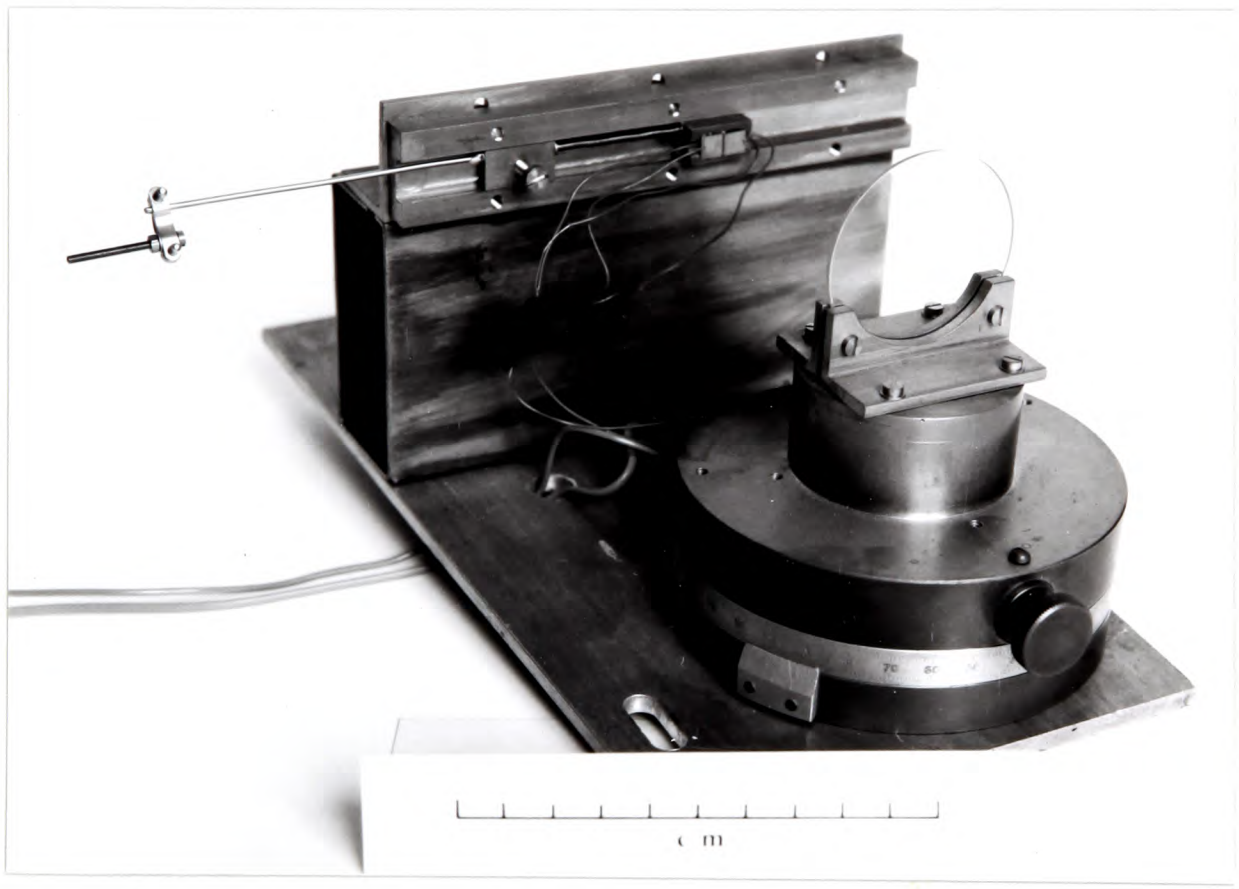


Plate 12.

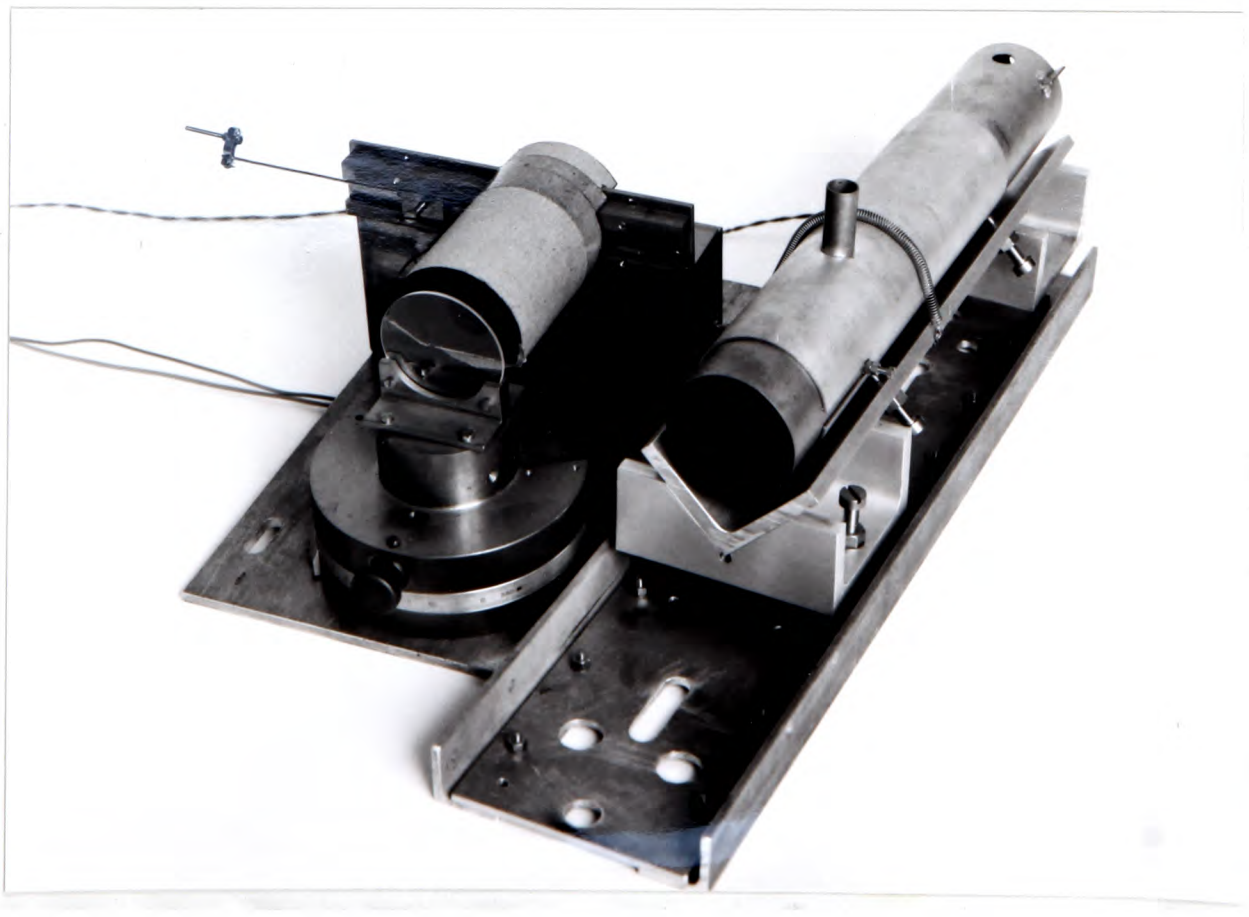


Plate 13.

the torsion balance mirror as the size of the laboratory would allow (approx. 1.5m) and the luminance was maximised with a carefully designed light source described below.

Stray light was prevented from falling on the cells by a matt black screen with a narrow entry angle directed towards the torsion balance mirror. Spurious signals were further minimised by conducting experiments in near blackout conditions.

The light source

The light source is shown as component parts in plate 11. The optical system was designed so that two lenses immediately in front of the filament bulb formed an image of the filament at the torsion balance mirror. A bulb with a small cylindrically coiled filament, approximately 0.5 mm diamter and 3 mm long with a blemish free glass was chosen. Thus a significant fraction of the incident light was reflected towards the cells.

It was discovered that if the light energy was allowed to fall on the torsion balance beam its zero position drifted (1). Thus the filament axis was mounted vertically, the image positioned symmetrically on the mirror and an infra red filter introduced into the incident light path. A 50 mm path of pure water provided a suitable filter and was conveniently contained between the two plano faces of the lenses (2) in front of the bulb.

The provision for fine adjustment of bulb filament with respect to the optical axis and alignment of the whole light source with respect to

---

(1) Presumably non-uniform thermal expansion caused a change of mass balance

(2) A water tight seal between lenses and tube was made with paraffin wax.

the mirror was found to be invaluable in obtaining the maximum amplification from this first stage.

An additional lens mounted close to the window of the vacuum envelope (section A) formed a sharp image at the cells of the vertical adjustable slit in the light source.

6.6.3 Second stage of amplifier

The electrical output of the photocells, see figure 8, was connected to a mirror galvanometer [1] with a sensitivity of 1.2 radians per microamp (reflected beam). Its resistance of 450 ohms was suitable for the photo cells and its period of 2 seconds was conveniently short with respect to the torsion balance period (8.4 seconds). A shunt resistor of 12000 ohms provided critical damping. Deflections of a light beam reflected by its mirror were sensed by a Photodyne [2] pen recorder about 1.6 m from the galvanometer mirror.

High frequency mechanical vibrations of the galvanometer mirror disturbed the pen recorder response. This was alleviated by standing the galvonometer on a sub-frame isolated from the laboratory by rubber mountings [3].

6.6.4 Calibration of the optical amplifier

Whilst the section A was filled with gas at high pressure and the damping of the torsion balance was large, the whole optical amplifier was carefully calibrated by two different means. It was found to be linear over a considerably greater range than that required by subsequent experi-

---

(1) Kindly made available by the Clarendon Laboratory
(2) Photodyne Model PDH8 made by SEFRAM of Paris
(3) The author is grateful to Dunlop Polymer Engineering who suggested a suitable anti-resonant design and provided the rubber mountings

mental results.

The first means of calibration was to shift the photocells transversely on their horizontal mounting by a fine screw drive . The shift was calculated from measurements made of the pitch.

The second means was to rotate a parallel sided glass disc (see plate 12) through a known angle in a horizontal plane. Refraction at each of the air-glass interfaces causes a transverse shift of the light beam which is not accompanied by a significant change in shape or luminance of the light image on the photocells. Knowledge of the refractive index of the glass (μ), the thickness of the glass (t) and the angular rotation (θ) allows the shifts to be calculated from the formula:-

$$s = t \sin\theta \left(1 - \frac{1}{\mu} \frac{\cos\theta}{\cos\phi} \right)$$

where ϕ is the angle of refraction corresponding to angle of incidence θ. For this particular case $\mu = 1.523$ and $t = 1.869$ mm.

The relation between s and θ is effectively linear for $-20^{o}<\theta<20^{o}$. This was confirmed by direct measurement on the glass and angle measuring head used.

The results of these calibrations are shown at figure 9 in terms of the deflection of the Photodyne pen recorder over the range -108 to +102 mm. Deflections from experiments did not exceed the range ±56 mm. During experimental work check calibrations were frequently made using the second means described and over a range appropriate to experimental

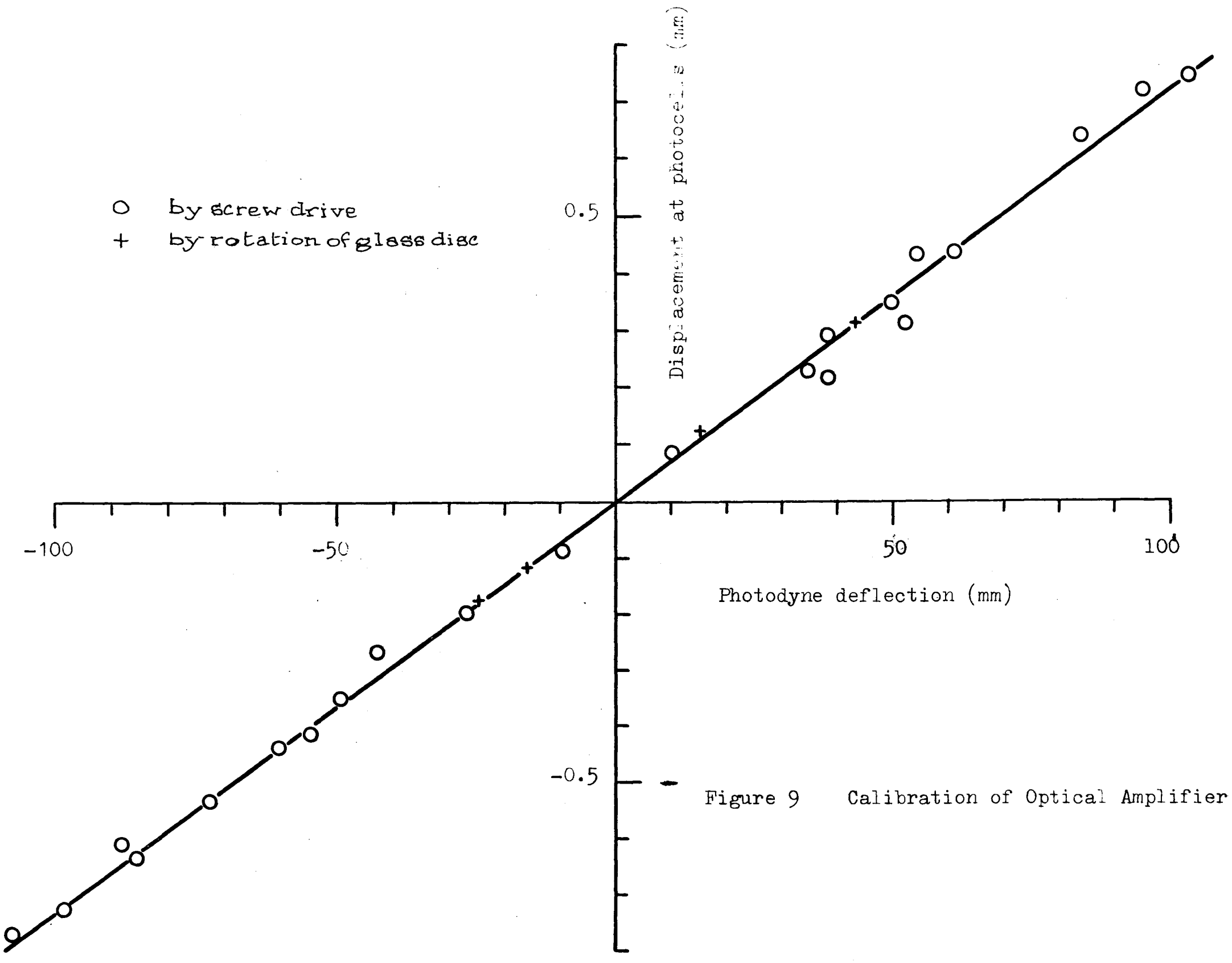


Figure 9 Calibration of Optical Amplifier

deflections. These calibrations never differed by more than 2%. The electrical power supply to the filament bulb was stabilized and the potential difference applied to the bulb carefully monitored and adjusted to 2 parts in 6000.

6.6.5 Sensitivity of the experimental apparatus

From the data contained in figure 9 and the photo cell torsion balance separation, (1474 mm) it may be calculated that 100 mm deflection at the Photodyne pen recorder results from rotation of the torsion balance of 0.229×10^{-3} radians. Also from section 6 the sensitivity of the torsion balance was 34.5×10^{-3} dynes radian^{-1} which leads to the result that 100 mm deflection of the Photodyne results from a force on the torsion balance of 7.90×10^{-6} dynes.

It is possible to detect a Photodyne deflection of 1 mm (1), so that the apparatus is capable of detecting a force of order 10^{-7} dynes (2).

6.7 The Vacuum Apparatus

This important part of the experimental apparatus has already been briefly described in section 6.1. The three parts called sections A, B and C are described below.

6.7.1 Section A. The ultra high vacuum envelope and its appendices

The outer vacuum envelope consisted of a cylinder of stainless steel of height 267 mm, internal diameter 124.5 mm and wall thickness about 1 mm.

---

(1) The Photodyne pen leaves a trace 0.3 mm wide

(2) Greater sensitivity could be obtained by further development of the optical amplifier, see for example Jones (1961)

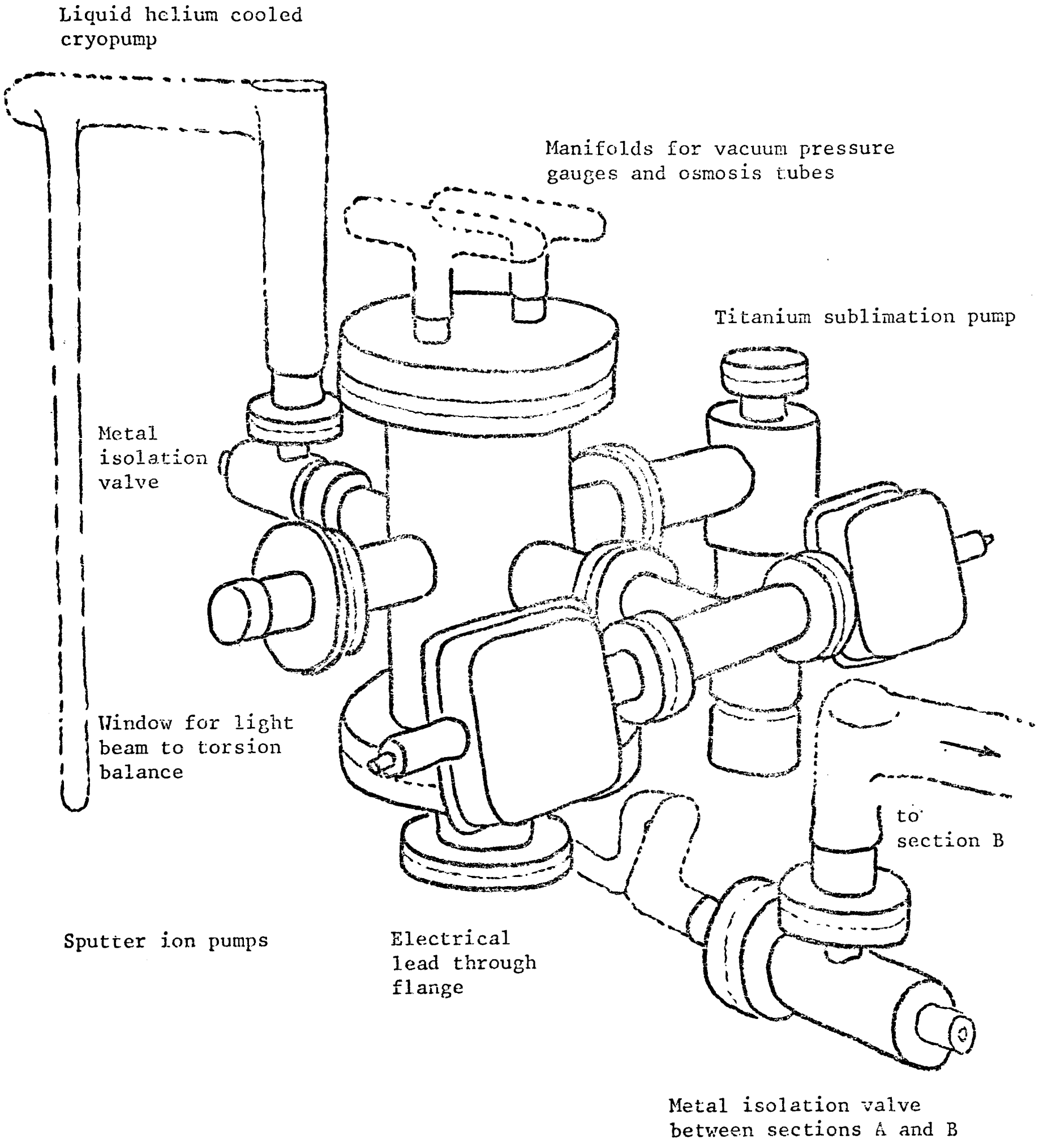


Plate 14. Details of section A

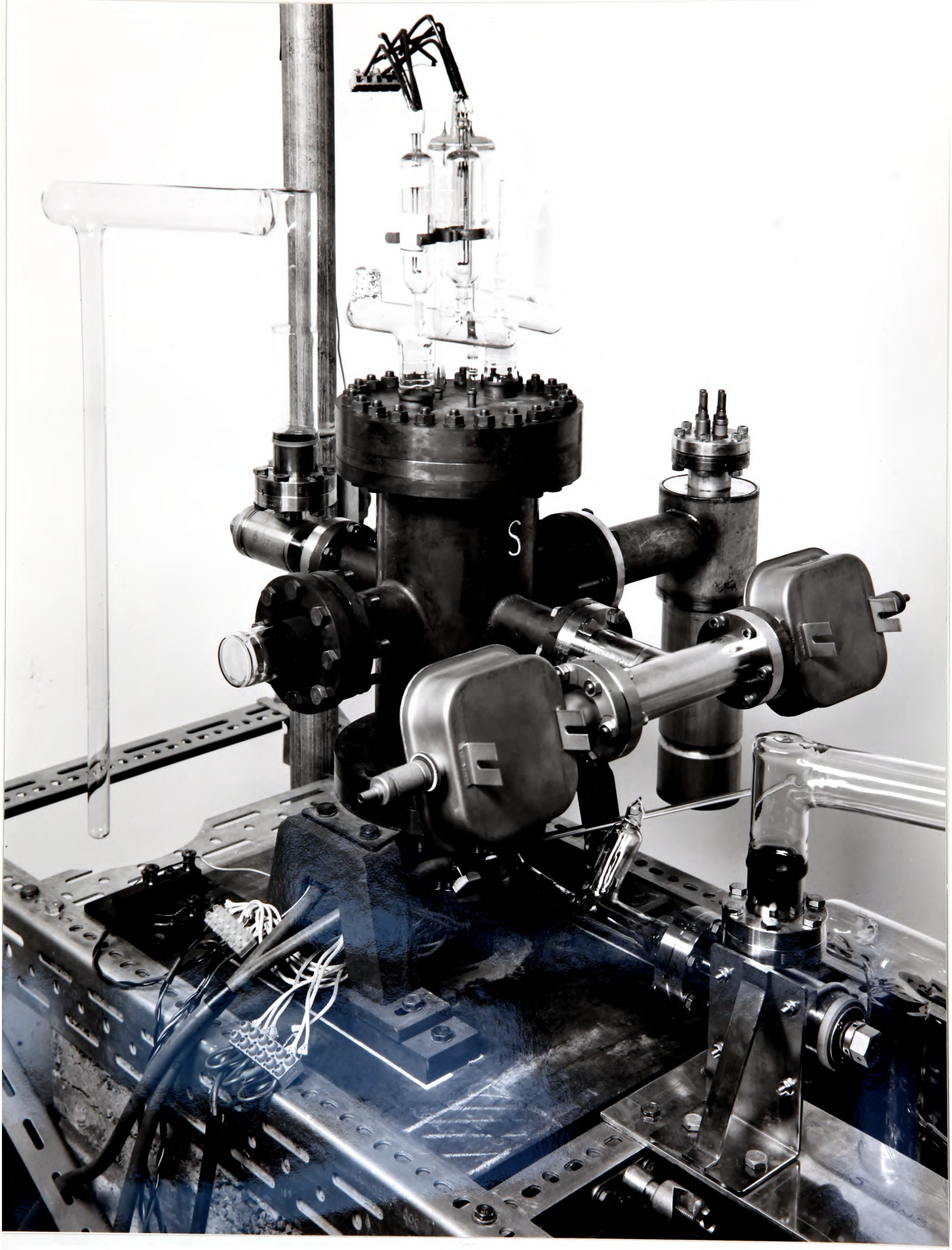


Plate 14. Section A of experimental apparatus viewed from South West (x 0.25 approx.). See cover sheet for details. Note woven glass insulation on electrical leads which remain in place during baking.

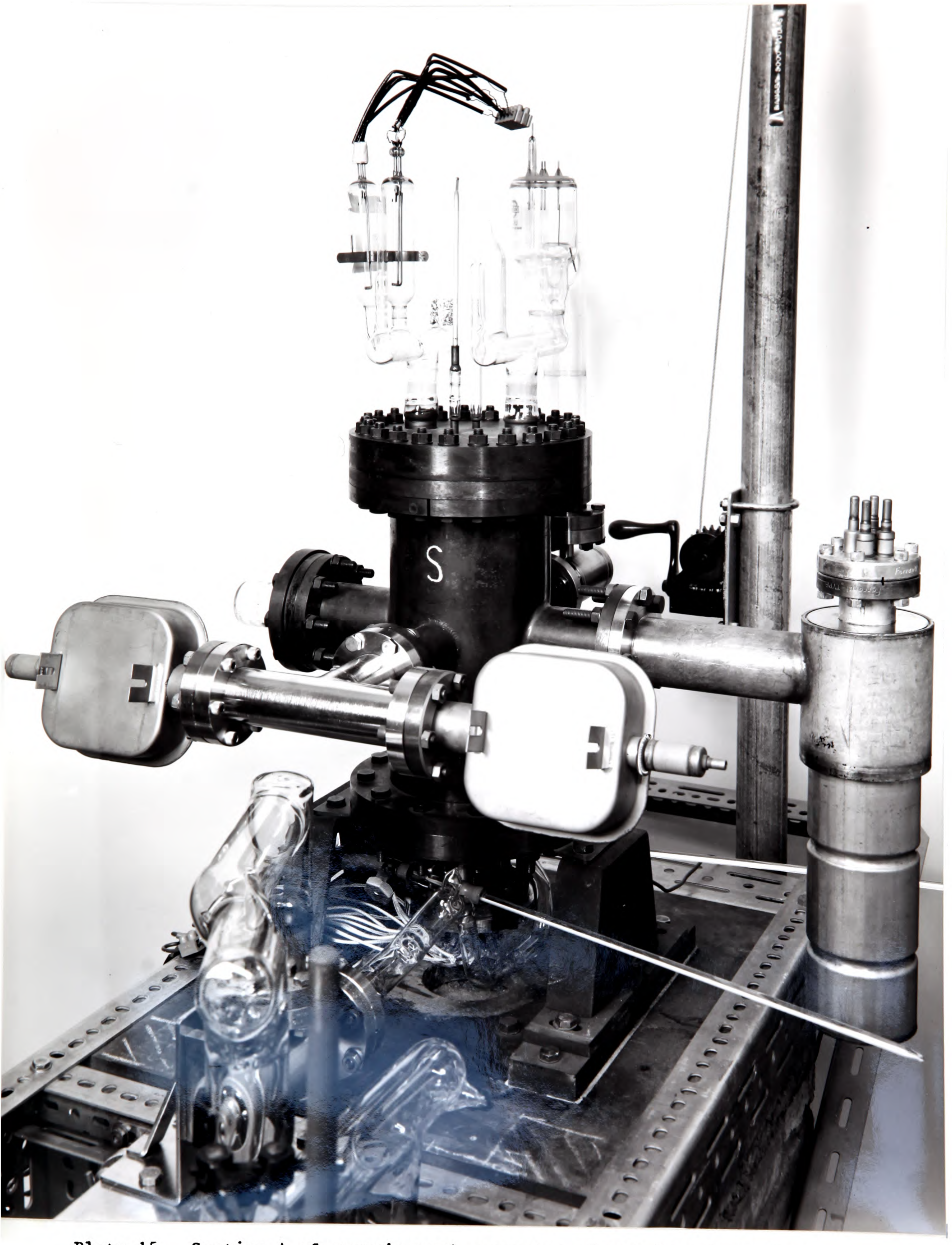


Plate 15. Section A of experimental apparatus viewed from South East (x 0.25 approx.). Note the two thermometers to measure temperature of water to internal isothermal chamber and also winch to lift baking oven.

The cylinder was provided with four horizontal side ports and so orientedin the laboratory so that it is convenient to refer to them as north, south, east and west. Plates 14 and 15 provide two different views of this section. The north and south ports were each 30 mm diameter and 70 mm long, the east and west ports 50 mm diameter and 90 mm long. The cylinder was closed at each end by stainless steel plates. The lower plate had a central port 50 mm diameter and 100 mm long. The upper plate had two metal-glass ports 25 mm diameter each to a glass (1) manifold and two metal-glass ports approximately 5 mm diameter. All metal ports terminated in plain stainless steel flanges except the north and south ports which had Conflat (2) flanges. The plain metal flanges were sealed with gold wire seals (3).

Vacuum pressure gauges and osmosis tubes.

The upper plate is most easily seen in plate 16. Two glass manifolds provide a simple means of connecting the gas admitting osmosis tubes (see appendix 11) and the various gauges to monitor gas pressure.

The Pirani gauge, used during initial evacuation over the range 100×10^{-3} to 0.1×10^{-3} torr is linear in the range 20×10^{-3} to 0.1×10^{-3} torr. In use a similar dummy tube and pair of filaments form a total of four filaments in a Wheatstone bridge circuit.

A Bayard-Alpert gauge was able to monitor the pressure from 0.1×10^{-3} to 0.1×10^{-9} torr. It was of a special type with wide tubulation to minimise

---

(1) Unless otherwise stated glass refers to the borosilicate glass, Pyrex
(2) Trade name of Varian Ltd. Seal made between identical sharp edged flanges which form a seal by plastically deforming an originally plain copper ring. It is bakeable, very reliable and easily made or demounted
(3) Hand made from 0.64 mm diameter fine gold wire by fusing the ends in an oxygen-hydrogen flame. They are annealed and formed into shape around, for example, a suitably sized beaker. They are deformed between flanges to about half their original cross-sectional thickness. They are bakeable, reliable and simple. The gold is recoverable.

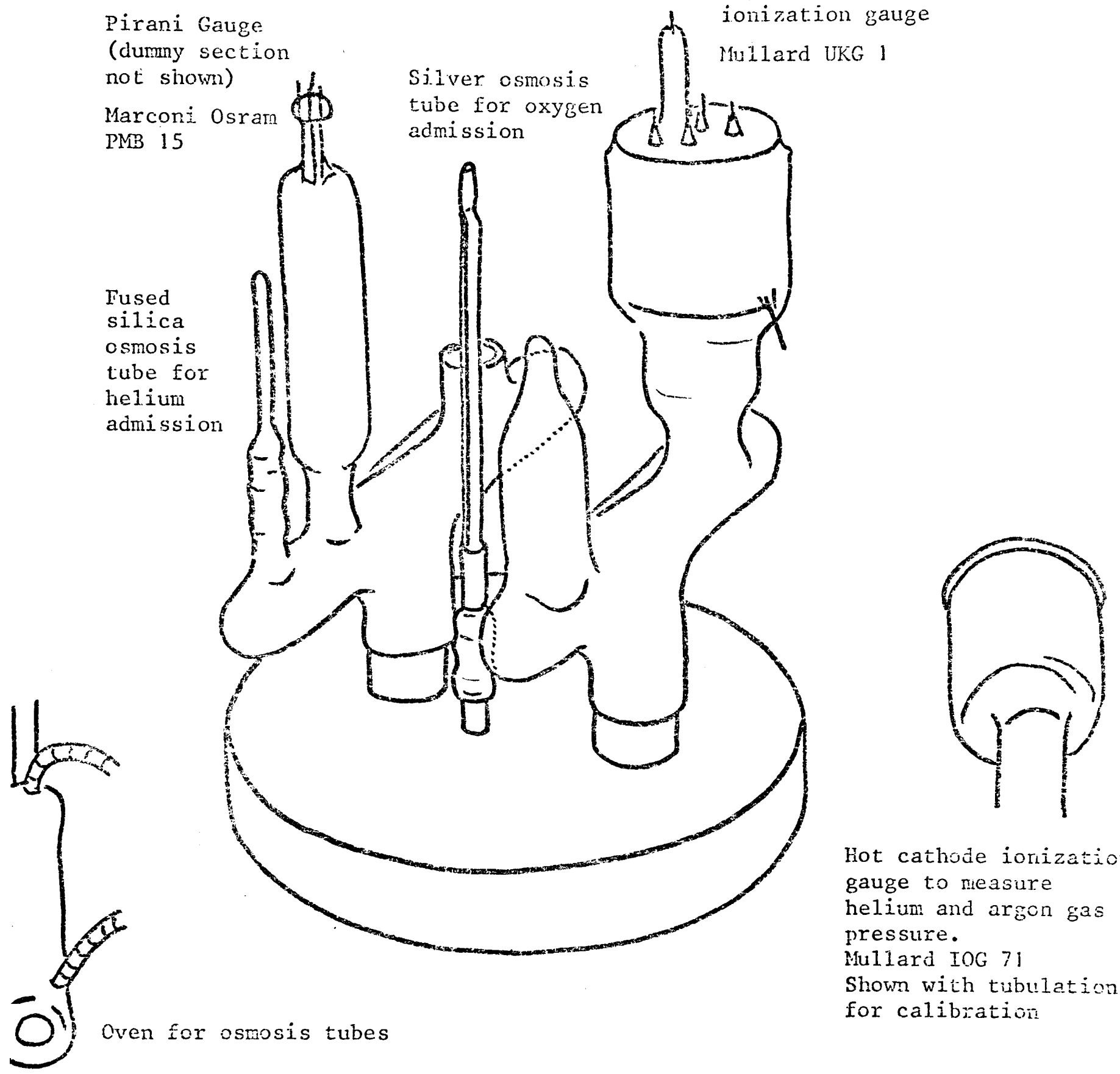


Plate 16. Details of top flange of section A.



Plate 16. Top flange of section A showing manifolds to vacuum pressure gauges and osmosis tubes (x 0.5 approx.). See cover sheet for details. Note foil covered port from which IOG71 has been removed.

any errors due to the pumping effect of its filament.

The early type of hot cathode ionization gauge, the IOG71, was used to measure the pressure of the helium and argon gas (in the range 0.1×10^{-3} to 1.0×10^{-3} torr of helium and argon) admitted to section A. Details of its calibration and use appear in appendix 8. The Pirani gauge was not suitable for this purpose since it relies on heat loss from the filaments by gaseous thermal conduction and under the very clean conditions of section A the gas-filament interaction would have been changing with an accommodation coefficient less than unity. This effect was confirmed under clean conditions.

Vacuum pumps

The pumps on section A were of three types, sputter ion, liquid nitrogen cooled titanium sublimation and liquid helium cooled cryogenic cold finger.

Two Ferranti FJD8 sputter ion pumps were connected via a "tee" piece and Conflat flanges to the south port. The speed of these pumps decreases linearly with pressure and is different for various gases.

Pressure	Pump Speed
10^{-5} torr	8 litre s^{-1}
10^{-10} torr	5.2 litre s^{-1}

Variation of pump speed for nitrogen with pressure, for Ferranti FJD8 sputter ion pump. Speed for argon is about 100 times less in each case, similarly for helium.

The combined speed of the two pumps on the port was approximately 9 litres s^{-1} for nitrogen at 10^{-5} torr. Their main purpose was to reduce the pressure in section A after it had been isolated during the baking procedure and to maintain an equilibrium pressure of about 10^{-6} torr of oxygen (admitted via the silver osmosis tube) during the oxygen treatment on the hot tungsten ribbons. They were turned off whilst section A contained either helium or argon for experiments.

Details of the operation of these pumps and their application to ultra high vacuum requirements were obtained from Robinson (1968).

A titanium sublimation pump cooled with liquid nitrogen was connected to the large east port. It provided a high speed (55 litres s^{-1}) for active gases by gettering and its design and operation are fully described in appendix 9. After baking it was used in conjunction with the sputter ion pumps to reduce the pressure to $\sim 10^{-10}$ torr. It was then maintained in its active condition throughout all the experiments to help provide the necessary purity of helium or argon gas. Valuable information about the combined use of titanium sputter ion and getter pumps was obtained from Newton and O'Neill (1966), Redhead, Hobson and Kornelsen (1968) and Cyranski (1970).

It was estimated that the probable total leak rate of section A when isolated was 10^{-6} lusecs (1). Whilst the titanium sublimation pump would maintain a satisfactory low pressure of the active gases, approximately 1% of the earth's atmosphere is argon. A relatively small fraction of argon in an experiment with helium would have been very undesirable since argon was known to have an accommodation coefficient an

---

(1) A unit of rate of flow of gas in (pressure)x(volume) units. 1 lusec is 1×10^{-3} torr litres s^{-1} for a pressure differential of 760 torr

order of 10 greater than that for helium on tungsten (see eg Watt et al 1974). For this reason a liquid helium cooled cold finger was connected to the north port via a 12 mm bore metal valve. This pump is fully described in appendix 10. Its speed was limited by the valve to about 2 litres s^{-1}. It was used in combination with the titanium sublimation pump during helium experiments with and additional advantage that it was used to adjust the helium gas pressure by physical adsorption. In argon experiments it was used only to adjust the gas pressure.

6.7.2 Section B

This section was constructed mainly of Pyrex with metal valves and was completely grease free. It served two purposes; first to provide a channel by which section A was initially evacuated and second to introduce pure argon gas into section A.

The 12 mm bore valve between sections A and B and the relatively small bore of the pumping port into section A resulted in a communicating conductance of about only 1 litre s^{-1}. It was provided with a sputter ion pump, a Monax liquid helium cold finger with isolation valve, a liquid nitrogen cold finger and vacuum pressure gauges to operate satisfactorily over the range 100×10^{-3} to 0.1×10^{-9} torr as shown in figure 3.

A pair of metal valves separated a 1 litre Pyrex flask of Research (X) Grade argon with a break seal. When this was broken, argon could be let into section B in controlled amounts and thence into section A. The typical impurities of this grade of argon are given in table 4.

Nitrogen	2	Carbon dioxide	0.5
Oxygen	<1	Hydrocarbons	0.5
Hydrogen	<1	Water vapour	1

Table 4 Typical analysis of impurities in research grade argon as supplied by the British Oxygen Company. Values expressed as volume parts per million.
Argon purity 99.997 %.

The whole of this section was bakeable. After initial evacuation whilst warm, sections B and the whole of A were baked initially into the sputter ion pump on B and then the liquid helium cooled cold finger. After section A was isolated, B was maintained at low pressure to minimize any gas leakage from B to A.

6.7.3 Section C

Apart from a stainless steel liquid nitrogen vapour trap adjacent to the metal valve of section B, section C was of copper and plastics pipe with elastomer seals and Apiezon greases. It was used as a two stage rough pumping system for sections A and B. A water jet pump separated the whole system from the atmosphere.

A pair of liquid nitrogen cooled sorption pumps (1) were capable of reducing the pressure sufficiently in order to start the sputter ion pump on section B. A diaphragm gauge and a Pirani gauge indicated the progress of initial evacuation.

---

(1) These pumps were filled with artificial zeolite, Union Carbide type 5A

6.7.4 Evacuation of the vacuum apparatus

During the course of the experiments the whole apparatus was evacuated several times following modifications or mishaps. Thus a carefully planned routine was developed to reliably produce the required conditions in section A in the minimum time. The important details of this lengthy procedure are given in appendix 14.

Chapter 7

The Experimental Procedure

7.1 Introduction

When the apparatus had been satisfactorily evacuated, section A to a pressure of $3x10^{-10}$ torr or less, section B to $3x10^{-9}$ torr and acceptably low leak rates confirmed, the isothermal chamber and the tungsten ribbons were subjected to final cleaning procedures. Trial experiments were conducted with each of the tungsten ribbons at their maximum experimental temperature of 1900 K and a gas pressure of $3x10^{-10}$ torr to ensure that no significant "no-gas" deflections were observed. The experimental gas was then admitted to section A and the experiments conducted.

7.2 Cleaning procedures

In order to remove any surface carbon picked up by the tungsten ribbons during their transfer from the preliminary apparatus (1) to section A the oxygen treatment (2) was applied in section A for a further 10 hours. Here the ribbons were ohmically heated to 2240 K in $1x10^{-6}$ torr of oxygen, produced by the equilibrium between oxygen admission via the silver osmosis tube, at about $550^{o}C$, and its removal by the sputter ion pumps on section A.

The area of copper septum (see figure 1) "seen" by the balance beam was very large compared with the area of the apertures. Thus a very small desorption of gas from the septum, caused for example by heat from a

---

(1) The bell jar of the auxilliary vacuum apparatus in which the tungsten ribbons were pre-treated and temperature calibrated

(2) See section 6

hot ribbon, would produce a signal comparable with that produced by hot gas atoms of helium or argon coming through an aperture. The isothermal chamber was therefore given a final outgassing for about 2 hours at 100°C immediately prior to an experiment. This was done by passing steam through channels in the septum normally cooled by water to a temperature equal to that of the laboratory. The tungsten ribbons were maintained at a temperature of about 300°C during this procedure.

7.3 Procedure in the argon experiments

After the above preliminaries, the break-seal of the argon flask on B was broken and the metal valves in B manipulated to produce, by successive expansions, a pressure which gave a suitable working value in A ($\sim 1 \times 10^{-4}$ torr). The titanium sublimation pump in A was reactivated by subliming more titanium and the reactivation repeated at regular intervals in order to sorb all gases but argon, which the titanium film did not significantly pump. The cold finger on A was chilled with liquid helium and the metal valve about it (normally closed) was cautiously manipulated to reduce the argon pressure when required.

Owing to traffic disturbance the torsion balance was subject to continual oscillations of random amplitude. However, it was found that during the early morning between the hours of 2 to 6 the random amplitude was usually small enough to be damped out by use of the electrostatic damping plates. This was done by rapid and judicious manual switching of the potential of the plates in suitable phase relation to the observed oscillations of the light beam reflected from the torsion balance mirror. Immediately prior to an experiment the balance oscillations were damped to an amplitude small compared with that of the expected deflection and

the optical amplifier calibrated by rotating the glass disc as described in section 6.

One of the tungsten ribbons was then flashed to 2500 K for approximately 1 second to remove adsorbed gases [1] - in particular adsorbed oxygen resulting from the carbon removing oxygen treatment. Then the tungsten ribbon current was reduced directly to a lower value corresponding to the tungsten ribbon temperature desired in that particular experiment [2], the oscillations again damped (usually obtained in about 60 seconds) and a steady deflection corresponding to the tungsten temperature was recorded on the Photodyne chart. The current was then switched off to obtain the zero of the deflection, switched on to repeat the deflection and again switched off to repeat the zero. Such an experiment was completed within about 200 seconds. Thus at any chosen tungsten temperature there were three separate values of the deflection due to gas and in general these agreed to within about 5 per cent.

7.4 Procedure in the helium experiments

The helium experiments followed the argon ones, the argon being removed by repeated filling of the apparatus with dry nitrogen at atmospheric pressure and evacuation by water jet pump. The sorption pumps on section C were then chilled, producing a pressure of about 10^{-3} torr. The sections A and B were then pumped and rebaked as described in appendix 14.

The tungsten ribbons were again given the oxygen treatment (2 hours) and the isothermal chamber outgassed (2 hours).

---

(1) Some calculations on desorbtion of gases from tungsten at high temperature are given by Carpenter, Humphries and Mair (1963)

(2) A technique suggested by Yamamoto and Stickney in 1970

The cold finger on A was immersed in liquid helium and the valve above it left open, thus effectively forming a "sink" for all gases except helium itself, since the vapour pressure at 4.2 K of the most volatile gas other than helium (viz. hydrogen) is less than 1×10^{-6} torr (see appendix 10). As in the argon experiments the liquid nitrogen cooled titanium sublimation pump was also regularly activated to assist in maintaining the desired low background pressure.

The silica osmosis tube was then heated for about 10^3 seconds at about $475^{o}C$ in helium at atmospheric pressure, producing a pressure of about 10^{-3} torr in the 7 litre volume of A (see appendix 11).

The observational procedure in the helium accommodation experiments was the same as in the argon ones, save that the helium gas pressure was increased when required by reheating the silica osmosis tube in a helium atmosphere or small adjust ments in pressure made by raising or lowering the liquid helium dewar on the cold finger on section A (see appendix 10).

Chapter 8

The Experimental Results and Analysis

8.1 The selection of results for analysis

A large amount of experimental data was obtained. However, for reasons primarily concerning the cleanness of the gas or tungsten surface and desorption of gas from parts of the isothermal chamber, most of the data was discarded. Only results for those experiments where the conditions were judged to be satisfactory are presented and analysed here.

The criteria used to judge and hence select those experiments were as follows:-

1. The ultra high vacuum conditions should be maintained with only those pumps and gauges intended to be used during an experiment and with the tungsten ribbon at the top of the intended temperature range.

2. The deflection of the Photodyne pen recorder should be small, during a dummy or no-gas experiment, when compared to experiments in argon or helium at the same tungsten ribbon temperature.

3. The tungsten ribbons should have been subjected to the oxygen treatment before the set of experiments and flashed to 2500 K immediately before that particular experiment.

4. On admission of the argon or helium to section A, the hot filament cathode IOG71 should indicate no change in electron emission (see appendix 8).

5. Similar deflections should result from use of either of the tungsten ribbons at the same temperature.

6. The amplitude of background "noise" should be small compared to the "real" deflection.

Some difficulties were experienced in satisfying criterion 4 for argon (when admitted from section B) so that satisfactory results were only obtained for the higher temperatures of tungsten ribbon.

8.2 The net force on the torsion balance

The rotation of the torsion balance and hence the net force on it B, was calculated from the average Photodyne pen recorder deflection for that experiment and the data for the sensitivity of the torsion balance and calibration of the optical amplifier given in section 6. For convenience of presentation and analysis the values of B were normalized to a gas pressure of 1 torr [1]. These results are presented for argon and helium as a function of tungsten surface temperature at figure 10. Since there could be no net force on the torsion balance under isothermal conditions the curves have been extrapolated to pass through the point T_s = 293 K, B =0.

The normalization was justified because the Photodyne deflection was found to be directly proportional to the gas pressure at a given tungsten temperature (see figure 11) and the calibration of the optical amplifier

---

(1) 1 torr is that gas pressure equivalent to 1.336×10^3 dynes cm^{-2}

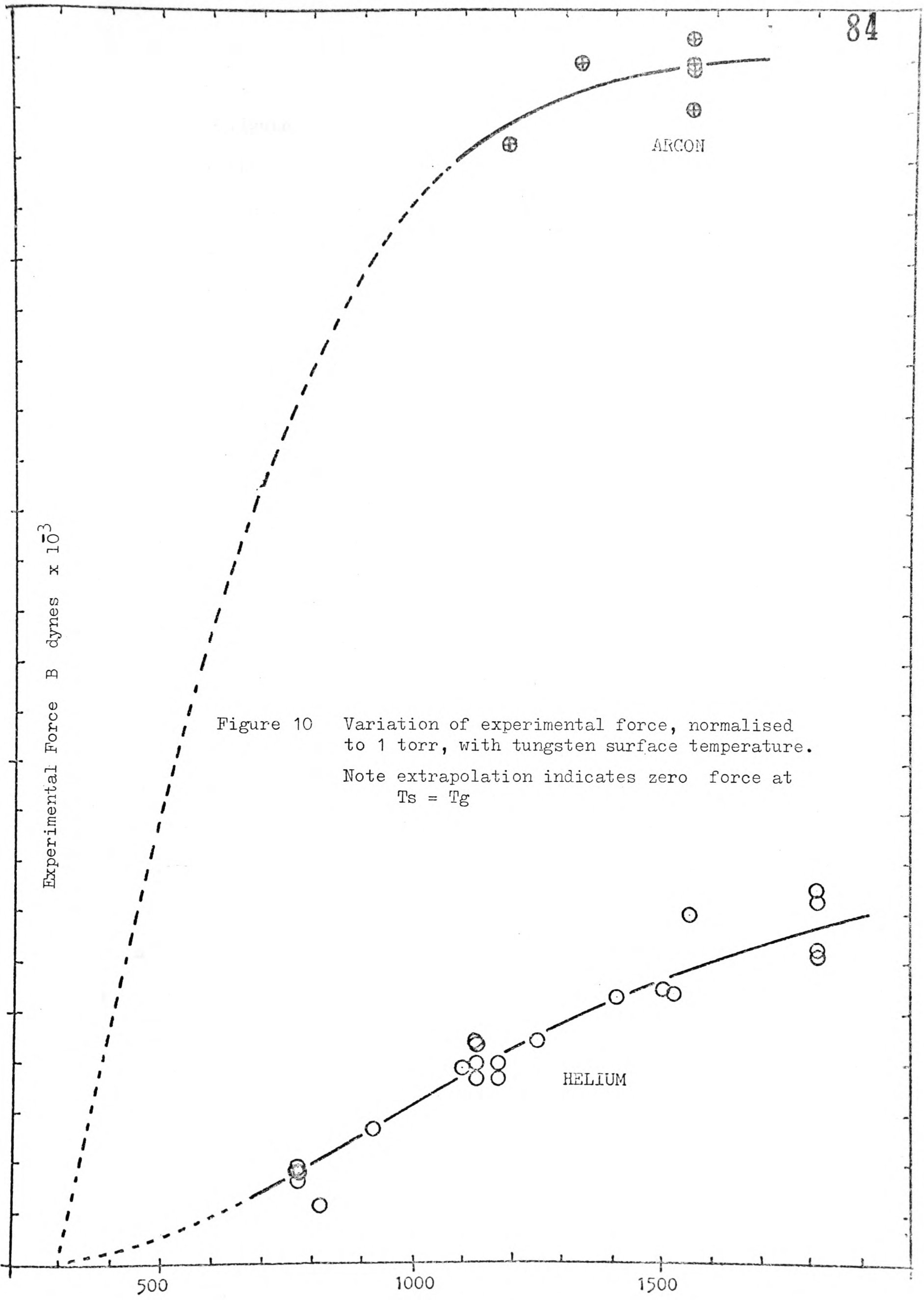


Figure 10 Variation of experimental force, normalised to 1 torr, with tungsten surface temperature.

Note extrapolation indicates zero force at Ts = Tg

was linear (see figure 9). Notice that the curve in figure 11 may be extrapolated to the origin. This reinforced data on the "no-gas" experiments and confirmed the estimations made that deflections of the torsion balance due to radiometer effect, sublimation of tungsten and radiation pressure were negligible. The actual pressures were about 0.1×10^{-3} torr for argon and ranged from 0.35×10^{-3} to 3×10^{-3} torr for helium. Hence the mean free path of the gas was always large compared with the distance between the tungsten ribbons and the torsion balance (<35 mm).

Figure 10a for the case of argon displays the effect on B of increasing the time interval between flashing the tungsten ribbon and the experiment. In comparison with the argon curve [1] in figure 10a, the value of the net force B decreased by about a factor 4 when the ribbon was kept at room temperature between observations for times up to 1020 seconds. For longer times, up to 3600 seconds, the signal recovered somewhat. The cause was believed to be changing coverage of the clean surface, of newly flashed tungsten, by readsorbed gas. The same procedure applied to helium did not show this effect up to the longest "cold time" interval tried (530 seconds). It is perhaps significant that in the helium experiment the liquid helium cooled cold finger continuously pumped all gases but helium.

8.3 Analysis of experimental data

8.3.1 Introduction

A knowledge of the force on the torsion balance due to gas atoms from the hot tungsten impinging on its surface (G, see later) does not of

---

(1) The usual procedure involved a holding time at the experimental temperature of about 60 seconds as measured from the 2500 K flash

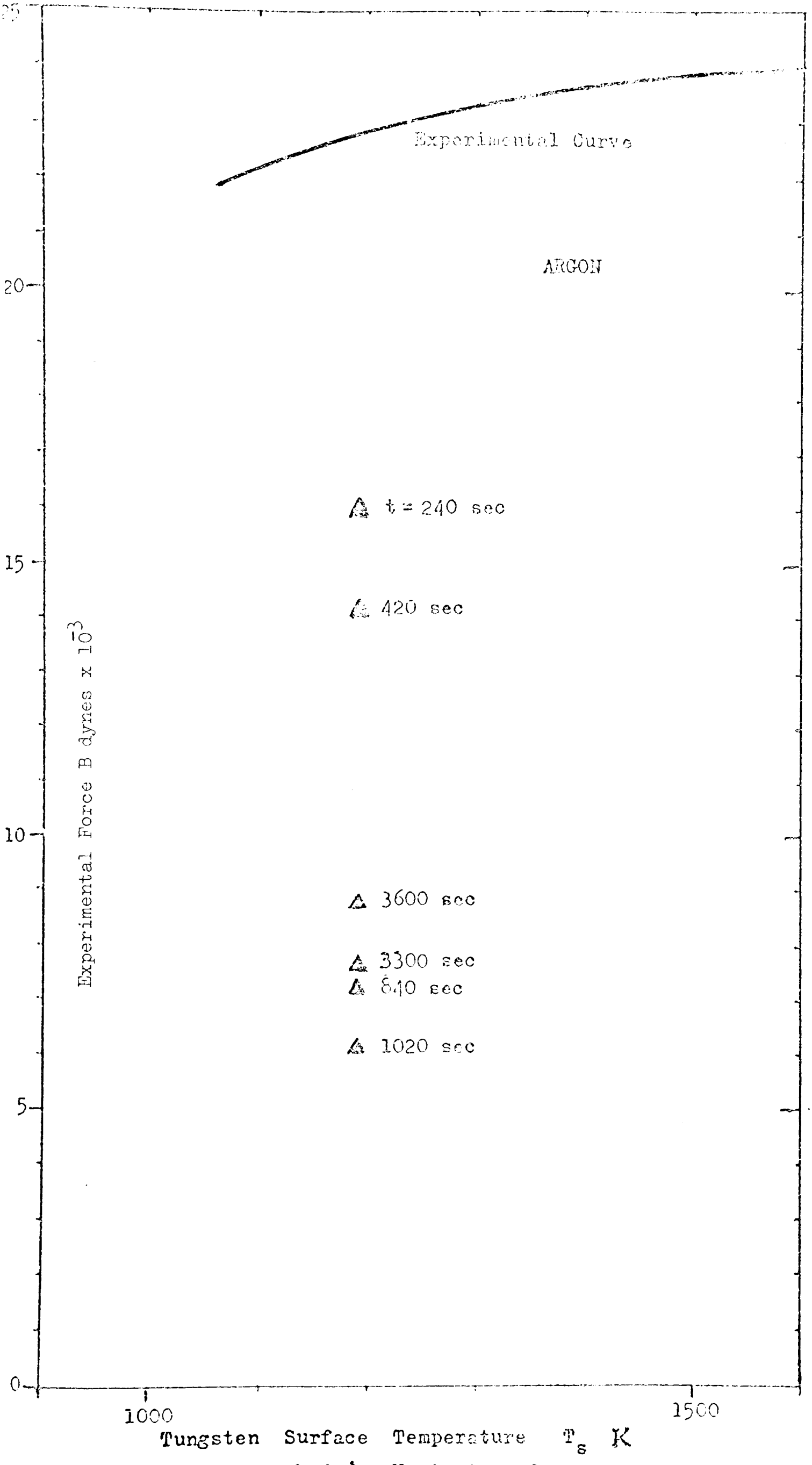


Figure 10a Points marked Δ : Variation of experimental force, normalised to 1 torr, with time after 2500 K flash

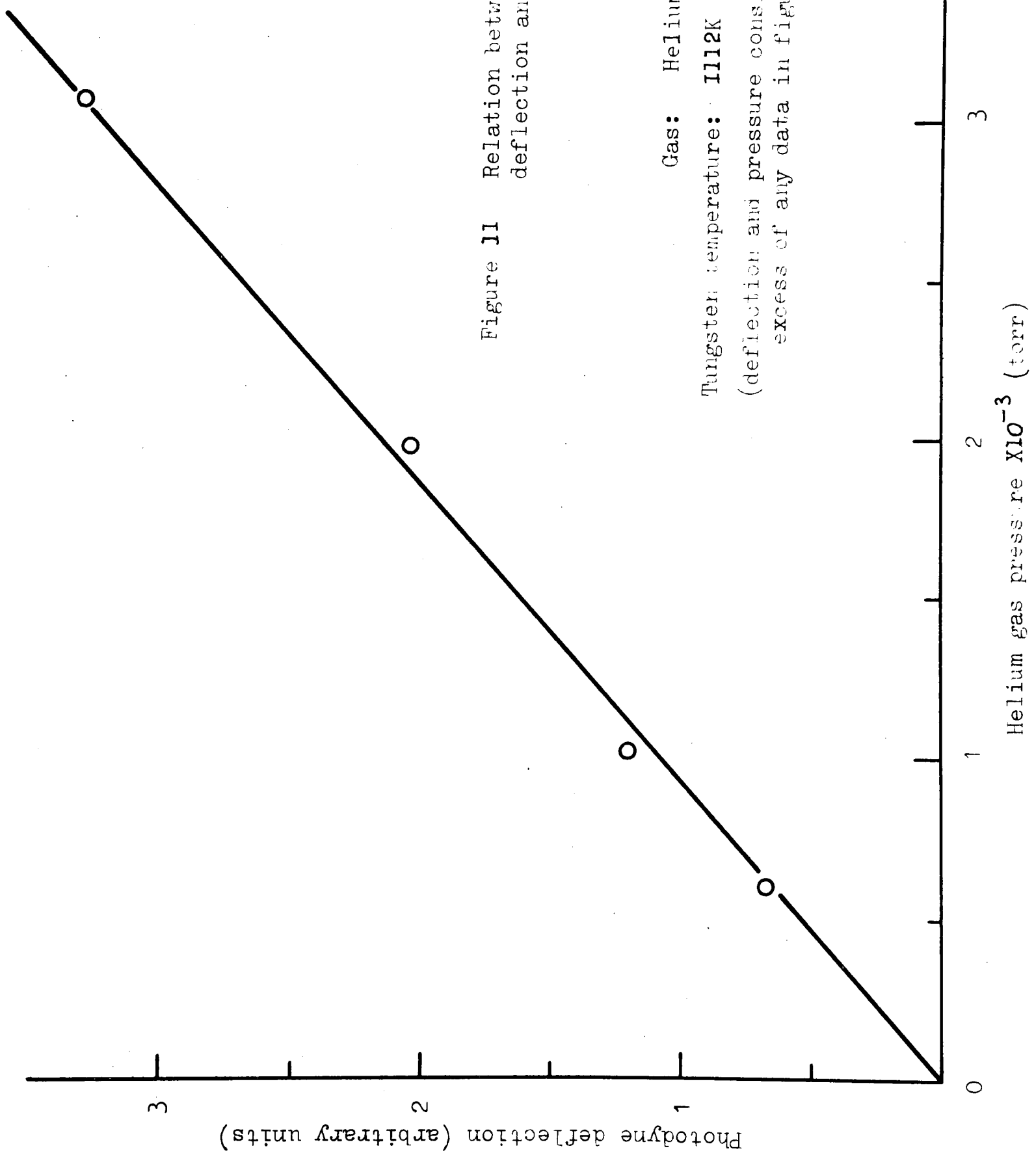


Figure 11 Relation between photodyne deflection and gas pressure

Gas: Helium

Tungsten temperature: 1112K

(deflection and pressure considerably in excess of any data in figure 10)

itself provide information about accommodation of the gas at the hot tungsten surface unless the number flux through the aperture system is known. This requires an hypothesis about the angular distribution of atoms remitted from hot tungsten. It is also necessary to make some assumptions about the behaviour of the gas at the torsion balance (1) and this is discussed in appendix 5.

Two hypotheses are used to interpret the experimental data.

The first hypothesis is that the gas leaves the hot tungsten as if it had come into thermal equilibrium with a notional surface at a temperature T'. The second hypothesis is that the gas is remitted with a particular non-isotropic temperature distribution. It is then possible in the case of each hypothesis to deduce a value for the accommodation coefficient of the gas at the hot tungsten surface.

8.3.2 Calculation of accommodation coefficients on the hypothesis that the gas is remitted from hot tungsten in thermal equilibrium with a surface at temperature T'.

The raw data are:- the net force B (figure 10), exerted on the balance arm, the tungsten temperature T_s, the temperature T_g and pressure P_o of the cold gas before impingement on the tungsten, and the geometry of the apparatus.

From these data is deduced the gross force G which would be exerted on the balance arm if the stream of hot atoms, remitted normal to the surface of the tungsten ribbon and traversing the aperture system, had

---

(1) This is not an inherent limitation of the method. It is technically possible, as W.N. Mair and B.W. Viney (1970) have shown, to construct of thin aluminium foil a 'crab pot' on the balance arm from which the remission would be cosine and the effective accommodation coefficient unity. Limitation of time prevented the author doing this.

T_s K	α_W^{He}	α_W^{Ar}
700	0.16	-
900	0.20	-
1100	0.22	3.5
1300	0.23	3.0
1500	0.23	2.6
1700	0.23	2.3
1900	0.22	-

Table 5. Values for thermal accommodation coefficient α_W^{He} of helium and α_W^{Ar} of argon incident at T_g = 293 K on hot clean tungsten at various temperatures T_s.

Hypothesis: cosine remission from the tungsten.

For details of assumption at torsion balance, see Appendix 5.

emerged into a vacuum in which the balance was situated, impinged on its arm and been adsorbed without recoil.

Values of G, and hence of the gas-tungsten accommodation coefficient α_W^g given in table 5 are obtained (see appendix 1 for analysis). These are based on the assumptions that the gas atoms are remitted from the hot tungsten surface in a cosine wise angular distribution (see Knudsen 1908 and 1909) discussed earlier in section 3.

The conditionsat the copper torsion balance are discussed in appendix 5 and it was on these assumptions that the table 5 results were calculated. However, values of α_W^g are obtained for the extreme conditions possible at the torsion balance. These are discussed in section 9.

8.3.3 Calculation of accommodation coefficients on the hypothesis that tangential momentum is conserved on remission of the gas from the hot tungsten.

Here the data are interpreted on the hypothesis that the tangential components of momentum of the impinging molecules are conserved on remission. This assumption was suggested for instance by Devonshire (1937) and later became a major assumption of the "cube" models which have had success when applied to scattering data (Yamamoto and Stickney 1970 and Trilling 1967).

The treatment of the experimental data is similar to that above. The main difference is that the translational energy of the remitted helium or argon can no longer be expressed in terms of a single "isotropic" temperature T'. Consequent upon adopting this hypothesis are two

T_s K	α_W^{He}	T_n K	$\tau = T_n/T_g$	ρ
700	0.023	312	1.07	1.08
900	0.026	324	1.11	1.13
1100	0.028	338	1.15	1.20
1300	0.028	350	1.19	1.25
1500	0.028	361	1.23	1.29
1700	0.027	368	1.26	1.33
1900	0.025	375	1.28	1.35

Table 6. Values for thermal accommodation coefficient α_W^{He} and other related parameters, of helium incident at T_g = 293 K on hot clean tungsten at various temperatures T_s.
Hypothesis: conservation of tangential momentum.
For details of assumptions at torsion balance, see Appendix 5.

T_s K	α_W^{Ar}	T_n K	$\tau = T_n/T_g$	ρ
1100	0.17	559	1.91	2.19
1300	0.14	571	1.95	2.24
1500	0.12	575	1.96	2.26
1700	0.10	577	1.97	2.27

Table 7. Values for thermal accommodation coefficient α_W^{Ar} and other related parameters, of argon incident at T_g = 293 K on hot clean tungsten at various temperatures T_s.
Hypothesis: conservation of tangential momentum.
For details of assumptions at torsion balance see Appendix 5.

"enhancement" ratios τ and ρ. τ gives the enhancement [1] number flux and ρ the enhancement [1] momentum flux for atoms remitted in a direction normal to the tungsten surface. The values of the gas-tungsten accommodation coefficient α_W^{He} and α_W^{Ar} together with appropriate values τ and ρ are given in tables 6 and 7 respectively. The conditions at the torsion balance are as discussed in appendix 5. However a set of values of α_W^{He} and α_W^{Ar} are obtained for a range of conditions at the torsion balance and these are also in appendix 5.

8.4 Accuracy of results

The anisotropic model for the temperature of atoms remitted from the hot tungsten may be oversimplified though it does yield (as any acceptable model must) values of α, derived from our data, which are of the same order as those found by other workers using the entirely different total heat loss methods.

However, the α values obtained may have significant systematic error introduced by limitations of the model that has been chosen. It would therefore be misleading to attempt to put error limits on the values of α given in tables 6 and 7.

An indication of the magnitude of the experimental error in B is given by the scatter in the normalized signal from the torsion balance displayed in Fig. 10. This figure includes all the readings, obtained after a satisfactory degree of cleanness of tungsten and of gases had been achieved.

---

(1) With respect to cosine remission, see appendix 1

Chapter 9

Discussion of Results and Development of Apparatus

9.1 Introduction

The net experimental force due to gas molecules remitted from the hot tungsten onto the torsion balance was obtained by calculation from the deflection of the pen recorder, using the experimental data for the sensitivity of the torsion balance and the calibration of the optical amplifier. This force is shown as a function of tungsten temperature in figure 10 for both helium and argon.

Assumptions were made about the interaction of the gas and the torsion balance surface. Thus, graphical solutions were obtained for the value of thermal accommodation coefficient based on two separate hypotheses about the gas-tungsten interaction. Details of the analysis appear in appendix 1 and the results are summarized in tables 5 , 6 and 7.

Information about the sensitivity of these results to the assumptions made about the gas at the torsion balance is given in section 8 for the first hypothesis and appendix 5 for the second hypothesis.

9.2 Results obtained using the first hypothesis

This hypothesis is hereafter referred to as "cosine remission". The graphical solutions to the analysis of the results are shown in tables 5 and 8 .

The values of α_W^{He} are all improbably large being about one order larger

than those of Watt, Moreton and Carpenter (1974) who worked over about the same temperature range (1073 to 1875 K) using the total-heat-loss method. They are also unreasonable as an extrapolation of those results due to Wachman (1966), Thomas and Schofield (1955) and Kouptsidis and Menzel (1970). For details of the values obtained by these workers (see section 4).

The values of α_W^{Ar} are impossibly high, being in excess of unity [1].

Thus it is evident that the experimental data cannot be reconciled with the hypothesis of cosine remission from the hot tungsten, characterised by a single temperature T' which is independent of direction. This is a major conclusion of this work and depends only on the assumption (see Appendix 5) made about the remission [2] from the copper torsion balance. This conclusion however would still be valid even if the values of α_{Cu}^{g} adopted in appendix 5 were seriously in error. To confirm this, values of α_W^g were evaluated on the two possible extreme assumptions about the copper torsion balance, $\alpha_{Cu}^{g} = 0$ with specular remission and $\alpha_{Cu}^{g'} = 1$ with cosine remission. The resulting values of α_W^g remain improbably high, see table 8.

assumption about copper torsion balance	α_W^{He}	α_W^{Ar}
$\alpha_{Cu}^{g} = 0$, specular remission	0.06	0.79
$\alpha_{Cu}^{g} = 1$, cosine remission	0.36	2.6

Table 8. Values of accommodation coefficient α_W^g at $T_s = 1500$ K for extreme assumptions about copper torsion balance. Cosine remission hypothesis.

(2) cosine remission and $\alpha_{Cu}^{He} = 0.4$ and $\alpha_{Cu}^{Ar} = 1.0$

(1) Goodman (1974) discusses the upper limiting value for α (see pp 265 and 362)

Thus the supposition that the remission from hot clean tungsten is cosine and isotropic in temperature is not supported by the results of this work and would appear to be incorrect.

Since the work and apparatus described in this thesis is a direct development of the method used by Carpenter et al. (1963a), it initially seems surprising that the results for thermal accommodation coefficient obtained here should be significantly larger than those from the original work. These were based on the same assumption of cosine remission of gas atoms from the hot tungsten surface and led to reasonable preliminary values. It was admitted that the original work was not especially clean, except possibly at the highest tungsten temperatures, but this fact would tend to increase the values of accommodation coefficient since there was some evidence that the likely surface contaminant was oxygen with its relatively low atomic mass. However, whilst the principle of the experimental method was the same the geometry of the hot tungsten surface with respect to the torsion balance was significantly different in the two cases.

In the work described here the gas atoms originating from the hot tungsten, that were incident on the torsion balance, were remitted from a plane surface of the tungsten ribbon and in a direction essentially perpendicular to its surface as defined by the narrow aperture system. In the original work[1] the tungsten surface was that of a fine wire filament (50μm diameter). The aperture system was large, so that gas atoms from all possible remission angles, from tangential to normal to the tungsten surface, might reach the torsion balance. If, as it is believed to be reasonable, the gas atoms were in fact remitted with their tangential momentum unchanged, this would satisfactorily explain

---

(1) Full details of this are unfortunately not available in the published literature but are given in Carpenter et al. (1963b)

the relatively low values of thermal accommodation coefficient obtained in the original work at the highest temperature.

The aperture system of the original apparatus was not of a simple geometry so that values of thermal accommodation coefficient, incorporating the conservation of tangential momentum assumption, are not readily calculable.

9.3 Results obtained using the second hypothesis

This hypothesis is hereafter referred to as "tangential conservation". The graphical solutions to the analysis, incorporating the suggestion made by Goodman (1973), are shown in tables 6 and 7. These values for accommodation coefficient are of the same order of magnitude as those obtained by other workers (see section 4). However, the author is only aware of two other sets of results with the same gas-solid combination at the high solid temperatures of this work. These are due to Carpenter, Humphries and Mair, (1963b) using an early form of the torsion balance apparatus and Watt, Moreton and Carpenter (1974) using a conventional heat loss method in combination with a very sensitive electrical bridge. The tungsten surface in the work of Carpenter et al. was probably significantly covered with adsorbed gas except at the highest temperature of 2800 K. The work of Watt et al. (for a similar tungsten temperature range to this work and where considerable precautions were taken to maintain cleanness of gas and solid) gives values of accommodation coefficient in close agreement with other reliable work at lower tungsten temperatures and in reasonable agreement with the results of this work. Although there is an increasing amount of work using molecular beams (see e.g. Bernasek and Somorjai 1975) to investigate gas solid interactions at high surface temperatures, there are to the authors knowledge no results which may be expressed in the form of values of accommodation coefficient. The majority of this

work is unfortunately restricted to observations of remissions in directions in the plane of the incident beam. In those cases where the remission has been observed in three dimensional space, considerable practical restrictions have limited the observable directions. Thus, the necessary molecular beam data from which values of thermal accommodation coefficient might be calculated is not available.

The application of the hypothesis of "tangential conservation" to the interpretation of the experimental data obtained here was suggested by a combination of contributing factors. The "consine remission" hypothesis was clearly incorrect since it led to values of accommodation coefficient which were an order of magnitude too large. These results implied some enhancement of remitted momentum flux in the direction normal to the hot tungsten. Evidence in support of this was obtained when these results were compared with the preliminary results for remission from a wire of circular cross-section as discussed above. Devonshire (1937) was probably the first to suggest that conservation of tangential momentum was appropriate to a gas interacting with a solid surface. Tangential conservation is a major assumption of the cube theories and more recently classical calculations using these theories have been successfully applied to experimental scattering data (Yamamoto and Stickney 1970 and Trilling 1967). Goodman (1971) discusses the effect of the values of dimensionless parameters relevant to the scattering of gas atoms by solid surfaces and the applicability of classical and quantum theoretical treatments to the variety of practical situations. In general it would seem that classical theories produce a good fit with experimental data even into the regions where quantum theories might be expected to be more appropriate. This is not yet understood. It would be reasonable to expect that the tangential conservation hypothesis would apply where the gas atoms impinge on an effectively smooth solid surface. This would tend to be the

case for a relatively large interaction radius which would result from small values for the incident energy of the gas atoms and the adsorption energy of gas on the surface. In the gas-solid systems which are the subject of this work, these values[1] are especially low (gas energy corresponds to a temperature of 293 K and see section 3). In these circumstances the cubes models, and thus the hypothesis of tangential conservation, should work well.

Whilst the values of thermal accommodation coefficient obtained from this data, using the above hypothesis, are consistent with those of other workers, some limited calculations were made to discover the sensitivity of the accommodation coefficient to varying degrees of tangential accommodation[2] α_t. Details of the analysis are given in appendix 1. For helium on a tungsten surface at 1500 K, $\alpha_w^{He} = 0.028$ for $\alpha_t = 0.0$. If the value of α_w^{He} was required to be 0.018 (i.e. that obtained by Watt et al. (1974) at the same tungsten temperature, using the total heat loss method) the value deduced for α_t would be -0.01. This negative quantity is a mathematical result and unlikely to represent a realistic value but does indicate the relative size of α_t. For argon on a tungsten surface at 1500 K $\alpha_w^{Ar} = 0.117$, $\alpha_t = 0.0$. If the value of α_w^{Ar} was required to be 0.24 (Watt et al. 1974) $\alpha_t = 0.1$. Thus, even if the Watt et al. results are accepted as definitive, the tangential conservation hypothesis is still a reasonable approximation. More detailed results are given below.

---

(1) Data for the inert gases and tungsten are presented in Trilling (1970) and Goodman and Wachman (1967)

(2) A partial accommodation coefficient defined as $\alpha_t = \frac{T_t - T_g}{T_s - T_g}$

$\tau = \frac{T_n}{T_t}$	α_w^{He}	α_t
1.00	0.23	0.23
1.22	0.033	0.006
1.23	0.028	0.000
1.24	0.022	-0.006
1.25	0.017	-0.012

$\tau = \frac{T_n}{T_t}$	α_w^{Ar}	α_t
1.00	2.59	2.59
1.80	0.26	0.12
1.90	0.18	0.05
2.00	0.10	-0.01
2.10	0.05	-0.05

Relationship between τ, α_w^g and α_t for T_s = 1500 K and the experimental momentum flux

9.4 Dependence of results on conditions at torsion balance

Whilst it was necessary here to make assumptions about the accommodation of the gas at the torsion balance it is important to note that the results obtained are very insensitive to extreme changes of accommodation co-

efficient at the balance as shown by table 10 in appendix 5. Also, it is certainly possible to provide the torsion balance with a device (1) that would ensure that gas incident on it was remitted cosine wise and at the balance temperature. The sensitivity of the balance would not be altered but its period of oscillation would be increased. This would not be a disadvantage providing the period remained short compared to the time taken to observe an experimental result (typically between 60 and 200 seconds). In addition to this it has already been suggested by Carpenter et al (1963a) that the tungsten ribbon might be replaced by a small furnace from which gas molecules would be emitted in a cosine angular distribution at a known temperature.

9.5 Development of the apparatus and experimental method

9.5.1 Investigation of remission from hot solid in directions other than normal

The results of this work are limited in that only the normally remitted molecules from the tungsten were investigated, hence the requirement for a satisfactory (second) hypothesis about the angular remission from the hot tungsten .It be would be possible to investigate other remission directions by rotating the plane of the hot solid with respect to the axis of the aperture system. Indeed in this work it had been the intention, but lack of time prevented this. The tungsten ribbon used was sufficiently wide to allow a rotation of up to $\pm 45^{o}$ whilst still "filling" the $\pm 2\frac{1}{2}^{o}$ acceptance angle of the aperture system.

A preliminary rotating ribbon model was constructed and a design for flexible electrical heating current leads considered. The problems associated with rotating bearings in ultra high vacuum has been investi-

---

(1) Consisting of a "crab pot" of thin corrugated aluminium - Alfol

gated (Osborn 1964) and a simple design would be satisfactory.

9.5.2 Measurement of remitted number flux

This experimental method results in a measurement of the momentum flux remitted from a surface in a particular direction. More detailed information, about the number flux in a particular direction, could be obtained by introducing an ionization detector similar to that used by Yamamoto and Stickney (1970). Concurrent experiments using both sides of the tungsten ribbon could provide torsion balance and number flux data under the same conditions of remission from a hot solid impinged upon by a (near) isothermal gas.

Chapter 10

Conclusions.

The apparatus described here is a development of that used by Carpenter, Humphries and Mair (1963a). The experimental details have been fully described and evidence given for the results of considerable efforts to conduct the experiments under clean conditions.

If helium or argon atoms at room temperatures impinge in a cosine manner from an isothermal source on a clean hot tungsten ribbon (of which the (100) planes are mainly parallel to the surface) the momentum flux of atoms remitted in a direction normal to the ribbon surface, is significantly greater than can be plausibly explained if the remission, like the impingement, is cosine-wise.

If it is assumed - one of the assumptions of cube theories - that only the normal component of velocity is increased on remission (i.e. that the tangential component of the impingement velocity is conserved) a greater-than-cosine number flux in the normal direction is obtained.

The data, obtained by experimental measurement of the momentum of atoms remitted from the hot tungsten in a direction normal to the surface, supplemented by the hypothesis of tangential conservation, allow the calculations of the accommodation coefficient α. This α is defined in the same way as in the total heat loss method and the results obtained here are of the same order as those clean and reliable results using that method.

The method of determining α described here becomes more sensitive the

higher the temperature of the hot solid. This contrasts with methods which become increasingly insensitive at high temperature as radiation flux becomes dominant over gas-born heat flux.

The potentialities of the present method include investigation of the angular distribution of the translational energy of gas atoms remitted from the hot solid which may be metal, alloy or non-metal and for polyatomic gases on metals, the deduction of the internal contribution to the total energy, by comparing the total heat loss of conventional methods with the translational loss to which alone the method described here is sensitive.

Appendix 1

Details of Analytical Treatment of Experimental Data

This appendix is divided into two parts (a) and (b) corresponding to the sections 8.3.2 and 8.3.3.

Part (a)

Calculation of accommodation coefficients on the hypothesis that the gas is remitted from hot tungsten in thermal equilibrium with a surface at temperature T'.

The net experimental force on the torsion balance is given by B where:-

$$B = G + G' - (F + F') \qquad (1)$$

G = Force from gas atoms remitted by hot tungsten, traversed aperture system, recoilless impingement on torsion balance. (Numerically equal to momentum flux of atoms).

G' = Recoil force on torsion balance of atoms causing G.

F = Value of G when tungsten is at temperature of gas T_g

F' = Recoil force analagous to G'.

The momentum flux of atoms at T_g may be calculated from the analogy between the rectilinear propagation of photons and gas molecules. Assuming the remission of atoms from the cold tungsten is cosine-wise a formula due to Milne (1929), for the probability of transmission of photons through two separated, parallel and co-axial apertures gives

$$F = \frac{3\pi}{4} P_o \frac{a^4}{l^2} \qquad (2)$$

when applied to the aperture geometry for which $\frac{a}{l} >> 1$

where a = radius of the apertures

l = axial separation of apertures

P_o = gas pressure

Since atoms at T_g, striking a surface at T_g must be remitted cosine-wise in direction, and unchanged in temperature from appendix 2

$$F' = \frac{2}{3}\frac{3\pi}{4} P_o \frac{a^4}{l^2} \tag{3}$$

The value of G + G' is now directly calculable from equation (1) since B is an experimental quantity and F and F' are given by equations (2) and (3) above, P_o, a and l being known. It is possible to express G' in terms of G by defining the conditions at the torsion balance surface. Numerical values from the literature may be adopted for the thermal accommodation coefficients of He and Ar on the copper torsion balance arm (see appendix 5) and cosine remission assumed from the copper. Then, at the copper surface

$$\alpha^g_{Cu} = \frac{T' - T^*}{T' - T_g} \tag{4}$$

and

$$\frac{G'}{G} = \frac{2}{3}\left(\frac{T^*}{T'}\right)^{\frac{1}{2}} \tag{5}$$

or

$$G = (G + G') \frac{(T')^{\frac{1}{2}}}{(T')^{\frac{1}{2}} + \frac{2}{3}(T^*)^{\frac{1}{2}}} \tag{6}$$

Where α^g_{Cu} is the thermal accommodation coefficient of helium or argon on copper, T* is the effective temperature of atoms remitted from the torsion balance arm and it is assumed that the speeds of the hot atoms are appropriate to gas temperature T'.

Thus with (1)
$$G = (B + F + F') \frac{(T')^{\frac{1}{2}}}{(T')^{\frac{1}{2}} + \frac{2}{3}(T^*)^{\frac{1}{2}}} \qquad (7)$$

By virtue of equation (4) this expression for G contains only one unknown namely T'.

Now if it is assumed that the angular remission from the hot tungsten is cosine, i.e. the same number flux of atoms traversing the aperture system as when $T_s = T_g$

then
$$G = \left(\frac{T'}{T_g}\right)^{\frac{1}{2}} F \qquad (8)$$

the value of F being calculable from (2). If it is further assumed that the effective temperature (T') of the atoms which traverse the aperture system is the same as the effective temperature of atoms remitted from the hot tungsten in directions other than normal (i.e. that the temperature is "isotropic", the mean velocity components in the normal and tangential directions being equal)

then
$$\alpha_W^g = \frac{T' - T_g}{T_s - T_g} \qquad (9)$$

so that T' may be expressed in terms of α_W^g (whose value we wish to deduce) and the known temperatures T_g and T_s. Hence both in equations (7) and (8) T' can be expressed in terms of a single unknown α_W^g.

For cosine remission from torsion balance equation (7) becomes:

$$G = (B+F+F') \frac{\left[1 + \alpha_W^g\left(\frac{T_s}{T_g} - 1\right)\right]^{\frac{1}{2}}}{\left[1+\alpha_W^g\left(\frac{T_s}{T_g} - 1\right)\right]^{\frac{1}{2}} + \frac{2}{3}\left\{\left[1+\alpha_W^g\left(\frac{T_s}{T_g} - 1\right)\right](1-\alpha_{Cu}^g) + \alpha_{Cu}^g\right\}^{\frac{1}{2}}} \qquad (10)$$

and for specular remission from the torsion balance equation (7) becomes

$$G = (B+F+F') \frac{\left[1 + \alpha_W^g \left(\frac{T_s}{T_g} - 1\right)\right]^{\frac{1}{2}}}{\left[1+\alpha_W^g\left(\frac{T_s}{T_g} - 1\right)\right]^{\frac{1}{2}} + \left\{\left[1+\alpha_W^g\left(\frac{T_s}{T_g} - 1\right)\right] (1-\alpha_{Cu}^g) + \alpha_{Cu}^g\right\}^{\frac{1}{2}}} \qquad (11)$$

where $(F + F') = \frac{5\pi}{4} P_o \frac{a^4}{l^2}$

Equation (8) becomes:

$$G = \frac{3}{4} P_o \pi \frac{a^4}{l^2} \left[1 + \alpha_W^g \left(\frac{T_s}{T_g} - 1\right)\right]^{\frac{1}{2}} \qquad (12)$$

Equating (10) and (12) or (11) and (12) a unique expression for α_W^g is obtained (for a given assumption about α_{Cu}^g and the angular remission from the torsion balance).

In practice this is most conveniently done graphically. Values of G for a range of α_W^g are plotted and a value of α_W^g for a given T_s is obtained. These graphs appear at figure 12 for helium and figure 13 for argon and the results are presented in table 5 for the most likely conditions at the torsion balance. Values of α_W^g for alternative conditions at the torsion balance are obtained from figure 12 for helium and figure 13 for argon and the results are discussed in section 9.

For the conditions of the experiment, deflections normalized to 1 torr gas pressure, F becomes 9.88×10^{-3} dynes $torr^{-1}$ and (F + F') becomes 16.47 dynes $torr^{-1}$.

Figure 12
Helium - cosine remission

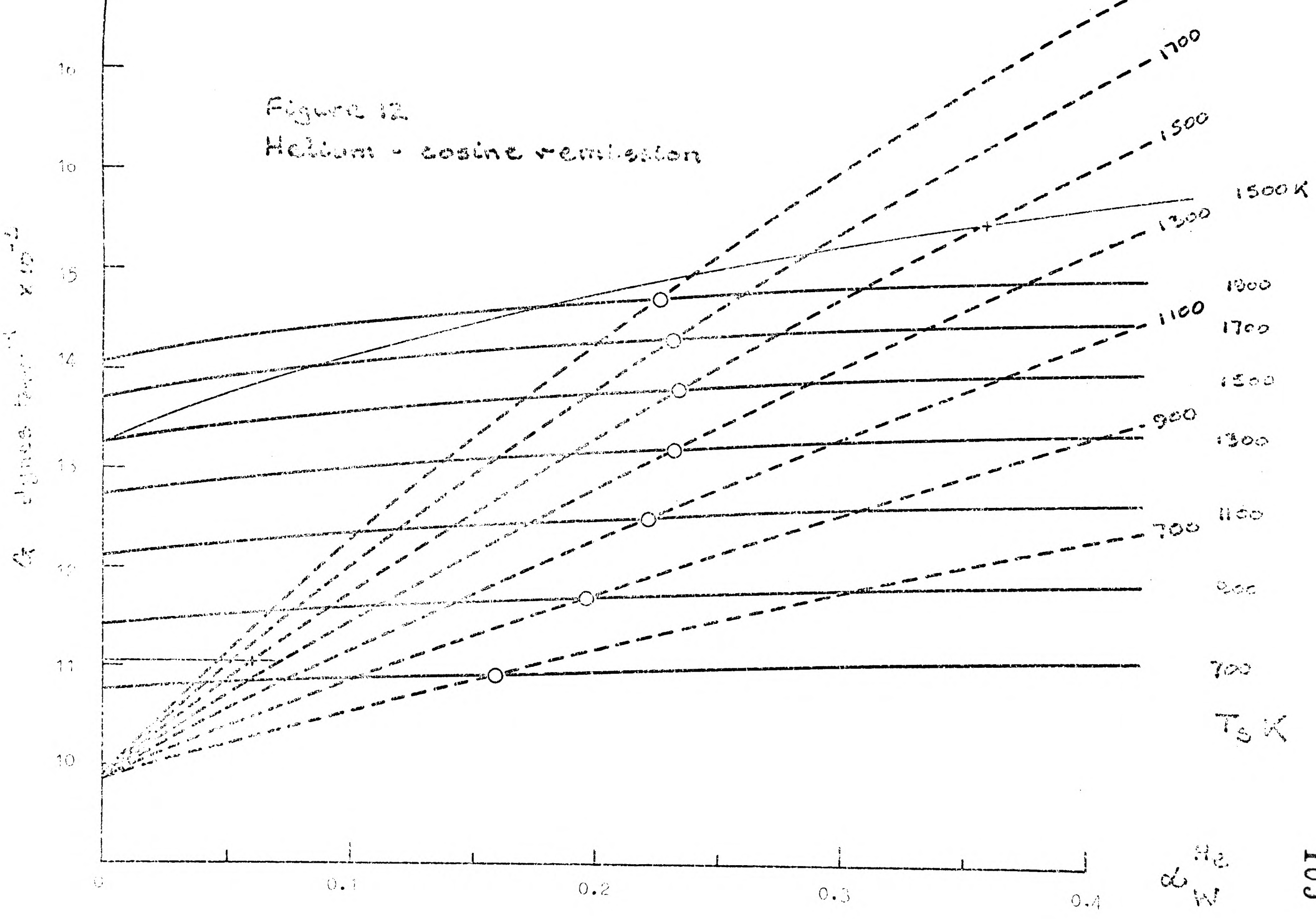
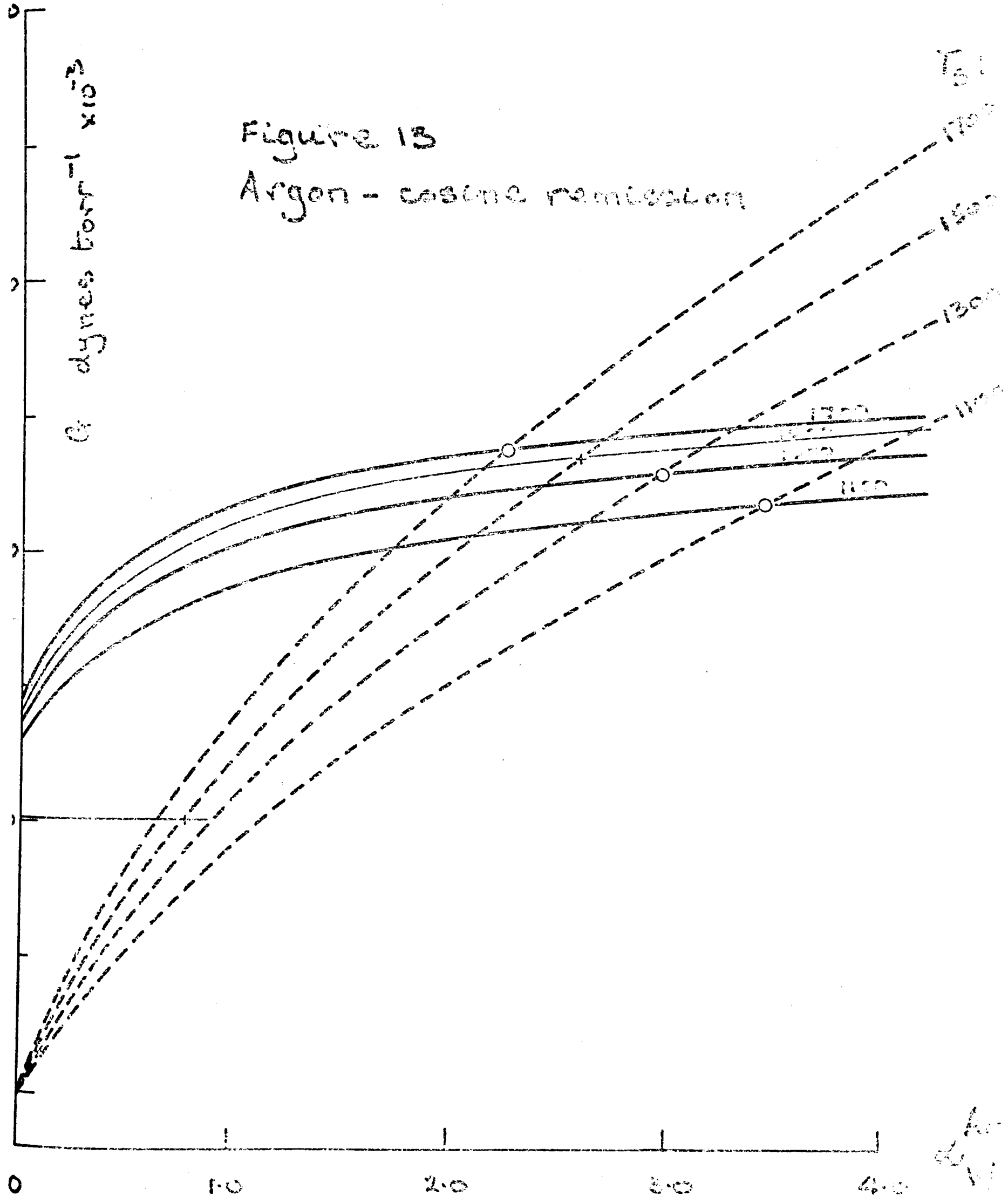


Figure 13
Argon - cosine remission



Part (b)

Calculation of accommodation coefficients on the hypothesis that tangential momentum is conserved on remission of the gas from the hot tungsten.

The treatment of the experimental data is similar to that above. The main difference is that the translational energy of the remitted helium and argon can no longer be expressed in terms of a single "isotropic" temperature T'. The mean values of component velocities parallel to the ribbon surface (say $\bar{u}$ and $\bar{v}$) are now appropriate to T_g, while the mean values of those normal to the surface (say $\bar{w}$) are appropriate to a higher temperature T_n.

This hypothesis biases the speed distribution and thus the angular distribution in the z direction. It is a special case of a more general model proposed by Goodman (1972a) for the desorption of molecules from a surface in which the desorbed molecules have normal velocity components distributed according to a Maxwellian temperature T_n and tangential components according to T_t. But choosing conservation of tangential momentum we write:

$$T_t = T_g$$

and for T' we substitute T_n

Equation (4) becomes:

$$\alpha^{g}_{Cu} = \frac{T_n - T^*}{T_n - T_g} \qquad (13)$$

and Equation (7) becomes:

$$G = (B + F + F') \frac{(T_n)^{\frac{1}{2}}}{(T_n)^{\frac{1}{2}} + \frac{2}{3}(T^*)^{\frac{1}{2}}} \qquad (14)$$

In order that α_W^g shall retain its usual meaning (i.e. ratio of actual heat flux to the heat flux if the remitted gas had attained complete thermal equilibrium with the heated solid) and therefore agree with the values obtained by total heat loss methods, it must be written as

$$\alpha_W^g = \frac{\left[kT_n + 2(\tfrac{1}{2}kT_g)\right] - 2kT_g}{2kT_s - 2kT_g}$$

or

$$\alpha_W^g = \tfrac{1}{2}\,\frac{T_n - T_g}{T_s - T_g} \qquad (15)$$

This expression replaces equation (9) of the preceding part (a) α_W^g is defined (as α_W^g of equation (9) is defined) in terms of the <u>total</u> heat flux from the hot tungsten. It is a definite experimental quantity whose value is independent of the particular hypothesis invoked to interpret it. The hypothesis of tangential conservation excludes $\overline{u^2}$ and $\overline{v^2}$ from contribution to the heat loss. Hence a compensating large value of $\overline{w^2}$, and consequently of T_n, result. Thus $(T_n - T_g)$ for the anisotropic temperature hypothesis is twice $(T' - T_g)$ for the isotropic temperature hypothesis.

The other modification of the equations of the previous part (a) is that equation (8) is no longer valid. As angular remission from the hot tungsten is no longer cosine, but biased in the z direction, the number flux of atoms through the aperture is now greater when the tungsten is hot than when it is at T_g and so the momentum flux G can no longer be obtained merely by multiplying F by the ratio of the mean speeds appropriate to T_n and T_g.

A treatment[1] by Goodman (1973) leads to a factor ρ for the enhancement of the momentum flux remitted normal to the surface of the hot tungsten

(1) See page 115(a).

viz.

$$\rho = \frac{\left[1 + 2\alpha_w^g\left(\frac{T_s}{T_g} - 1\right)\right]^{\frac{3}{2}}}{\left[1 + \alpha_w^g\left(\frac{T_s}{T_g} - 1\right)\right]^{\frac{1}{2}}} \qquad (16)$$

where α_W^g has the value determined by experiment, and ρ is defined as the ratio of G, assuming conservation of tangential momentum, to its value if both normal and tangential momentum were augmented on impact with hot tungsten.

Thus equation (8) becomes

$$G = \rho\ F\left(\frac{T_n}{T_g}\right)^{\frac{1}{2}} \qquad (17)$$

By a procedure analogous to that described for the cosine remission hypothesis in part (a) the two equations for G i.e. (14) and (17) can both be expressed in terms of known quantities and the unknown α_W^g. Hence the value of α_W^g may be deduced.

For cosine remission from the torsion balance equation (14) becomes:

$$G = (B+F+F')\ \frac{\left[1 + 2\alpha_w^g\left(\frac{T_s}{T_g} - 1\right)\right]^{\frac{1}{2}}}{\left[1+2\alpha_w^g\left(\frac{T_s}{T_g} - 1\right)\right]^{\frac{1}{2}} + \frac{2}{3}\left\{\left[1+2\alpha_w^g\left(\frac{T_s}{T_g} - 1\right)\right](1-\alpha_{Cu}^g)+\alpha_{Cu}^g\right\}^{\frac{1}{2}}} \qquad (18)$$

and for specular remission from the torsion balance equation (7) becomes

$$G = (B+F+F')\ \frac{\left[1 + 2\alpha_w^g\left(\frac{T_s}{T_g} - 1\right)\right]^{\frac{1}{2}}}{\left[1+2\alpha_w^g\left(\frac{T_s}{T_g} - 1\right)\right]^{\frac{1}{2}} + \left\{\left[1+2\alpha_w^g\left(\frac{T_s}{T_g} - 1\right)\right](1-\alpha_{Cu}^g)+\alpha_{Cu}^g\right\}^{\frac{1}{2}}} \qquad (19)$$

Equation (17) becomes:

$$G = \frac{3}{4} P_o \pi \frac{a^4}{l^2} \left[1 + 2\alpha_W^g \left(\frac{T_s}{T_g} - 1\right)\right]^{\frac{3}{2}} \qquad (20)$$

Equating (18) and (20) or (19) and (20) a unique expression for α_W^g is obtained (for a given assumption about α_{Cu}^g and the angular remission from the torsion balance).

This is done graphically. The graphs appear at figures 14 and 15 for helium and argon respectively and the results are presented in tables 6 and 7 for helium and argon respectively for the most likely conditions at the torsion balance. Values of α_W^g for alternative conditions at the torsion balance are obtained from figures 16 and 17 for helium and argon and the results presented in table 10 of appendix 5.

Calculation of T_n and of the number flux of remitted atoms

In Goodman's model (1972a) of desorption from a surface described above it is shown that the ratio (τ) of the number flux in the normal direction corresponding for $T_n \neq T_t$ to the number flux for $T_n = T_t$ is given by

$$\tau = \frac{T_n}{T_t} \qquad (21)$$

which in the case of this hypothesis of conservation of tangential momentum becomes

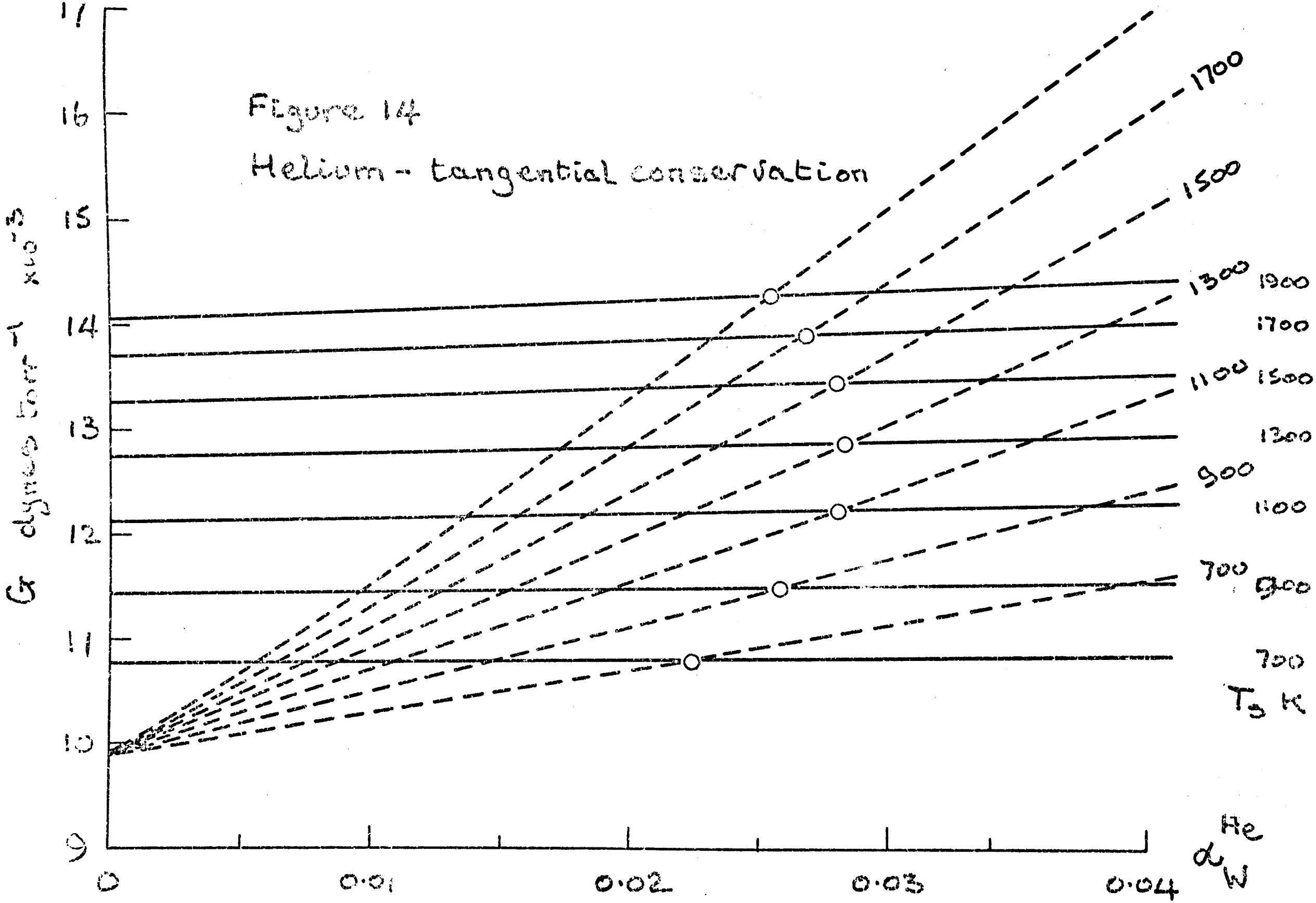
$$\tau = \frac{T_n}{T_g} \qquad (22)$$

Where T_n is related to α_W^g by equation (15).

In tables 6 and 7 (section 8) T_n has been calculated from α_W^g and hence τ deduced from (22).

Figure 14

Helium - tangential conservation



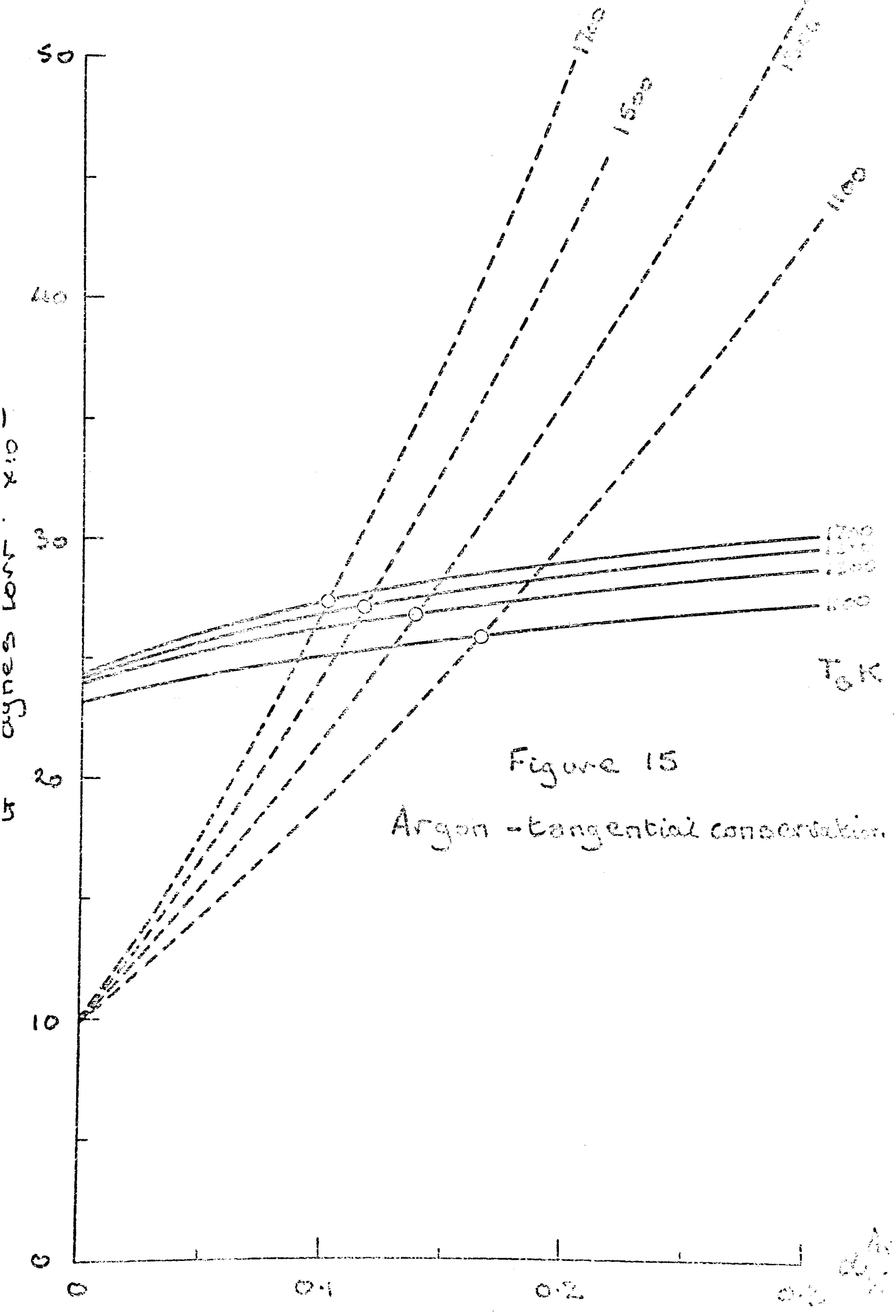
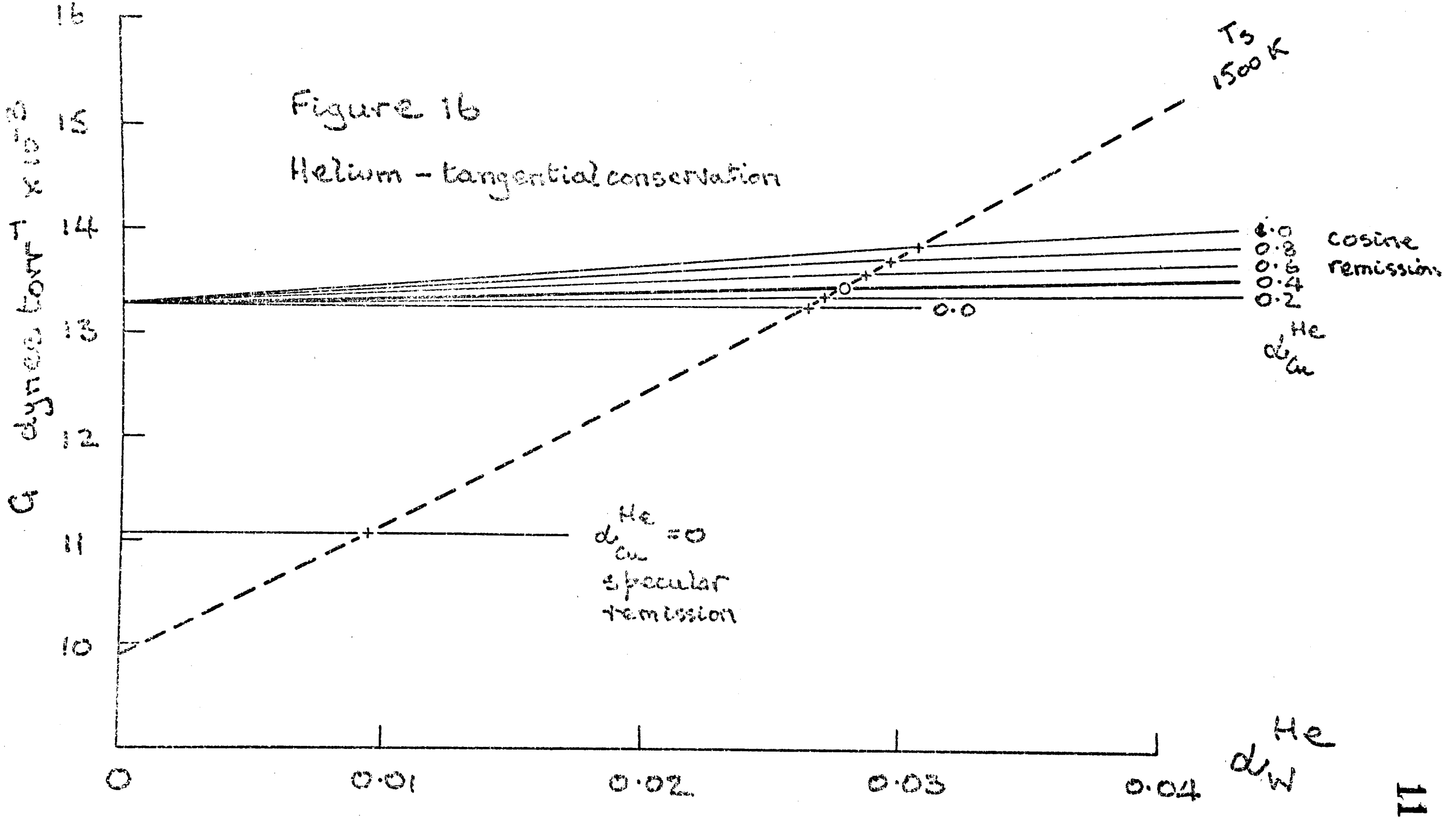


Figure 15

Argon - tangential conservation

Figure 16

Helium - tangential conservation



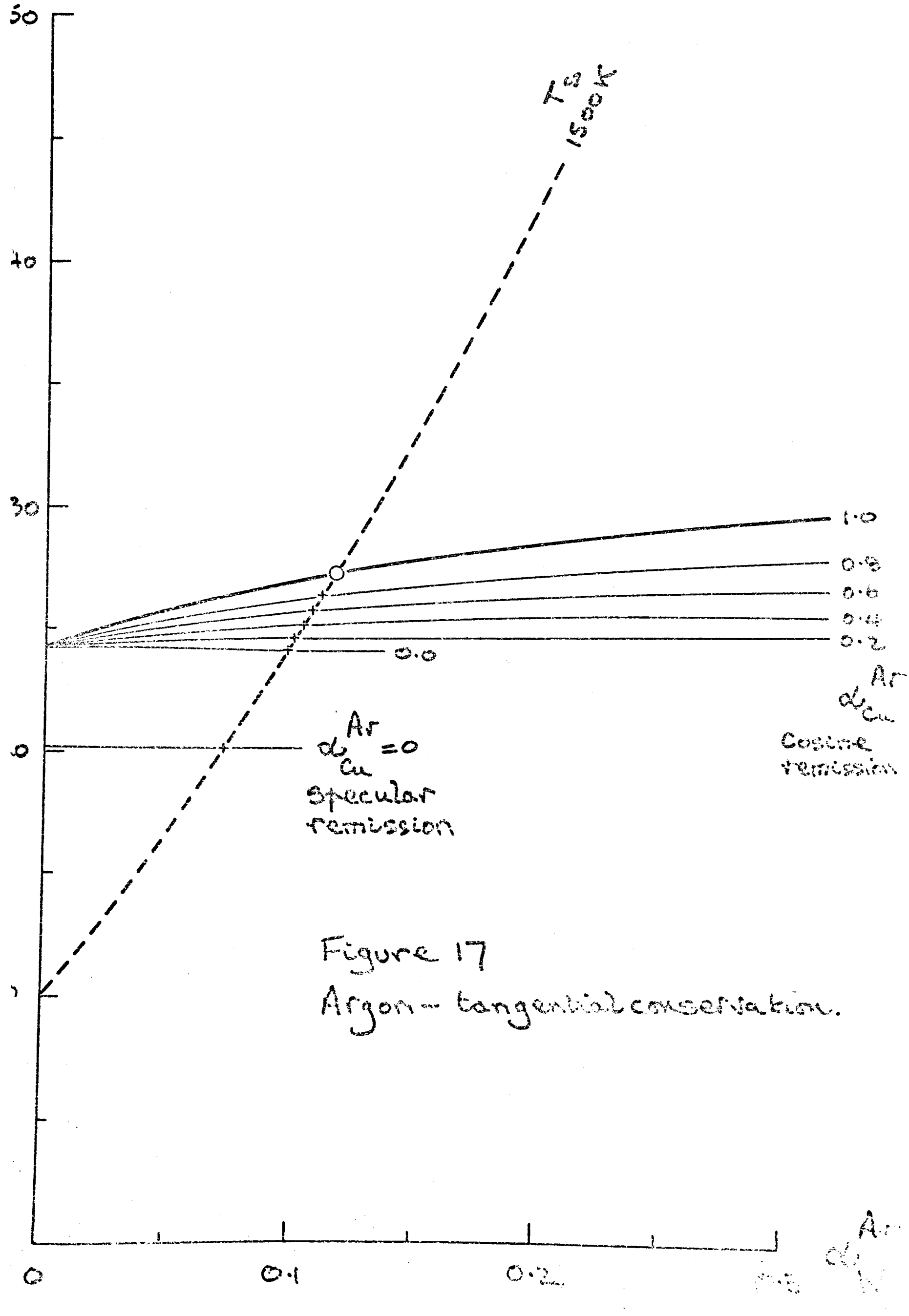


Figure 17
Argon -- tangential conservation.

Both τ and ρ are "enhancement" ratios, consequent upon adopting the hypothesis of conservation of tangential momentum, (as opposed to cosine remission with equal mean speeds of remission in all directions). τ gives the enhancement of number flux and ρ the enhancement of momentum flux for atoms remitted in a direction normal to the tungsten surface.

Since the relation between T_n and the mean energy of the atoms, which traverse the aperture system and hit the torsion balance is

$$\tfrac{1}{2}m\overline{c_e^2} = 2kT_n \qquad (23)$$

the mean velocities $\bar{c}_e$ of the helium and argon atoms which are remitted normal to the surface of the ribbon and emerge from the aperture system can be calculated directly from the values of T_n in Tables 6 and 7 (section 8) since from appendix 3:

$$\overline{c_e^2} = \frac{32}{9\pi}(\bar{c}_e)^2 \qquad (24)$$

Goodman's Treatment for the Momentum Enhancement Ratio ρ

The distribution $f(v,\Omega)$ of gas atoms remitted from a surface with tangential and normal temperatures T_t and T_n respectively is, from Goodman 1972a:-

$$f(v,\Omega) = \frac{m^2}{2\pi k^2 T_t T_n} v^2 \cos\theta \exp\left(-\frac{mv^2\sin^2\theta}{2kT_t}\right) \exp\left(-\frac{mv^2\cos^2\theta}{2kT_n}\right)$$

where; m is the gas molecular mass, v the speed

$$\int_0^\infty dv \int_0^{\pi/2} \sin\theta d\theta \int_0^{2\pi} d\phi f(v,\Omega) = 1 \quad \text{and } d\Omega = \sin\theta d\theta d\phi$$

Then $$f(\Omega) = \int_0^\infty dv f(v,\Omega) = \frac{1}{\pi}\frac{\tau\cos\theta}{\cos^2\theta + \tau\sin^2\theta}$$

where $$\tau = \frac{T_n}{T_t}$$

Thus for $\theta = 0$ i.e. $\cos\theta = 1$

$$f(\Omega) = \frac{\tau}{\pi} \quad \text{Note that for } T_n = T_t \; f(\Omega) = \frac{1}{\pi}$$

Hence for a given number rate of gas atoms remitted from the surface, the number flux leaving in $d\Omega$ at $\theta = 0$ (i.e., normal to surface) is proportional to $(\tau/\pi)d\Omega$, provided that $d\Omega$ is sufficiently small. Therefore the remitted normal number flux is enhanced by the factor τ, above the "equilibrium" value where $T_n = T_t$.

Now remitted normal speed = constant x $T_n^{\frac{1}{2}}$.

Thus remitted normal momentum flux = constant x τ x $T_n^{\frac{1}{2}}$.

Consider gas at T_g impinging on a surface at T_s and remitted with

non isotropic speed components according to temperatures T_t and T_n as above.

Then $$\alpha = \frac{\bar{E}' - \bar{E}_g}{E_s - \bar{E}_g}$$

where $\bar{E}' = k(T_n+T_t)$, $\bar{E}_g = 2kT_g$ and $E_s = 2kT_s$

and remitted normal momentum flux

$$= \text{constant} \times \tau \times \left\{\frac{2T_g\left[1+\alpha\left(\frac{T_s}{T_g} - 1\right)\right]}{\left(1 + \frac{1}{\tau}\right)}\right\}^{\frac{1}{2}}$$

Consider now a gas at T_g impinging on a surface at T_s and remitted with isotropic speed components according to the single temperature T'. The above expression reduces to the simpler form, remitted normal momentum flux

$$= \text{constant} \times \left\{T_g\left[1 + \alpha\left(T_s/T_g - 1\right)\right]\right\}^{\frac{1}{2}}$$

Thus the ratio $\rho = \dfrac{\text{remitted normal momentum flux, nonisotropic temperature}}{\text{remitted normal momentum flux, isotropic temperature}}$

Thus,

$$\rho = \tau\left[\frac{2}{1 + \frac{1}{\tau}}\right]^{\frac{1}{2}} \qquad (25)$$

In the special case where $T_t = T_g$ the above ratio may conveniently be expressed as:

$$\rho = \frac{\left[1 + 2\alpha\left(T_s/T_g - 1\right)\right]^{3/2}}{\left[1 + \alpha\left(T_s/T_g - 1\right)\right]^{1/2}} \qquad (26)$$

Calculation of Sensitivity of α_w^g to α_t

A "partial" tangential accommodation coefficient α_t is defined

$$\alpha_t = \frac{T_t - T_g}{T_s - T_g} \tag{27}$$

and in general for a non isotropic remitted gas with temperatures T_n and T_t

$$\alpha_w^g = \frac{kT_n + 2(\frac{1}{2}kT_t) - 2kT_g}{2kT_s - 2kT_g} \tag{28}$$

In a manner analogous to that used at p.107 two expressions for G are obtained:

Equation (18) becomes:-

$$G = (B+F+F') \frac{\left(\frac{2}{1+\frac{1}{\tau}}\right)^{\frac{1}{2}} \left[1 + \alpha_w(^{T_s}/_{T_g} - 1)\right]^{\frac{1}{2}}}{\left(\frac{2}{1+\frac{1}{\tau}}\right)^{\frac{1}{2}} \left[1+\alpha_w(^{T_s}/_{T_g}-1)\right]^{\frac{1}{2}} + \frac{2}{3}\left\{\left(\frac{2}{1+\frac{1}{\tau}}\right)\left[1+\alpha_w(^{T_s}/_{T_g}-1)\right](1-\alpha_{cu})+\alpha_{cu}\right\}^{\frac{1}{2}}} \tag{29}$$

and Equation (20) becomes:-

$$G = \tau\left(\frac{2}{1+\frac{1}{\tau}}\right)^{\frac{1}{2}} F\left[1 + \alpha_w(^{T_s}/_{T_g} - 1)\right]^{\frac{1}{2}} \tag{30}$$

For particular, convenient values of τ and T_s each of the equations (29) and (30) are plotted as a function of α_w^g. Thus a value of α_w^g is obtained graphically for a given τ and T_s. Then a value of α_t is calculated using equations (27) and (28).

Appendix 2

Relation between F' and F

Relationship between the force F due to gas molecules mass m, arriving at a surface normally at point O, at a mean speed $\bar{c}$ and the force F' due to the remission of those molecules in a cosine wise angular distribution at the same mean speed $\bar{c}$ which is independent of direction.

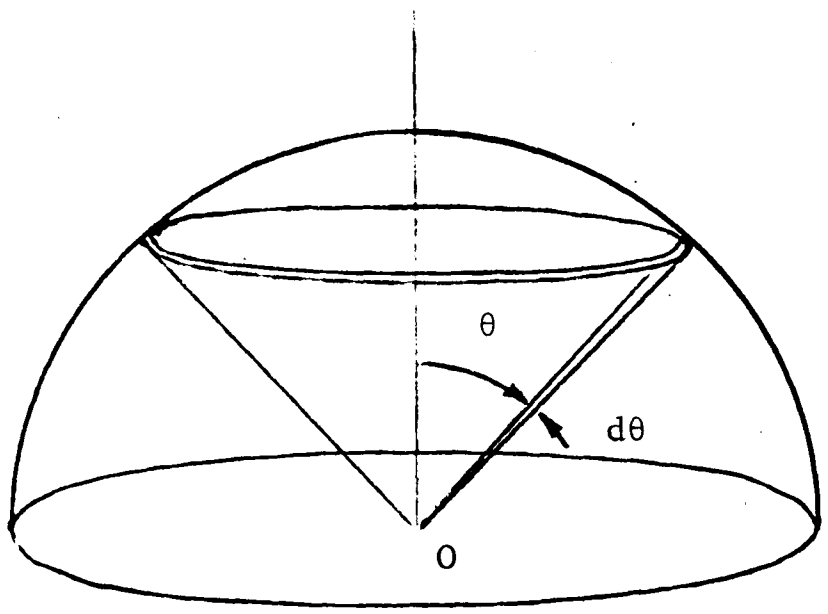


Figure 18

Consider the approaching molecules mean momentum $m\bar{c}$ and their rate of arrival at the surface n, and rate of remission in direction θ, n_θ

On remission the rate of leaving in a direction θ to the normal is n_θ where

$$n_\theta \alpha dw_\theta \cos\theta \qquad \text{(the cosine law)}$$

where dw_θ is the small solid angle between θ and θ + dθ.

$$\text{but } dw_\theta = 2\pi \sin\theta \, d\theta$$

$$n_\theta \propto 2\pi \sin\theta \cos\theta \, d\theta$$

Hence normal component of force due to molecules remitted at angle θ is proportional to

$$2\pi \, m\bar{c} \sin\theta \cos^2\theta \, d\theta$$

and the force due to molecules arriving normally is proportional to

$$2\pi \, m\bar{c} \sin\theta \cos\theta \, d\theta$$

$$\therefore F' = 2\pi \, m\bar{c} \int_0^{\pi/2} \sin\theta \cos^2\theta \, d\theta \Big/ 2\pi \, m\bar{c} \int_0^{\pi/2} \sin\theta \cos\theta \, d\theta$$

$$F' = \frac{2}{3} F$$

Appendix 3

Relationships between $\bar{c}$, $\overline{c^2}$, $\bar{c}_e$ and $\overline{c_e^2}$

$\bar{c}$ is the mean speed of the molecules in an isothermal gas at temperature T.

$\bar{c}_e$ is the mean speed of the molecules when considered arriving at a surface in an isothermal gas at temperature T.

m is mass of gas molecule and k is Boltzmann's constant.

(a) $\frac{1}{2} m\overline{c^2} = \frac{3kT}{2}$ and $\bar{c} = \left(\frac{8kT}{\pi m}\right)^{\frac{1}{2}}$

$\therefore \quad \overline{c^2} = \frac{3kT}{m}$ and $(\bar{c})^2 = \frac{8kT}{\pi m}$

$\therefore \quad \frac{\overline{c^2}}{(\bar{c})^2} = \frac{3\pi}{8}$

(b) $\frac{1}{2} m\overline{c_e^2} = 2kT$ and $\bar{c}_e = \frac{3}{4}\left(\frac{2\pi kT}{m}\right)^{\frac{1}{2}}$

$\therefore \quad \overline{c_e^2} = \frac{4kT}{m}$ and $(\bar{c}_e)^2 = \frac{9\pi kT}{8m}$

$\therefore \quad \frac{\overline{c_e^2}}{(\bar{c}_e)^2} = \frac{32}{9\pi}$

(c) Also $\frac{\bar{c}_e}{\bar{c}} = \frac{3\pi}{8}$

and $\frac{\overline{c_e^2}}{\overline{c^2}} \pm \frac{4}{3}$

Appendix 4

c	f_c	c	f_c	c	f_c
0	0	1.1	0.8142	2.2	0.0864
0.1	0.0223	1.2	0.7697	2.5	0.0272
0.2	0.0867	1.3	0.7036	3.0	0.0024
0.3	0.1856	1.4	0.6232	4.0	4.1×10^{-6}
0.4	0.3077	1.5	0.5350	5.0	7.8×10^{-10}
0.5	0.4393	1.6	0.4464	6.0	1.9×10^{-14}
0.6	0.5668	1.7	0.3624		
0.7	0.6775	1.8	0.2862		
0.8	0.7613	1.9	0.2204		
0.9	0.8129	2.0	0.1652		
1.0	0.8302				

Table 9. Values deduced from Maxwell-Boltzmann distribution laws when applied to a gas of molecular mass m and at isothermal temperature T.
Distribution function f_c as a function of random velocity c expressed in terms of the most probable velocity $= \left(\frac{2kT}{m}\right)^{\frac{1}{2}}$ when c = 1.

Extract from Dushman S. 1949 Scientific Foundations of Vacuum Technique, Wiley, N.Y.

Appendix 5

Characteristics of the surface of the copper torsion balance

Values for α_W^{He} and α_W^{Ar} have been derived assuming that α_{Cu}^{He} and α_{Cu}^{Ar} were, for the surface of our torsion balance, 0.4 and 1.0 respectively, the angular remission being cosine-wise. This Appendix presents the evidence for these assumptions and shows that the resulting values of α_W^{He} and α_W^{Ar} are not critically dependent on them.

The copper of the torsion balance received no special treatment. It was initially baked in vacuo, with the rest of the vacuum envelope to 220°C (see section 6.7). Subsequently, owing to a vacuum failure during a bake, the copper became slightly oxidized and acquired a dull appearance. Thus it may be described as "dirty" copper - a fortuitous but probably fortunate accident since, as appears below, it is assumed to have a high accommodation coefficient and to be cosine in remission.

There appears to be little published data on the thermal accommodation of helium and argon on copper. Waelbroeck and Zucherbrodt (1958) report for copper at 40°C and not specially cleaned

$$\alpha_{Cu}^{He} = 0.4$$

$$\alpha_{Cu}^{Ar} = 0.8$$

Klett and Irey (1969) report for α_{Cu}^{He} 0.407 and 0.564 for 243 and 77.4 K respectively. Their copper was cleaned in an acid bath, water rinsed and dried.

Later work by Cochran and Irey (1972) gives for helium at 243 K on copper at 77 K a value of $\alpha_{Cu}^{He} = 0.56$. Their copper was sand blasted, acid dipped, rinsed and wiped with acetone.

In general surfaces at room temperature are "dirty" and thermal accommodation tends to be high and remission cosine-wise unless high temperature flashing followed by extremely high vacuum is possible. The point is exemplified for instance by Yamamoto and Stickney (1970) who found that for He/W and Ar/W a tungsten temperature $\gtrsim$ 1000 K was necessary to maintain a "clean" surface.

We have therefore assumed cosine remission for helium impinging on the room temperature copper balance arm and a value of $\alpha_{W}^{He} = 0.4$.

As for a given substrate α tends to increase with increasing atomic mass of the impinging gas atoms, and as Ar is much more massive than He we have adopted $\alpha_{W}^{Ar} = 1$, and again assumed cosine remission. Table 10 displays the effect on the deduced values of α_{W}^{He} and α_{W}^{Ar} of varying assumptions about interaction with the copper balance arm. If we restrict the "range of credibility" for α_{Cu}^{He} to $0.4 \rightarrow 1.0$ and for α_{Cu}^{Ar} to $0.6 \rightarrow 1.0$ the resulting ranges of α_{W}^{He} and α_{W}^{Ar} for $T_s = 1500$ K are $0.028 \rightarrow 0.031$ and $0.11 \rightarrow 0.12$ respectively (see table 10).

In view of these figures we have adopted and used, in tables 5, 6, and 7, the assumptions about gas/balance arm interactions stated in the first paragraph of this Appendix.

α_{Cu}^{He} or α_{Cu}^{Ar}	Remission of He or Ar from Copper	α_{W}^{He}	α_{W}^{Ar}
0	Specular i.e. Normal to surface	0.010	0.07
0	Cosine	0.027	0.10
0.2	"	0.027	0.10
0.4*	"	0.028	0.11
0.6	"	0.029	0.11
0.8	"	0.030	0.11
1.0**	"	0.031	0.12

Table 10. Values of thermal accommodation coefficient α_{W}^{He} of helium and α_{W}^{Ar} of argon incident at T_g = 293 K on hot clean tungsten at T_s = 1500 K for various assumptions of helium and argon accommodation at the 293 K copper torsion balance.

* Condition taken for values quoted in table 2 for helium.

** Condition taken for values quoted in table 3 for argon.

α	T'								
0.00	293	293	293	293	293	293	293	293	T_g
0.01	295	297	299	301	303	305	307	309	
0.02	297	301	305	309	313	317	321	325	
0.03	299	305	311	317	323	329	335	341	
0.04	301	309	317	325	333	341	349	357	
0.05	303	313	323	333	343	353	363	373	
0.06	305	317	329	341	353	365	377	389	
0.07	308	321	335	349	363	378	392	406	
0.08	310	326	342	358	366	390	406	422	
0.09	312	330	348	366	384	402	420	438	
0.10	314	334	354	374	394	414	434	454	
0.20	334	374	414	454	494	534	574	614	
0.30	355	415	475	535	595	655	715	775	
0.40	376	456	537	616	696	776	856	936	
0.50	397	497	597	697	797	897	996	1096	
0.60	417	537	657	777	897	1017	1137	1257	
0.70	438	578	718	858	998	1138	1278	1417	
0.80	459	619	779	939	1099	1259	1419	1579	
0.90	479	659	839	1019	1199	1379	1559	1739	
1.00	500	700	900	1100	1300	1500	1700	1900	T_s

Table 11. Tabulated values of T'K for a range of values of α and T_s.

where $\alpha = \dfrac{T' - T_g}{T_s - T_g}$, $T_g = 293$ K.

Apparatus and techniques

A tensioning spring for high temperature ribbon filaments

M J Watts
Engineering Science Laboratory, Oxford University, Parks Road, Oxford

MS *received 4 May 1972*

Abstract The design criteria of current-carrying springs for high temperature ribbon filaments are more demanding than for cylindrical wire filaments. A spring, which was found to be satisfactory for a tungsten ribbon up to 2500 K, is described.

Current-carrying springs and special geometries may be used to ensure that ohmically heated tungsten wire filaments of circular cross section remain taut when raised to high temperatures and do not fail mechanically when subject to thermal cycling (Blodgett and Langmuir 1934). However, if the filament is of rectangular cross section, i.e. a ribbon, as opposed to a cylindrical wire of the same cross-sectional area, the filament current required (and thus the current carried by the tensioning spring) to attain the same surface temperature is greater. But, whilst the tensioning spring for the ribbon filament must carry a greater current, the spring must not be of greater stiffness if the stress in the filament is to be the same in both cases.

Some recent work in this laboratory required that a tungsten ribbon 2·0 mm by 0·03 mm and 20 mm long be mounted vertically on a removable subassembly in a very restricted space of an ultrahigh vacuum apparatus. The tungsten contained no addition to inhibit the crystal growth. It was necessary continuously to heat the ribbon to 2200 K (requiring about 12 A) for periods of 8 h and to 'flash' repeatedly to 2500 K (about 16 A) for a few seconds. It was desirable that the ribbon should not move transversely and that the spring should operate at a low temperature to minimize outgassing.

Smithells (1952) quotes the strength of single crystal tungsten wires at 2600 K as 1·48 kg mm^{-2}, and, similarly, at 1000 K as 10 kg mm^{-2}. This gives a breaking load of about 89 and 600 g weight respectively when applied to the tungsten ribbon described above. The thermal expansion coefficient of tungsten in the range 300–2600 K is about 6×10^{-6} K^{-1}, so that a ribbon 20 mm long would increase in length by 0·28 mm when raised from 300 to 2600 K.

Smithells (1952) suggests that molybdenum is a suitable material for filament springs provided they do not operate at a temperature of greater than about 800 K. The tensioning spring designed was found to meet the requirements satisfactorily and is thought to be novel in its application. It consists of a piece of molybdenum foil 0·07 mm thick and 11 mm × 45 mm, rolled to form almost a cylinder, the shorter edges being about 1 mm apart (figure 1). Spot-welded to each of these edges was a molybdenum tag 0·26 mm thick and 11 mm × 20 mm. The upper tag was bolted to, but electrically insulated from, the subassembly mount (not shown). The lower tag was spot-welded to one end of the tungsten ribbon. Hence the ribbon was spring mounted at the upper end, the lower end being spot-welded to a further piece of molybdenum bolted to the subassembly and providing the earth connection. To increase the total thermal emissivity (Blodgett and Langmuir 1934) the cylindrical spring was sprayed before final assembly with several coats of a solution comprising Aquadag, alcohol and distilled water, the spring being maintained at

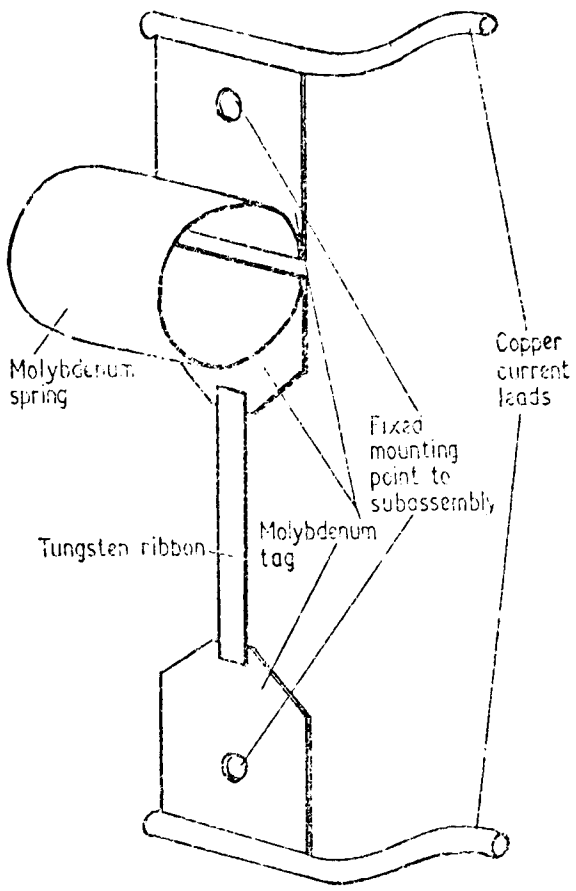


Figure 1 Molybdenum spring and tungsten ribbon assembly

about 70°C in air with a current of 15 A. This coating, when dry, was not easily damaged by handling.

The following results were obtained experimentally. The cylindrical spring stiffness of 1·1 g force per mm (at 20°C) was constant up to at least 10 g. It was possible to arrange that the total load was less than 3 g weight at 20°C, which was reduced at higher temperatures by the thermal expansion of the tungsten ribbon. The spring was allowed to carry 20 A in a vacuum environment of 10 μTorr when its temperature was below red heat. Similar springs have been life tested in a vacuum of 1 μTorr for more than 50 h, repeatedly cycled to 16 A and completely satisfying the requirements. Whilst extension and contraction of the cylindrical spring involves motion in a slightly curved path, this effect can be minimized by increasing the diameter of the spring.

In contrast to the above results, when two similar ribbons were mounted without the spring arrangement now described, unwanted transverse movement of about 1 mm on heating to 2200 K occurred and cracking appeared after 30 h service. In fact it was this failure which prompted the spring design here described.

Acknowledgments
Financial support from the Ministry of Technology and valuable discussion with L G Carpenter is greatfully acknowledged.

References

Blodgett K B and Langmuir I 1934 *Rev. Sci. Instrum.* **5** 321–33

Smithells C J 1952 *Tungsten* 3rd edn (London: Chapman and Hall)

Journal of Physics E: Scientific Instruments 1972 Volume 5
Printed in Great Britain © 1972

Appendix 8

Pressure Measurement of Argon and Helium

The gas pressure range in which experiments were conducted was $1x10^{-4}$ to $1x10^{-2}$ torr. The Mullardhot cathode ionization gauge (IOG71) was found to be suitable to measure accurately the argon and helium gas pressures in the above range in the absence of chemically active gases (1). The IOG71 was of the pre-Bayard-Alpert type and consisted of a central hot tungsten filament, a co-axial molybdenum grid and nickel collector. See plate 16 . Relative movement of the electrodes, causing changes in sensitivity, was unlikely since the electrodes were substantially constructed and mounted (2). Recalibration after the experimental work confirmed this, see below.

The gauge was used with an electron emission current of 50 μA corresponding to a filament temperature of about 1500 K. This produced very low outgassing and negligible pumping effect, yet sufficient collector current to be measured directly on a commercially available galvanometer (3) The electrical circuit diagram and electrode voltages (4) (recommended

---

(1) An ionization gauge was chosen in preference to a Pirani gauge. Although the sensitivity of the latter would have been suitable for the helium and argon pressures used, its reproducibility would have been dubious after the preliminary bake at pressures $\sim 10^{-9}$ torr. This treatment might have affected its surface cleanness and hence its thermal accommodation coefficient and calibration.

(2) The whole gauge was baked in the vacuum furnace (see appendix 13) for 20 hours between 250 and 300°C. This was intended to outgas the large nickel collector and glass envelope and to assist in relieving any stresses built into the electrode assembly. The filament and grid were further outgassed by resistive heating to manufacturers recommendations.

(3) The collector current for $1x10^{-4}$ torr of helium (lower than required) was 13 nA which could be read to ±2.5%. Same as footnote(2) p161.

(4) Additional experiments confirmed that small variations in each of the electrode potentials had negligible effect on the collector current.

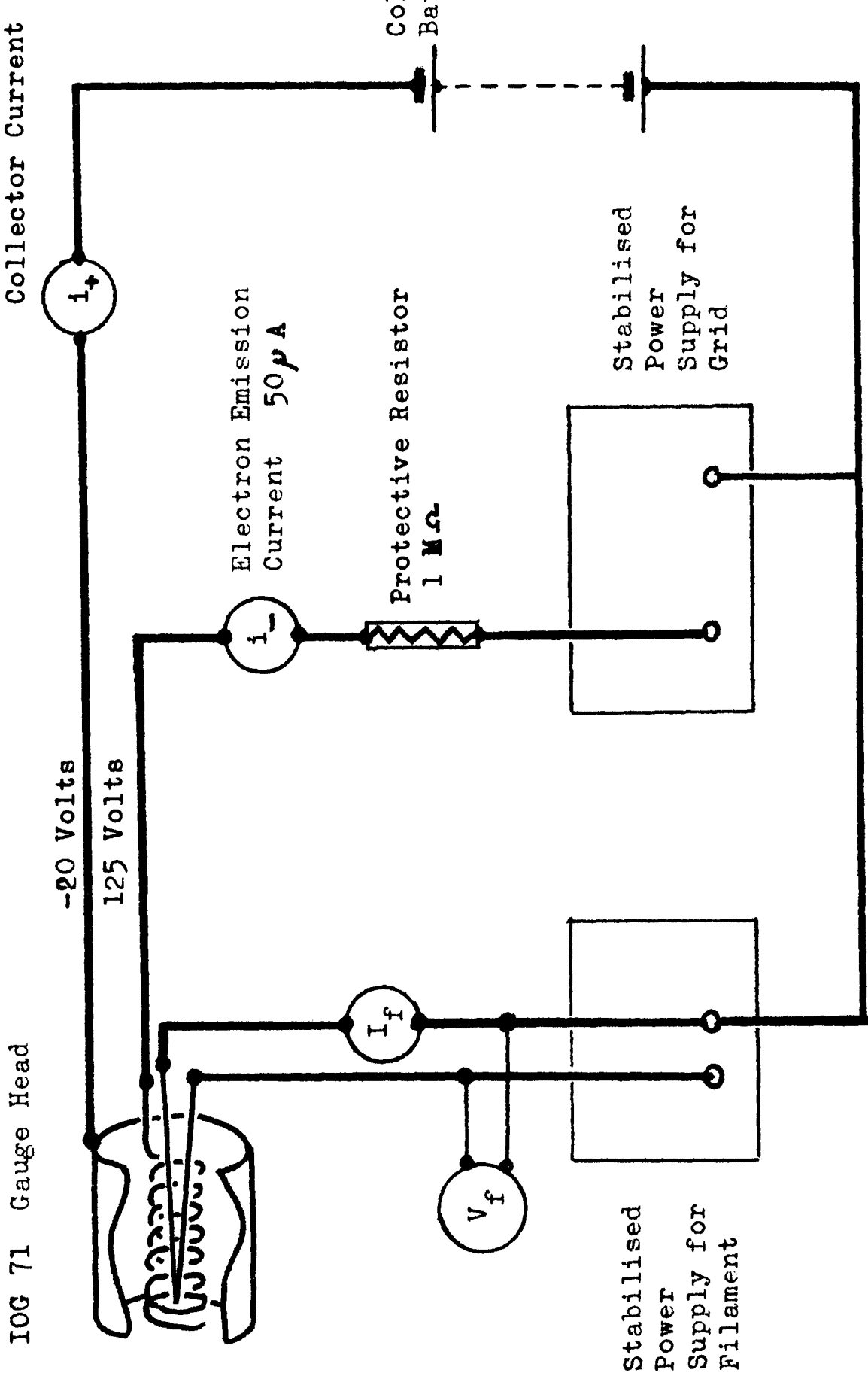


Figure 19 Circuit diagram and operating voltages of IOG 71 vacuum gauge.

by the manufacturer) were as shown in fig.19.

The gauge was calibrated for helium and argon (see figures 20 to 23) by the method of mixtures [1] using section 2 of the auxilliary apparatus, see appendix 12. The variation of collector current was linear with pressure up to 5×10^{-3} torr for helium and 0.7×10^{-3} for argon and the error estimated to be less than ± 1%. Recalibration of the gauge with argon after the completion of the experiment confirmed the above results. If a gauge sensitivity for nitrogen (K) of 20 $torr^{-1}$ quoted by the manufacturer is assumed to be correct and compared with experimental values for helium and argon from the present work, values of gauge factor (R) of 0.13 and 1.2 are obtained for the He and Ar respectively where

$$i_+ = R\,K\,p\,i_- \qquad [R = 1 \text{ for Nitrogen}]$$

where i_+ collector current
i_- electron emission current
p gas pressure in torr

The values of R obtained agree well with those quoted in Leck (1964)

Use of Gauge as a Monitor of Cleanness

It is well known that the thermionic work function of tungsten is a strong function of the surface cleanness, the work function increasing with surface contamination. (see eg: Blodgett and Langmuir 1932) This property was used qualitatively as a sensitive monitor of the cleanness of section A. Careful records were kept of the filament heating current necessary to produce 50 μA electron emission current. Low filament current was associated with low pressures (~ 10^{-10} torr) and clean conditions before an experiment. During a set of experiments, with a relatively high pressure of helium or argon, it was still possible to use the filament current as a continuous monitor of cleanness.

---

(1) A method by which a known quantity of gas is expanded through a series of known volumes. Errors due to sorption of the gas on the walls of the apparatus were both estimated and investigated experimentally but found to be negligible. The primary reference was atmospheric pressure, by courtesy of Oxford University School of Geography.

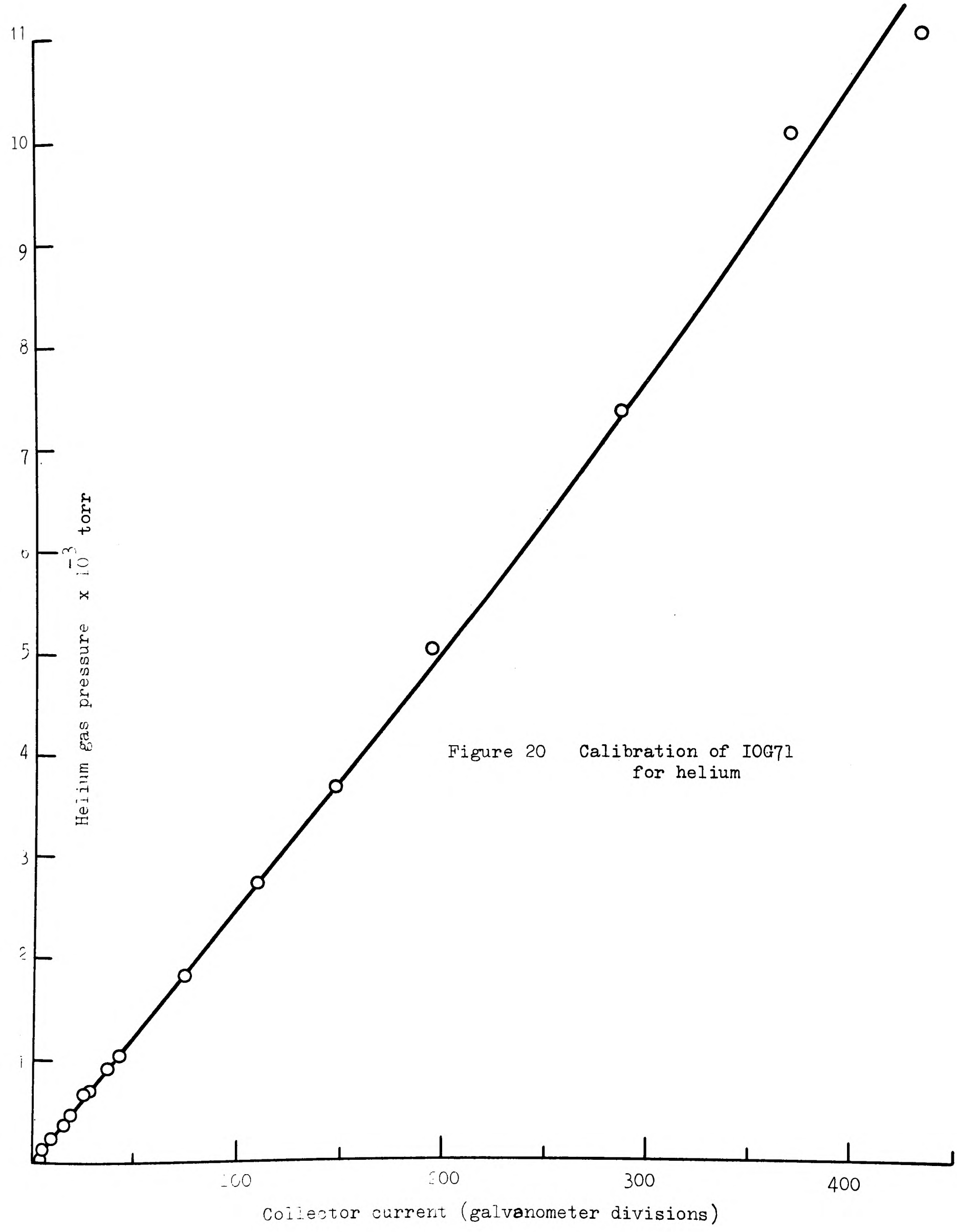


Figure 20 Calibration of IOG71 for helium

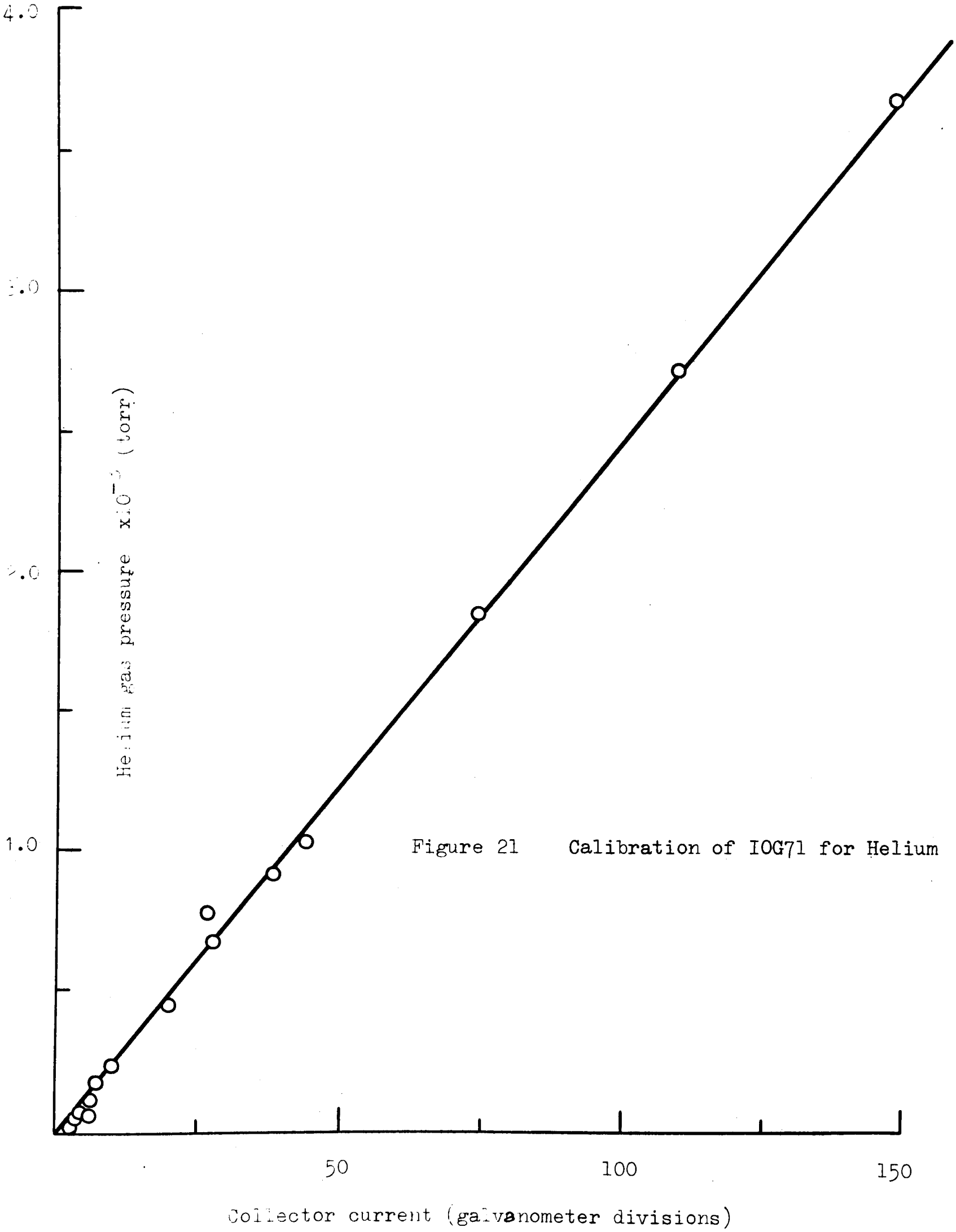


Figure 21 Calibration of IOG71 for Helium

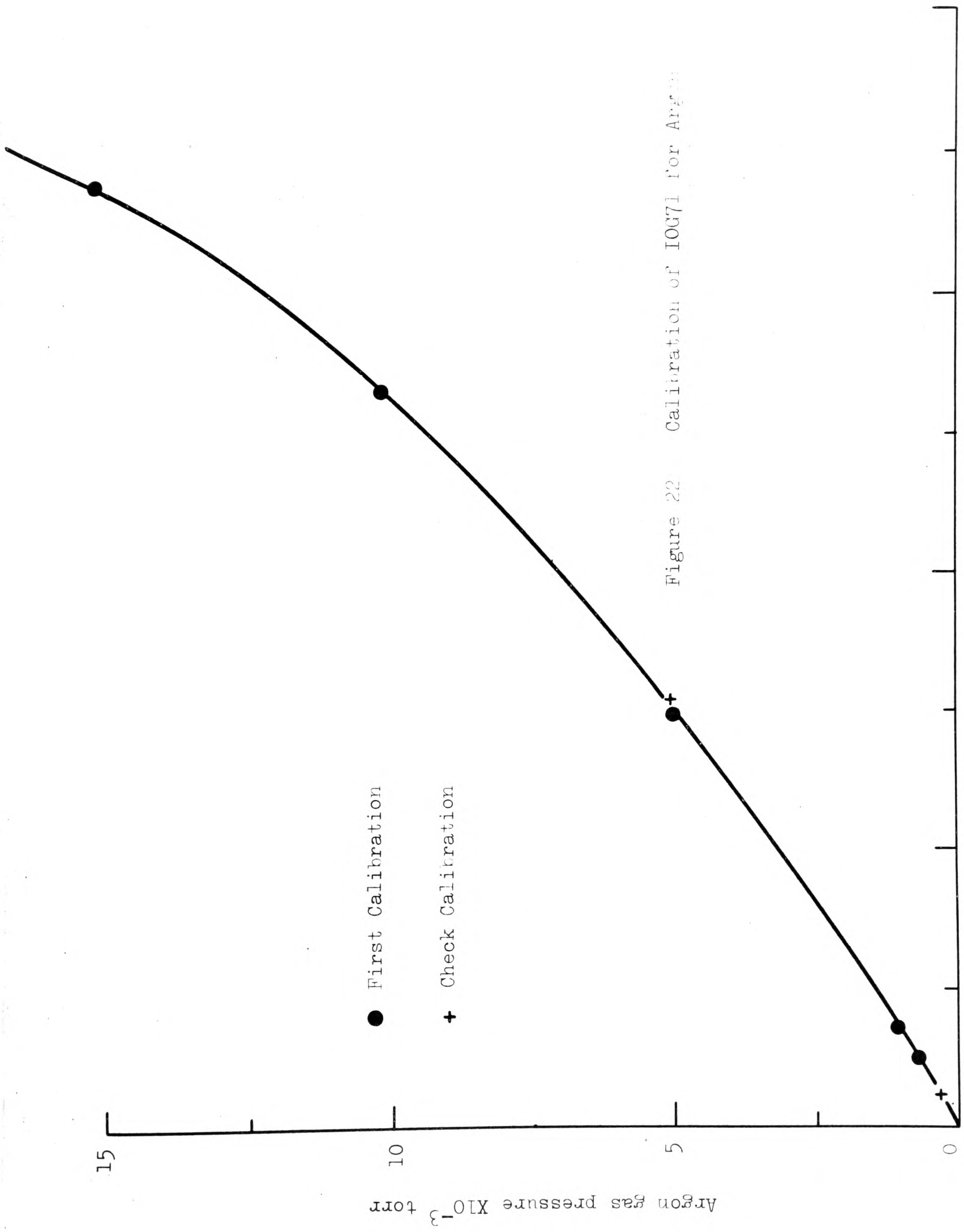


Figure 22 Calibration of IOG71 for Argon

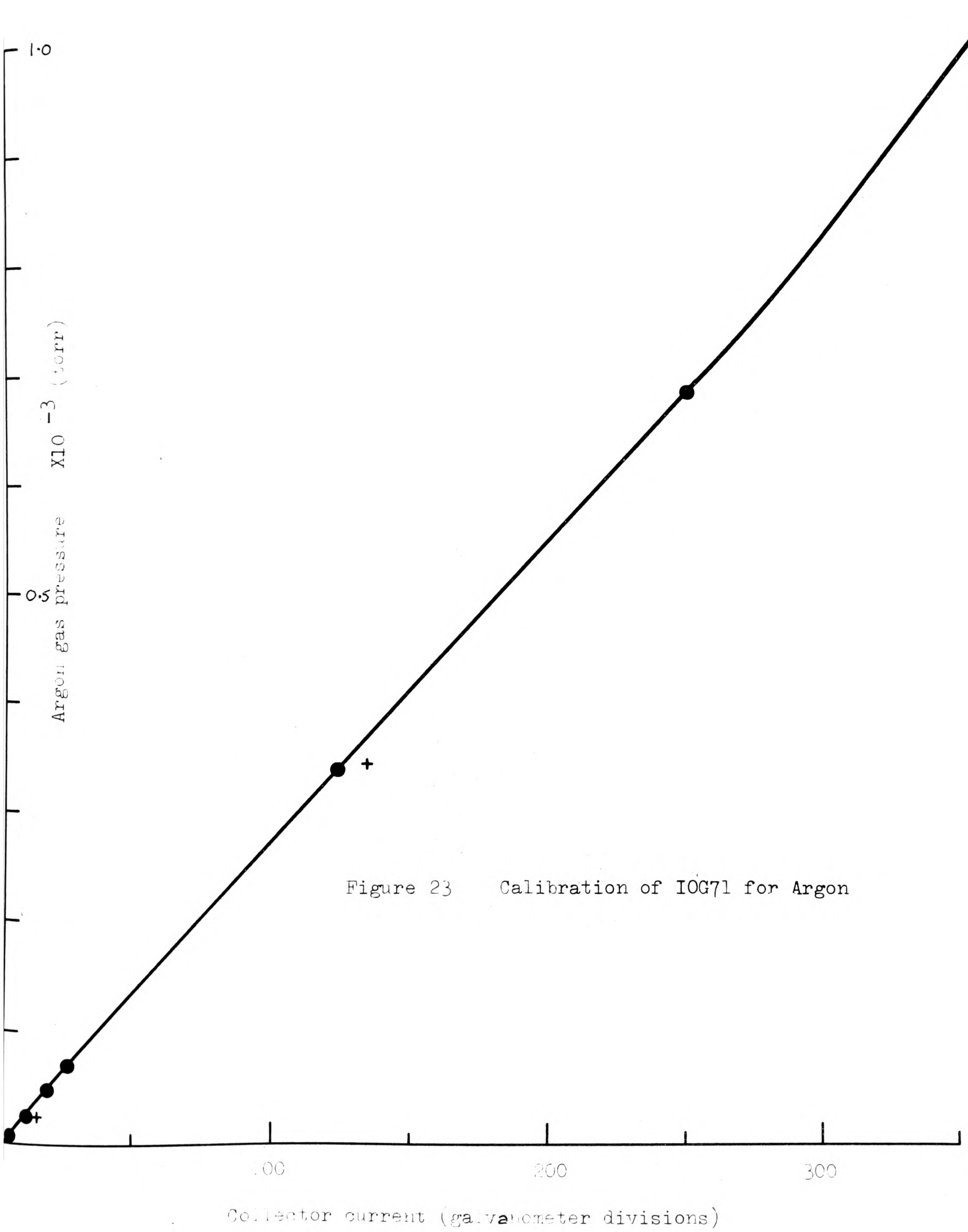


Figure 23 Calibration of IOG71 for Argon

Appendix 9

Titanium Sublimation Pump

General Principle of Operation

The pump provides a potentially high pumping speed for all the chemically "active" gases without pumping the inert gases significantly.

A thin layer of titanium is freshly deposited onto the large surface area of the pump. Gas molecules collide with this surface and those which are chemically active combine with the titanium. The deposition surface may be the inside of an appendage to the vacuum system or may be the inner surface of the vacuum chamber itself. The latter case is especially effective since the gas has the greater access to the pumping surface which can then approach its potential speed unrestricted by narrow channels. The surface may be cooled with water or a refrigerator, for example solid carbon dioxide or liquid nitrogen, which increases the potential surface pump speed. Reduction of the titanium surface temperature also improves pumping by sorption of, for example, methane (see below).

The titanium surface may be provided by sublimation from a filament of an alloy of titanium and molybdenum heated ohmically. The particular gas pressure and load will determine the necessary rate of sublimation of titanium, which may be continuous or for short duty cycles of a few minutes at intervals of several hours. The freshly deposited titanium both buries the pumped gas molecules and provides a new chemically active surface. In principle it is possible for inert gas atoms to be buried during deposition of the titanium surface but no experimental evidence of this effect was found in this work. It has been suggested

that deposition of titanium onto a very cold surface (e.g. one cooled by liquid nitrogen) significantly increases pumping speed. The hypothesis is that at low temperatures the titanium will tend not to migrate to form a uniformly flat surface, but grow as whiskers, increasing the specific area and the probability ofcapture of an active molecule approaching the surface. Thus both the speed and capacity for a given quantity of titanium would be enhanced. Whilst this effect was not observed, nor looked for in the work described, it would seem a sensible precaution to pre-cool the surface receiving the titanium. This would then act as an effective pump for condensible gases originating from the hot titanium filament and other components heated by radiation. The maximum possible pump speed for active gases is controlled by the bombardment rate of molecules on the surface.

The average bombardment rate β of a surface is given by

$$\beta = \frac{1}{4} n\bar{c} \quad \text{molecules cm}^{-2}\text{s}^{-1}$$

where n = molecular density (molecules cm^{-3})

$\bar{c}$ = mean speed

but $\bar{c} = \left(\frac{8kT}{\pi m}\right)^{\frac{1}{2}}$ for a Maxwellian speed distribution

where k = Boltzmann's constant 1.38×10^{-16} erg K^{-1}

T = Absolute temperature (K)

m = Molecular mass (g)

the atomic mass unit based on $^{12}_{6}C$

$= 1.66\times10^{-24}$ g

hence $\beta = \frac{n}{4}\left(\frac{8kT}{\pi m}\right)^{\frac{1}{2}}$ molecules $cm^{-2}s^{-1}$

Expressed as a speed F

$$F = \frac{1}{4000}\left(\frac{8kT}{\pi m}\right)^{\frac{1}{2}} \text{ litres cm}^{-2}\text{s}^{-1}$$

This is about 11.9 litres $cm^{-2}s^{-1}$ for nitrogen at 298K. Approximate values for other gases may be determined by noting the $(T/m)^{\frac{1}{2}}$ dependence

The Pump used in the present work

A high speed titanium sublimation pump was used to reduce the pressure within section A (see figure 3) from $\sim 10^{-9}$ to $\sim 10^{-10}$ torr and the selective pumping property enabled the low background pressure of $\sim 10^{-10}$ torr to be maintained whilst experiments were conducted in an environment of helium (at $\sim 10^{-3}$ torr) or argon (at $\sim 10^{-4}$ torr). This was an essential feature of the experimental procedure. Neither of these gases was noticeably pumped over a period of several days although fresh layers of titanium were regularly deposited and there was evidence that the background pressure was satisfactorily maintained (see section 7).

Design and Construction

It was necessary that the pump was of the appendage type (see plate 15) to minimise the possibility that critical surfaces in section A were contaminated with sublimated titanium. Figure 24 shows the general arrangement of the pump which was designed around a Ferranti electrical lead through flange and filament mounting assembly (FED.10). The specially constructed pump body of stainless steel was fabricated using argon arc welding techniques.

The major lower part of the body was made from 0.25 mm thick 750 mm diameter seamless "cryogenic" stainless steel tubing. These walls were strengthened by rolling in two convolutions as shown in figure 24

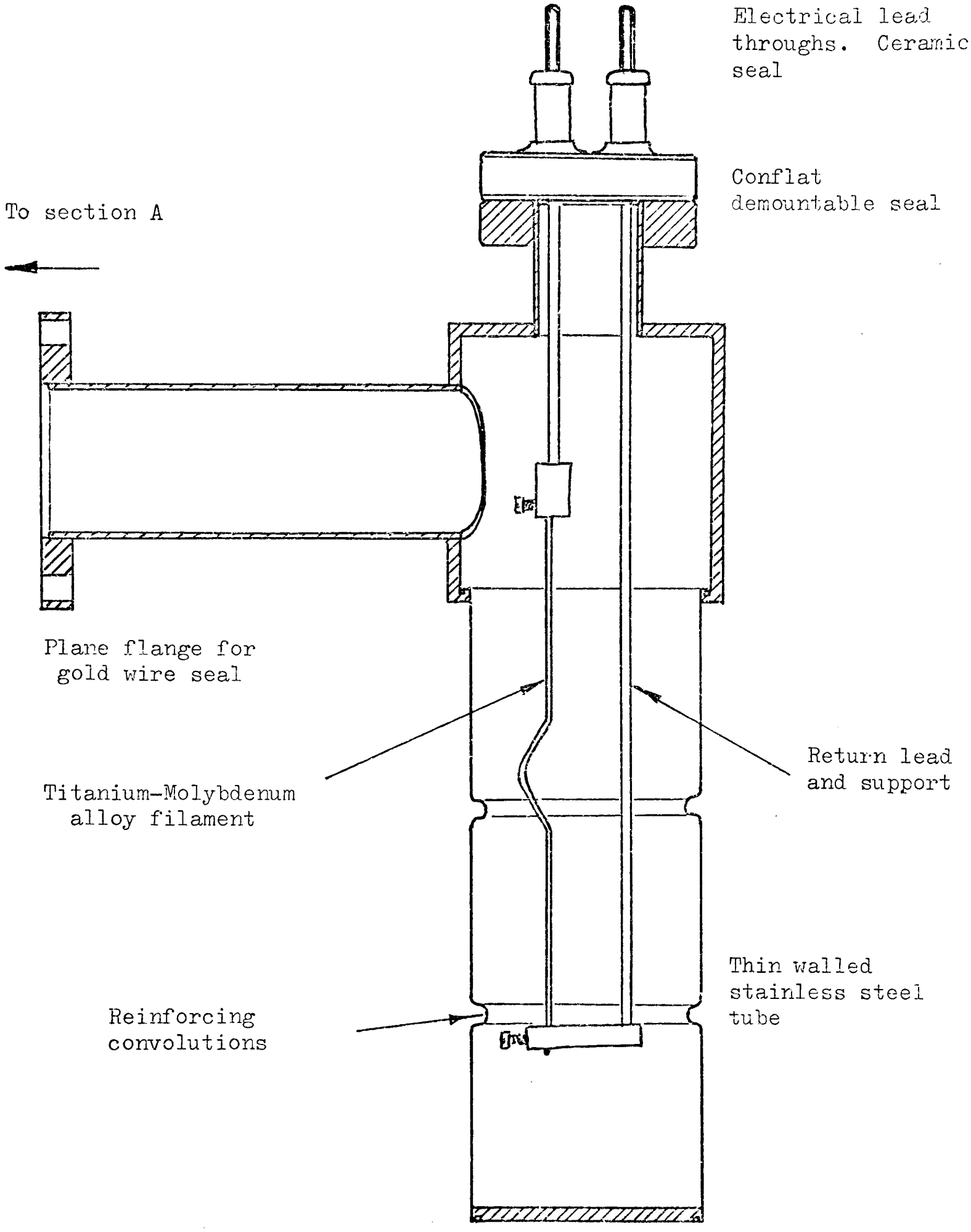


Figure 24 Titanium sublimation pump
Section (X0.5)

thus increasing the wall rigidity without the thermal mass or thermal conduction path to the liquid nitrogen coolant. The whole body was vacuum baked (1) at 500°C for 5 hours before testing on a helium mass spectrometer leak detector.

Sublimator Filaments

The Ferranti flange had provision for three evaporation filaments available from the same manufacturer and of an alloy of 85% titanium, 15% molybdenum, 170 mm long and 2.04 mm diameter. This alloy and dimensions combine a uniform rate of sublimation of titanium for a given filament current with the maximum utilization of the titanium, before burn out of the filament occurs, see McCracken (1965) and McCracken and Pashley (1965).

The filaments were arranged so that the majority of the titanium was deposited on-to the inside of the cryogenic walls comprising the lower part of the pump. This part was normally immersed in liquid nitrogen contained in a 4 litre glass dewar vessel. Thus titanium was deposited on a liquid nitrogen cooled area of approximately 500 cm^2. The potential pump speed for active gases was therefore a maximum of 6×10^3 litres s^{-1} (2). However this was severely restricted, by the port connecting the pump to section A, to approximately 55 litres s^{-1}, being the conductance of that port.

Filament Power Supply

The alternating current for ohmically heating the filaments was supplied from the mains via a controlling autotransformer and a transformer with a 6 volt secondary winding of 50 Amperes continuous rating. The filament

---

(1) by courtesy of the R.A.E. Farnborough
(2) for Nitrogen at 25°C

current was monitored directly with a 0-50 Ampere moving iron ammeter.

The resistance of the filament remained essentially constant at $\sim 0.085\Omega$ over the whole operating temperature range corresponding to currents from 0 → 50 Amperes.

All three filaments were initially outgassed for a total of 15 minutes at a current of 40 Amperes during the first pump down procedure of the whole apparatus.

Preparation and Operation of the Pump

The pump was baked to 150°C together with the whole of section A into the pumps (1) on section B. It was subsequently baked to 250°C, with the vacuum envelope of A at 220°C, into the two sputter ion pumps on A. The titanium sublimation pump was only used after the majority of the outgassing procedure was completed and section A isolated.

When used, the pump body was cooled with liquid nitrogen and then a filament fired at a constant current of 48 Amperes held for 2 minutes, the first half minute of which was taken with the filament warm up. Typically, firing or reactivation was repeated every few hours and immediately before each set of experiments to ensure the pump's activity (2) was maintained. A temporary pressure rise accompanied each reactivation. This was never greater than 10^{-8} torr as indicated by a Bayard-Alpert gauge on section A, and quickly diminished at the end of the firing. This rise of pressure was conveniently used to start the occasionally reluctant sputter ion pump when the pressure was of the order 10^{-10} torr.

---

(1) Sputter ion pump and liquid helium cold finger.

(2) It was estimated that at each reactivation, the 2 minute firing resulted in a deposition of 40 monolayers of titanium on the cooled surface, also the probable life of the reactivated pump was equivalent to an active gas load of 10^{-8} torr for 8 hours in section A.

The power required to fire the filament was approximately 200 Watts which only resulted in a small loss of liquid nitrogen. The main loss was due to heat conducted down the thin wall of the pump body. An indication of the loss rate of liquid nitrogen is given by the data that 2.3 litres evaporated in 11 hours. The top of the pump was well insulated with polystyrene and aluminium foil. When it was necessary to allow the pump to warm up to room temperature a filament was fired immediately before the warming, thus reducing the probability of gas molecules (especially methane) on or near the titanium surface from returning to the gas phase.

It has been reported that methane is produced by the interaction of hydrogen (from the outgassing of stainless steel) and carbon, (an impurity in the titanium molybdenum alloy) on the hot filament. Methane is apparently absorbed onto a titanium surface at liquid nitrogen temperature but released when raised to room temperature unless buried by a further layer of deposited titanium (see for example Holland, Laurenson and Allen (1961) and Redhead, Hobson and Kornelsen (1968).

After completion of the experiments the pump was examined. Only one filament had been used (2 hours at 48 Amperes) and this was still intact. Its appearance was very similar to those other two which had only been outgassed at a maximum current of 40 Amperes for 15 minutes. There was however some slight surface thermal etching. A silvery deposit was visible inside the pump and this had apparently adhered well to the stainless steel surface.

Some useful extracts from McCracken G M 1965 Vacuum 15 433-6 and McCracken G M and Pashley N A 1965 J. Vac. Sci. and Technol. 3 96-8.

Filaments of 85% titanium and 15% molybdenum wire 2.1 mm diameter. For steady current of 50 Amperes wire temperature is 1780K and rate of sublimation is 0.12 mg min^{-1} for each cm of wire length. At 40, 45 and 55 Amperes, rate of sublimation is 0.003, 0.03 and 0.65 mg min^{-1} respectively.

Typical titanium deposition layer needed for pumping was 5 µg cm^{-2} (1) on a liquid nitrogen cooled surface of area 3650 cm^2. This had a capacity for hydrogen equivalent to 1 torr litre.

(1) Equivalent to approximately 65 monolayers of titanium.

Appendix 10

Liquid Helium Pump

General Principle of Operation

A surface at the temperature of liquid helium (4.2K when subject to the normal atmosphere pressure) will effectively cryopump all gases except helium. At this temperature (4.2K) the equilibrium vapour pressure of hydrogen is 5×10^{-7} torr (Rose-Innes 1970) and that of all other gases, with the exception of helium, is less than 10^{-11} torr, see for example Honig (1957).

The speed of a pump using this principle will depend on the area of cooled surface and the thermal conductivity of the wall between the cryogenic liquid and the gas to be pumped. This includes the pump wall and the layers of already adsorbed gas. As with a titanium sublimation pump, for the intrinsically high speed available to be fully realised, the gas must have good access to the cooled surface and not be restricted by narrow channels. A pump with these characteristics was ideally suited for operation during an experiment requiring a helium environment with a low background (impurity) pressure of all other gases. It was not, however, suitable for similar experiments with an argon environment but might be used for removal of all or part of the argon if provided with a suitable isolating value. It is a relevant and important fact that many sputter ion pumps are not altogether suitable for the pumping of argon.

The Pumps used in the Present Work

Two liquid helium pumps were used. Both were of the cold finger type and they were provided with metal isolating valves. One, on section A

fig. 3 , was used to maintain a low background pressure during experiments with helium gas and to reduce the environmental gas pressure during experiments with argon [1]. A similar pump on section B fig. 3 , was used in the pump down and bake-out cycle of section A and also in the adjustment of argon pressure before its introduction into section A.

Requirements of the Pumps

Whilst it would have provided a very effective pump it was not possible to arrange for the liquid helium pump to be within the vacuum envelope of the section A for the following reasons. The presence of a cold surface within section A would have seriously disturbed the thermal equilibrium of the environmental gas which was an essential requirement of the experimental method. It was the particular purpose of this pump to remove impurities of outgassing before experiments and maintain the purity of the environment during experiments with helium. Thus it was considered essential that the impurities should be permanently contained within the pump and not allowed to return to section A [2]. The only design compatible with these conditions was a cold finger with an isolating valve. An isolating valve was also essential for the pumps on sections A and B when used for adjusting the pressure of argon.

Dimensions and Speed of the Pump

The pump used on section A is shown in plate 14 . Both liquid helium pumps shown in figure 3 are identical except for the type of isolation

---

(1) It was found possible to make small adjustments in helium pressure by altering the area of cooled surface - see later.

(2) It was periodically necessary to allow the pump to return to room temperature between experiments for economy of liquid helium.

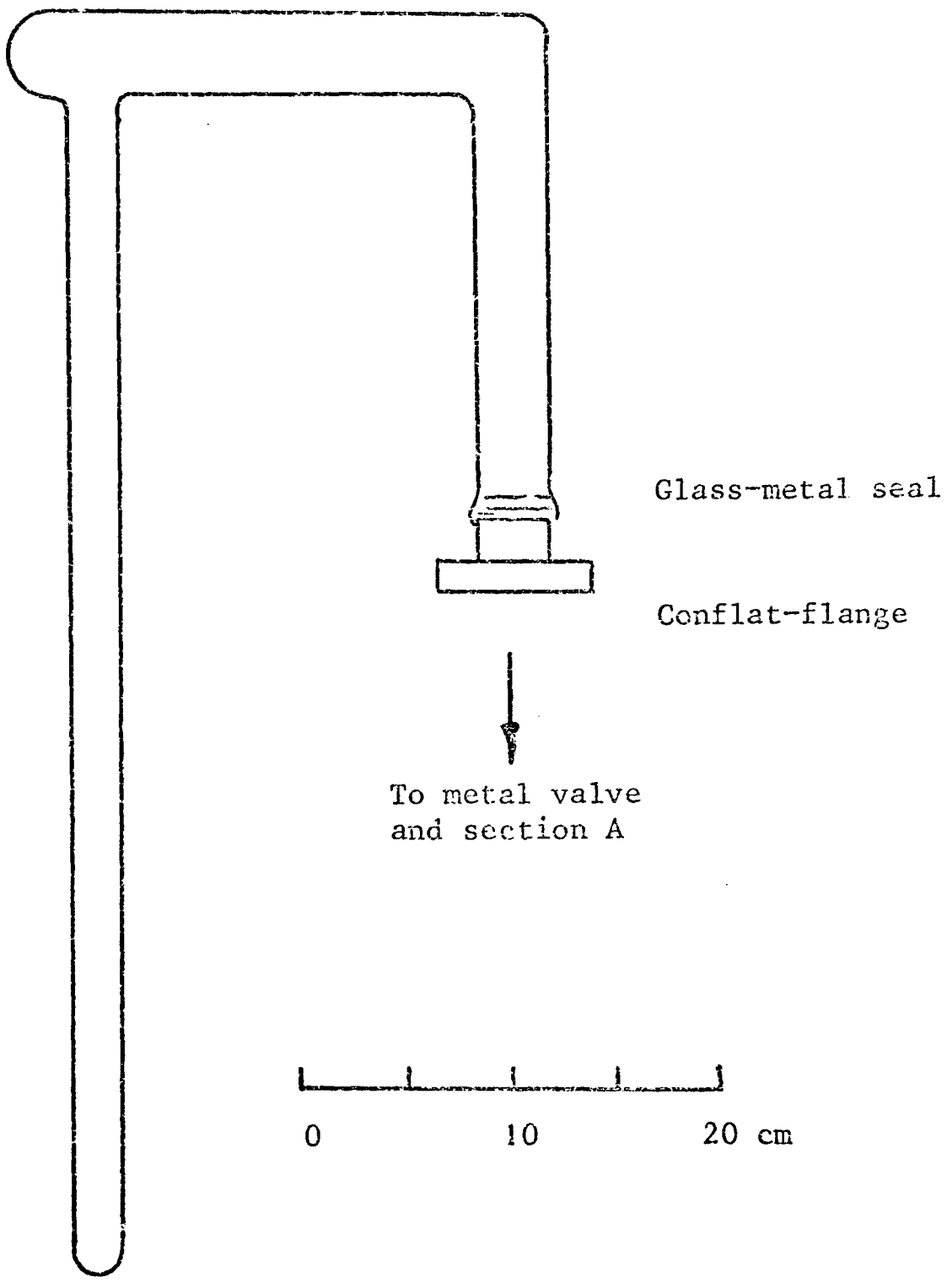


Figure 25 Liquid helium cold finger pump (Monax glass).

valve. The pump is shown here in figure 25 . It was made from Monax [1] glass tubing 570 mm long, 17.5 mm internal diameter and 1.5 mm wall thickness and was connected to section A via a 12 mm bore bakeable metal valve. The conductance of valve and connecting tube to the cooled section of the pump was estimated to be 2 litres$\cdot s^{-1}$ which was the maximum effective speed of this pump. Typically the area of Monax glass in contact with the liquid helium was 140 cm^2.

Preparation and Use of the Pump on Section A

The pump and its isolation valve (open) was baked to 150°C together with the whole of section A into the pumps [2] on section B. It was subsequently baked to 250°C, with the vacuum envelope of A at 220°C, into the two sputter ion pumps on A. When the pressure was as low as could be obtained using the sputter ion pumps and the titanium sublimation pump, the liquid helium cold finger isolation valve was closed [3]. The finger was pre-cooled with liquid nitrogen and then cooled [4] with liquid helium [5]. A period of 10 minutes was always allowed before the isolation valve was opened. No noticeable pressure change occurred at thisstage. When the pumping sequence was completed the isolation valve was again closed before the liquid helium was removed [6]. This valve

---

(1) Monax is a trade name for a borosilicate glass with a low permeability for helium. Manufactured by J. Moncrieff Ltd., North British Glass Works, Perth. Glass to metal seals can successfully be made direct to Kovar or Nilo-K (17% Co, 29% Ni, 54% Fe) since they both have similar thermal expansion coefficients $\sim 4.5\times10^{-6}{}^{o}C^{-1}$ (at 20°C).

(2) Sputter ion pump and liquid helium cold finger.

(3) This was a precaution taken least the subsequent cooling should break the Monax glass

(4) The liquid helium dewar was raised slowly, completely cooling the bottom tip of the finger first and thus concentrating the initial gas load at a point where it would remain until almost all the liquid helium had evaporated.

(5) A special dewar, on loan by courtesy of the Clarendon Laboratory, was used, see later.

(6) It is judicious to estimate the quantity of gas concentrated into the cold finger. When isolated and warmed to room temperature the pressure may be in excess of atmospheric pressure resulting in an explosion.

remained closed until the finger was again cooled. The effects of allowing a liquid helium dewar to warm up in position around a cold finger may not at first be appreciated. Monax at 20°C is relatively impermeable to helium. Whilst the effects of the permeability due to partial pressure of helium in the atmosphere ($\sim 4\times10^{-3}$ torr) may be acceptable, the effect of 760 torr of helium surrounding the cold finger may not be desired. Thus the liquid helium dewar was always removed from the cold finger when its pumping action was completed. The similar pump on section B was prepared and used in a similar way to obtain a low pressure in that section.

Adjustment of Helium Gas Pressure in Section A

It was discovered that the pressure of helium ($\sim 1\times10^{-3}$ torr) in the section A could reproduceably be adjusted by raising or lowering the liquid helium level relative to the cold finger. The corresponding decrease or increase in the helium gas pressure corresponded approximately to the adsorbtion or desorbtion of a monolayer of helium on the change in surface area cooled by liquid helium. These observations were in reasonable agreement with those of Hobson (1959) for helium on pyrex glass at 4.2K. The discovery resulted in a very convenient method of adjusting helium pressure and of providing a satisfactory check on the calibration of the pressure gauge (see appendix 8).

Adjustment of Argon Gas Pressure in Sections A and B

Since the equilibrium vapour pressure of argon or liquid helium temperature is considerably lower than the pressure required for the experiment ($\sim 1\times10^{-4}$ torr) the liquid helium cold finger technique could only be used for irreversible reductions in argon pressure by carefully

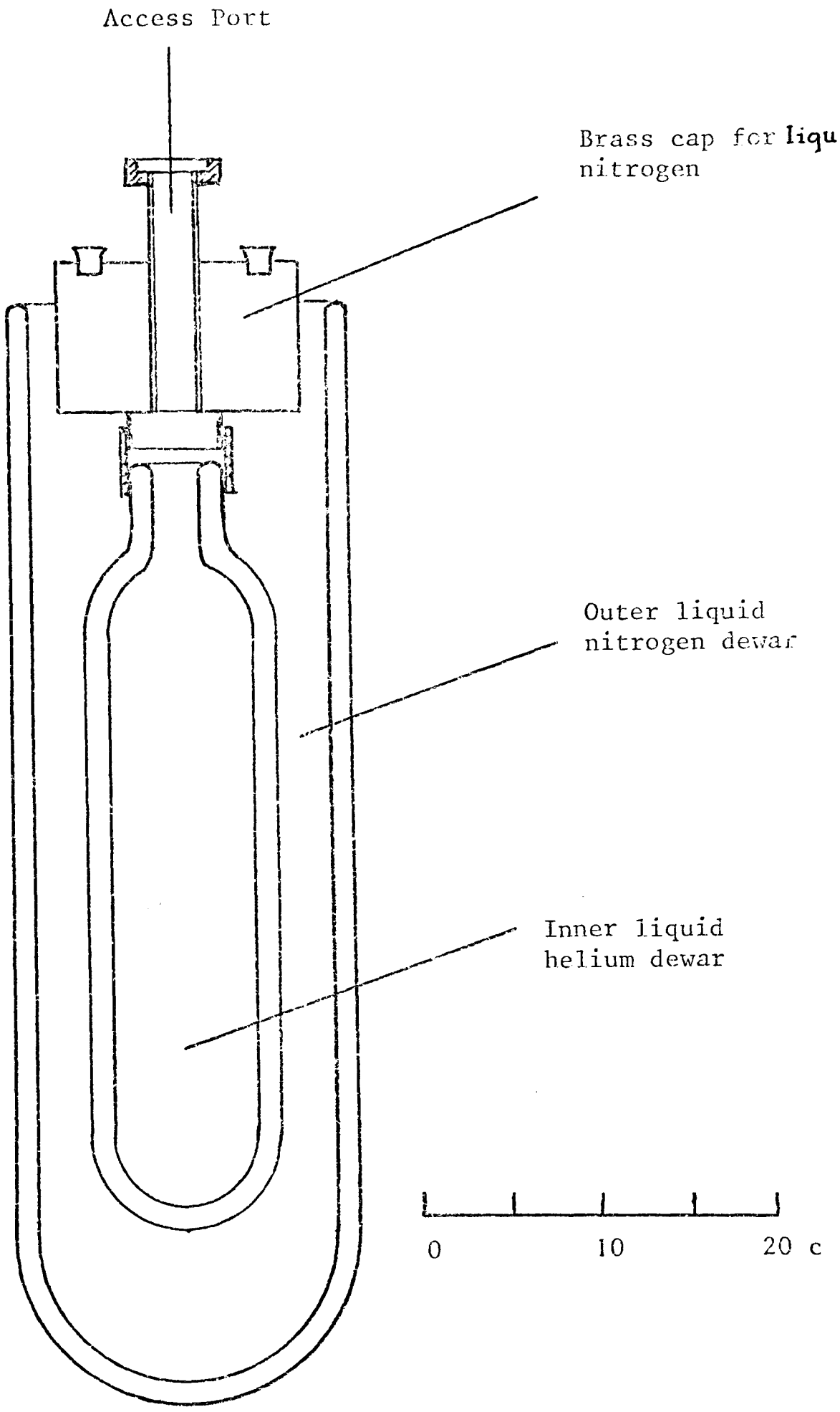


Figure 26 Liquid helium dewar with liquid nitrogen surround. (Monax glass).

cracking open the isolating valve for a short while.

The Liquid Helium Dewar

The liquid helium used to cool the cold finger was contained in a double Monax glass dewar designed by the Clarendon Laboratory see fig. 26. The entry neck of the top cap was small (about 25 mm diameter), restricting the maximum diameter possible for the cold finger. The outer dewar and the brass top cap, filled with liquid nitrogen, acted as protection for the inner liquid helium dewar of dimension 77 mm internal diameter, 470 mm deep (2.2 litres capacity).

Typically the inner dewar was charged with 1.5 litres of liquid helium. Cooling of the cold finger, after pre-cooling with liquid nitrogen, resulted in a loss of about 30 cm^3 of liquid helium. The natural loss with the cold finger immersed is at a constant rate and equivalent to 0.6 litres in 12 hours in a typical case. The liquid nitrogen protection required topping up every $1\frac{1}{2}$ hours.

Bibliography

Rose-Innes A C Low Temperature Techniques.

English Universities Press, London 1970

RedheadPA,HobsonJPand KornelsenEV. The Physical Basis of U.H.V.

Chapman and Hall, London 1968, p.101. Permeability of helium through pyrex.

MullardLtd Penetration of helium through glass.

Concern Symposium on Modern Vacuum Technology, May 1967 p.78.

Altemose V O Helium diffusion through glass

J. Applied Phys. 32(1961)1309-16

Hobson J P Can. J. Phys. 37(1959)300

(Ads orption of He on glass)

Hobson J P Cryopumping

J. Vac. Sci and Technol. 10 (1973) 73-9

Appendix 11

Osmosis Tubes

Certain gases may be admitted, by diffusion, into a vacuum system through a permeable membrane. The rate of diffusion is considerably increased by relatively small increases in membrane temperature (1). It was usual practice to make the membrane in the form of a tube, one end of which was closed and the other attached to the vacuum envelope via suitable graded glass and metal seals. A simple cylindrical oven surrounded the tube both heating it and concentrating the flow of gas around the tube (see later).

Admission of Oxygen via a Silver Tube

A partial pressure of about 1×10^{-6} torr of oxygen was required in which to pre-treat the tungsten ribbon surface before proceeding with a thermal accommodation experiment, see section 7 . A 99.9% pure silver tube fig. 2 , 4 mm diameter, 0.25 mm wall thickness and 140 mm long, was heated to $\sim 550^{\circ}C$ whilst surrounding it with commercial oxygen (2) at atmospheric pressure and at a flow rate of $\sim 500\ cm^3 min^{-1}$. The required partial pressure resulted from the competition between the oxygen thus admitted and the pumping action of the to 8 litre sec^{-1} sputter ion pumps on section A fig. 2 . Throughout the use of this tube (> 50 hours) there was no apparent change in the permeability for oxygen. The closed end of the silver tube was easily made by first crimping the end of the tube and then heating this crimp with an oxy-coalgas flame until the

---

(1) Diffusion rate and temperature are related exponentially. For a summary, with references to both theory and experiment, see eg. Dushmann S Scientific Foundations of Vacuum Technique, Wiley, New York 1947.

(2) Spencer (1923) obtained an oxygen purity of 95% at $400^{\circ}C$ and 97% at $500^{\circ}C$ when silver was surrounded by air

silver was seen just to flow. The other end was hard soldered, with the copper-silver eutectic alloy, to a Kovar-Koidal glass metal seal. Further details of diffusion of oxygen through silver at elevated temperatures are given by Spencer 1923 Whetten and Young(1959), Taylor(1935),Carpenter and Mair (1953).

Admission of Helium via a Fused-Silicon Tube

The thermal accommodation experiment of helium on tungsten was conducted in an environment of about $1x10^{-3}$ torr of helium, see section 7 . Helium was admitted to section A via a fused silicon tube fig. 2 , 5 mm outside diameter, 0.5 mm wall thickness and 52 mm long, heated to 475°C. Whilst surrounding it with high purity helium at atmospheric pressure and at a flow rate of ∿ 200 $cm^3 min^{-1}$. With these conditions the required pressure of ∿ $1x10^{-3}$ torr was obtained in the 7 litre chamber in 20 minutes. Altemose (1961) and Norton (1957) data suggests that the helium would be very pure and free from argon and nitrogen. The purity of the helium used to surround the silicon tube in these experiments was 99.998% ie the best currently available. A typical analysis is given at the end of this appendix. During the use of the silicon tube (> 2 hours) there was no apparent change in the permeability for helium. The fused silicon tube was specially made and joined to the pyrex glass apparatus via a graded seal.

The Oven and Gas Admission

The oven, see plate 16, was constructed from a piece of fused silicon tube 9 mm outside diameter 1 mm wall thickness and 290 mm long as used in domestic electric fire elements. On 100 mm of one end of this tube was wound a Nichrome 600 Watt coiled electric fire element. The windings were held in place by small pips of silicon fused onto the tube and an

insulating covering of fire cement (Pyruma). An alternating current of 1.75 Amps at 60 volts, controlled by a variac produced a temperature in the oven of 510°C. After > 50 hours at a temperature of typically 500°C, there was no evidence of the fire cement chemically attacking the Nichrome winding.

The gas to be admitted was passed down the silicon tube, on which the oven was constructed by connecting a flexible rubber gas supply pipe to the cool end. It would have been possible to utilize the partial pressure of oxygen and helium in the laboratory atmosphere but the gas flow into the vacuum system would have been thereby reduced, (drastically so in the case of helium). Increasing the osmosis tube temperature sufficiently may have compensated adequately for this but for other practical limitations.

Prevention of Gas Admission During Vacuum Chamber Bake-out

Calculations showed that if, during a vacuum bake-out at 450°C, the osmosis tubes were surrounded by the laboratory atmosphere, the partial pressures of both oxygen and helium inside the vacuum section A would be increased significantly (1), thereby increasing the gas load to the pumps. A manifold to surround the two osmosis tubes was made from stainless steel tube and a flow of commercial oxygen-free-nitrogen maintained in the manifold throughout the bake-out procedure (2).

---

(1) The partial pressures of oxygen and helium in the laboratory atmosphere are typically 180 torr and 4×10^{-3} torr respectively. However, the FJD8 sputter ion pump speed for helium is considerably less (by a factor of about 100, see section 6) than for oxygen. Thus, although the leak rate for helium is small, so is the pump speed, resulting in a relatively high partial pressure of helium within the vacuum envelope. Whilst estimations were made for a bake-out temperature of 450°C the actual temperature reached was not greater than 250°C.

(2) From early experimental trials, on both osmosis tubes at their operational temperatures, it was found that by replacing the helium or oxygen by oxygen-free-nitrogen the leak rates were reduced to values insignificant when compared to the leak rate of the whole of vacuum section A.

Neon	5	Hydrogen	<1
Nitrogen	10	Carbon dioxide	<1
Oxygen	2	Hydrocarbons	<1
Argon	<1	Water vapour	3

Table 12. Typical analysis of impurities in mineral helium as supplied by the British Oxygen Company. Values expressed as volume parts per million. Helium purity 99.998%.

Appendix 12

Auxiliary Apparatus

A high vacuum, oil diffusion pumped system [1] provided the facility for trials, conditioning, outgassing preliminary and calibration experiments. The whole apparatus was purpose built and considerable care was taken to maintain the whole apparatus in a "clean" condition. It was not used as a general purpose vacuum system.

The apparatus is shown schematically in fig. 27 together with additional information about the apparatus. The 2 stage 50 mm oil diffusion pump [2] was backed by a 2 stage rotary pump and provided with a P_2O_5 trap and 10 litre backing volume. Two valves V_1, V_2 and T_4 enabled each of the two main sections to be jointly or separately connected to, or isolated from, the diffusion pump. It was also possible to rough pump each section independently. Where elastomer seals were required, Nitrile rubber greased sparingly with Apiezon grease M, was used. Apiezon M was also used for the groundglass joints and taps.

Section 1

This consisted of a 40 mm diameter "backbone" pump line with the required components as appendices protruding from it. This section was separated

---

(1) This system was entirely separate from and in a different room to the ultra high vacuum apparatus described in section 6.

(2) The pump was filled with Apiezon B oil. Silicone oils were not used because of the possibility of electrically insultaing films forming on components associated with the torsion balance subsequently installed in the UHV apparatus. The diffusion pump was untrapped but the pump line between pump mouth and bell jar base plate was 50 mm diameter and 350 mm long.

CF_1 CF_x	Liquid nitrogen cold fingers
D	Diffusion pump
R	Rotary pump
T	P_2O_5 trap
VT_1 VT_2	Liquid nitrogen cooled vapour traps
I_x I_b	Bayard-Alpert ionization Vacuum gauges
P_x P_b	Pirani Vacuum Gauges
V	Vacustat McLeod gauge
B	Backing volume

Figure 27 Key for Auxilliary Apparatus. Gauges, Pumps and Valves.

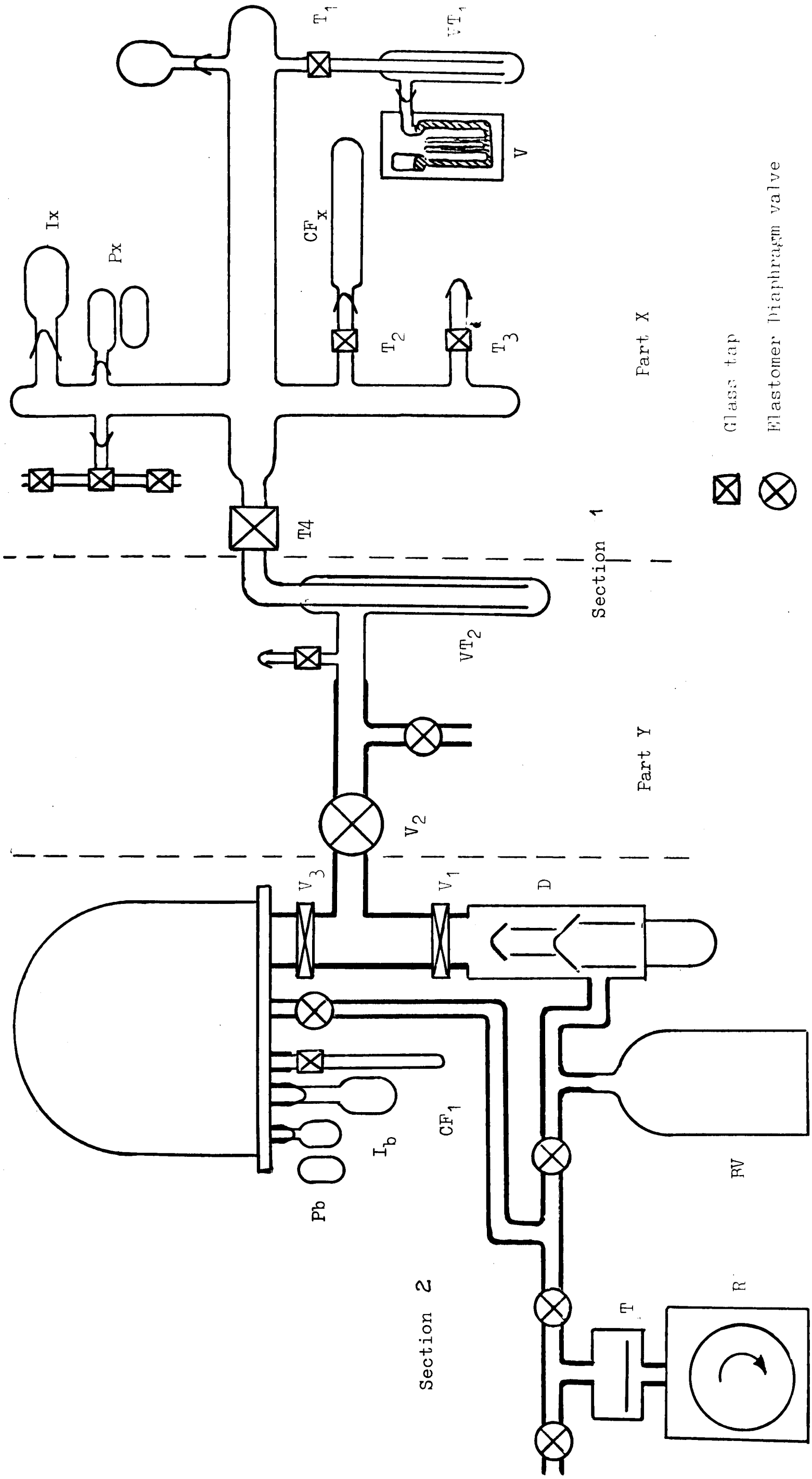


Figure 27 Auxil iary apparatus showing gauges, pumps and valves

into two parts X and Y by a large bore glass tap [1].

Part Y nearer to the diffusion pump, comprised the transition from metal to glass pump line and a pyrex, liquid nitrogen cooled, vapour trap.

Part X was used for the following work: calibration of vacuum pressure gauges (see appendix 8), experimental trials of the osmosis tubes (see appendix 11) and leak testing small vacuum components. This part was constructed entirely from pyrex, the components being attached with tapered ground glass joints. The gauges, taps and liquid nitrogen cooled traps were as shown in fig.27.

Typical operating conditions were: volume 1.4 litres, ultimate pressure [2] 5×10^{-7} torr, leak rate $\sim 10^{-5}$ lusecs of which $\sim$ 50% was condensible in a liquid nitrogen cooled finger.

Section 2

The section consists of a 300 mm diameter pyrex bell jar of 20 litres and brass [3] base plate 356 mm diameter and 19 mm thick. A spiral copper pipe was soft soldered to the underside of this base plate. The 50 mm diameter pumping part and other parts and apparatus (see fig. 27) were arranged around the edge of the base plate thus leaving a large uninterrupted working surface on which to arrange and conduct experiments. Typical operating conditions were: pump speed at base plate port

---

(1) This 20 mm bore tap was the largest that could conveniently be turned at 20°C without specially supporting the tap body to prevent breakage. It was greased with Apiezon "M".

(2) Whenever Part 1 was diffusion pumped the trap in Part 2 was cooled with liquid nitrogen.

(3) Naval Brass specification BS256 cut from 22 mm thick sheet as preference to a cut from the end of a billet thus reducing the possibility of leaks due to porosity. Typical composition, 60% copper, 1% tin, balance zinc

10 litre s^{-1} ultimate pressure 10^{-5} torr (1) obtained in 20 mins after 1 hour exposure to laboratory atmosphere, leak rate 10^{-2} luses of which 99% was condensible in a liquid nitrogen cold finger.

This section was used for the following work. Tungsten ribbon preliminary treatment and optical pyrometer temperature calibration, see section 6 , outgass ing of apparatus in conjunction with the vacuum furnace, see appendix 13 , trials of tungsten ribbon tensioning spring, see section 6.

---

(1) This ultimate pressure was improved, permanently, by a factor of 10 by heating the base plate to about 60 °C for 2 hours. The improve- was thought to be due to the outgassing of the Nitrile elastomer 'L' gasket between bell jar and base plate. The base plate was heated by passing steam through the copper pipe spiral soft soldered to its underside.

Appendix 13

Vacuum Furnace

Introduction

It was necessary to pre-bake several component parts [1] to outgas them and relieve internal stresses before their installation in the ultra high vacuum section A of the experimental apparatus (see fig.2)

An advantage of a separate vacuum furnace is that particular components, which require special treatment, are not limited to the typical bake of a complete vacuum apparatus at a maximum of 450°C [2].

The furnace was contained within a conventional 300 mm diameter, 20 litre volume pyrex vacuum bell jar with a water cooled brass base plate, part of the auxil iary apparatus described in appendix 12.

The Furnace Design

For the purposes required the furnace was designed as a simple muffle, cylindrical in shape with the axis vertical. Internal dimensions were 92 mm diameter and 153 mm height, large enough to contain each of the components to be baked. It was heated ohmically by a surrounding wire element adjacent to the muffle and used satisfactorily up to a maximum muffle temperature of 800°C. Several outer radiation shields minimized the electrical power requirement and the temperature of the surrounding bell jar. Access was via a bolted up top plate to the muffle. Overall dimensions were 140 mm diameter and 230 mm height.

---

(1) For example the torsion balance assembly (section 6), the tungsten ribbon mounts (section 6) and the ionization gauge 10G71 (appendix 8)

2) This 450°C limit is imposed when pyrex forms a part of the vacuum envelope, see for example Green(1968). In this work the maximum temperature was limited to about 220°C for the main envelope of section A.

Construction

The muffle. Plates 17 and 18 and figure 28 show the general arrangement of the furnace. The muffle cylinder, bottom and top plates were all of mild steel. Flanges were welded to each end of the cylinder. The cylinder was 92 mm internal diameter 5 mm wall thickness and 153 mm high. The removeable top and bottom circular plates were 9 mm thick and each held in close contact with the flanges by six OBA steel studs and nuts (1). The mating faces were fine ground to improve thermal contact. The studs at each end were of extended length, at reduced diameter, to provide locating pins for the radiation shields and supporting legs for the furnace. The legs stood in pyrex glass cups, improving thermal insulation and providing electrical insulation from the vacuum base plate. The interior of the muffle was evacuated via a 20 mm diameter vent in the top plate.

The heating element. The element consisted of 14.9 metres of 0.55 mm diameter nickel (2) wire giving a total resistance of 4.35Ω at 20°C and 29.5Ω at 827°C. (3) This was wound in a single layer helix on the muffle cylinder and insulated from it by cylindrical ceramic beads 3 mm diameter. The winding was more widely spaced in the centre than at the ends as shown in plate 17. Thermal cycling of the furnace annealed the element wire and caused it to stretch under its own weight so displacing some of the turns. Tightening and realigning after initial trials resulted in no further permanent changes. The ends of the element were of double thickness wire (twisted), led through holes in the muffle and radiation shields

---

(1) These were pre-oxidized in a bunsen burner flame which successfully prevented seizing. Occasional re-oxidation was necessary.
(2) Nickel was chosen as a suitable element material after Wong 1966, its high melting point (1453°C), high total emissivity (0.5 at 800°C) of oxidized surface and availability.
(3) Data for resistivity of nickel from Kaye and Laby
Note that the Curie point temperature is 360°C.



Plate 17. Vacuum furnace component parts (x 0.5)

Cylindrical nickel radiation shields.

Muffle with ceramic bead insulated nickel winding. Lower radiation shields in position.

Top plate of muffle.

Top nickel radiation shields.

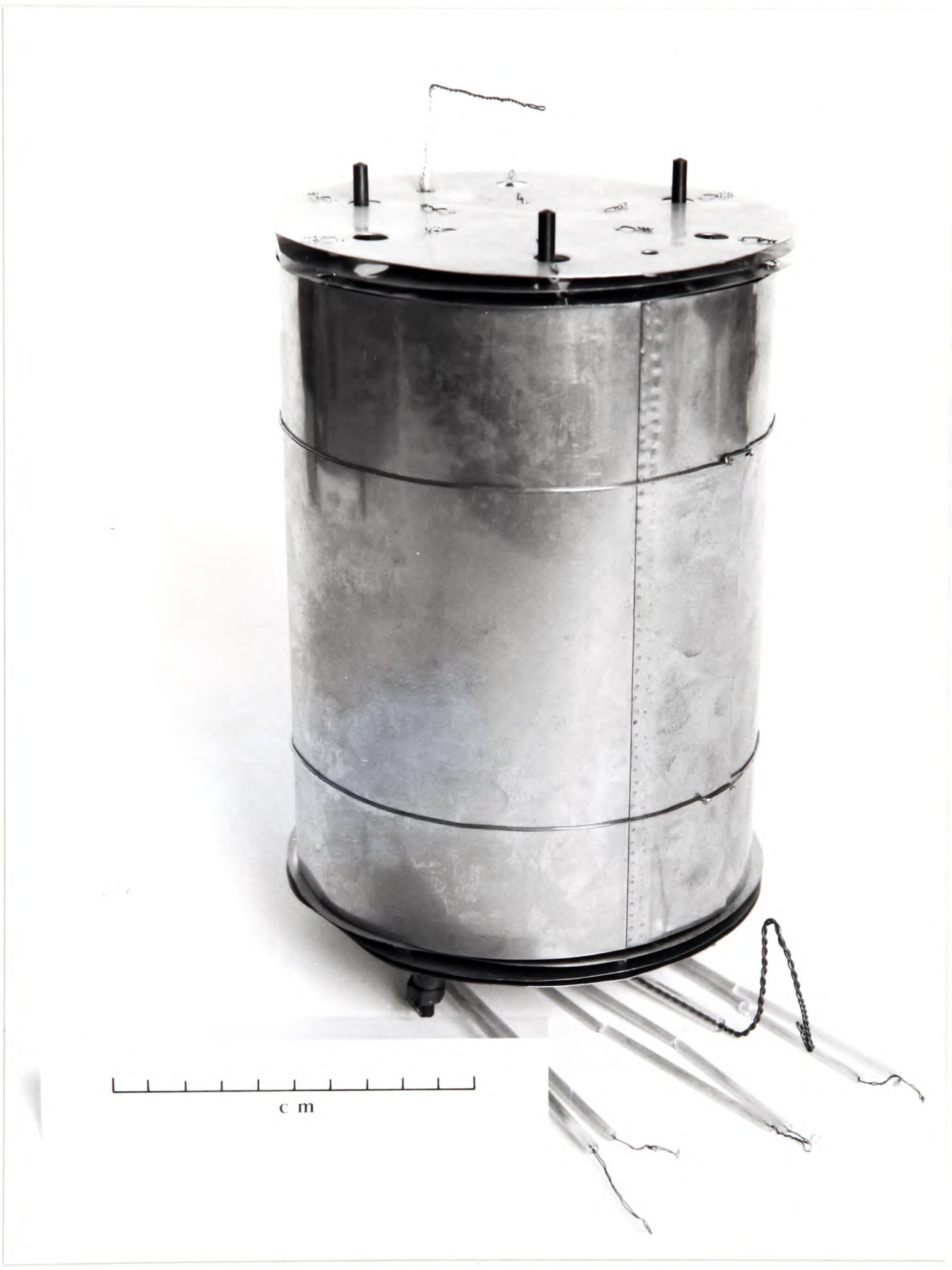


Plate 18. Vacuum furnace assembled (x 0.5). Fine wires within fused silica tubes are to thermocouples, thicker leads are to heating element.

and insulated from them with pieces of fused silica tube.

Radiation Shields.[1] The shields were made from nickel sheet (~ 0.5 mm thick) and arranged as shown in figure 28 . The innermost shield was in close contact with the insulating beads of the element and helped hold it in position. The six cylindrical shields (spot welded electrically where the available nickel was of insufficient width) were each wired in place using nickel wire. The four circular shields at each end were located on the stud extensions. The lower four of these were supported on small pins placed through holes in the legs. Ceramic beads wired to alternate shields prevented direct contact.

Temperature measurement. Three copper-constantan thermocouples were located within the muffle, oneeach at the top and bottom and the other, at about mid height, could be placed in contact with an object within the furnace. They were each led out through the bottom plate and radiation shields with fused silica insulation tubes. The temperature was indicated on a high resistance (7kΩ) galvonometer [2], Each thermocouple was calibrated with the same galvonometer (cold junction at 20°C) up to a hot junction temperature of 200°C. The calibration agreed well with Billing (1964) over the range calibrated so that the curve was extrapolated according to the (Billing) data up to 400°C [3] and linearly thereafter to 800°C as an indication within that range.

---

(1) Some useful design data was obtained from Sanders 1929 and Wadsworth 1963.

(2) This was a multirange instrument arranged so that the terminal resistance remained constant at 7kΩ. Maximum sensitivity was 2.31×10^{-3}V or 0.33×10^{-6}A, f.s.d. Manufactured by Evans Electroselenium Limited, Halstead, Essex.

(3) The normally accepted maximum for copper-constantan, limited by oxidation of the copper, is not relevant here since the thermocouple is in a good vacuum.

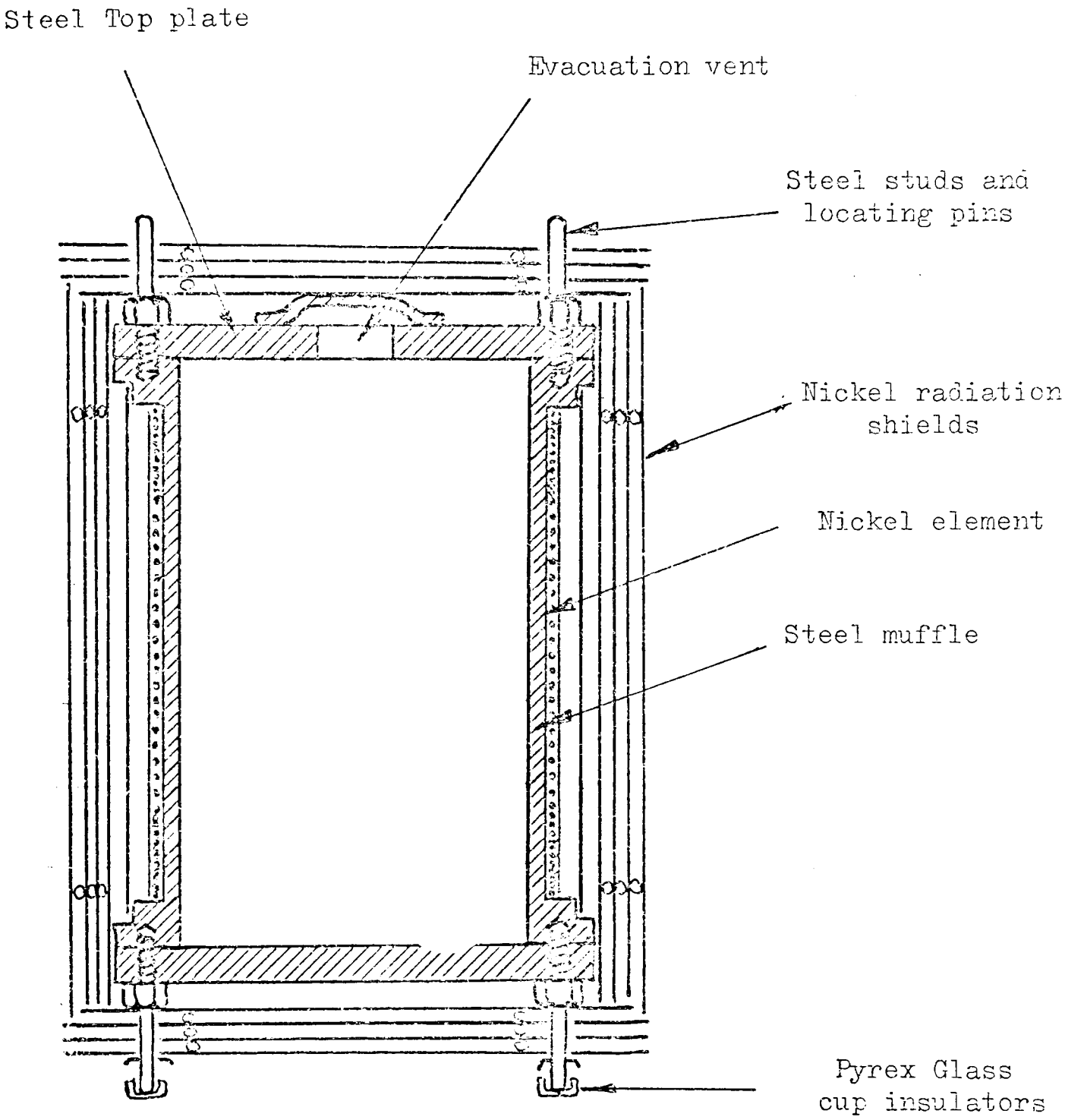


Figure 28 Vacuum furnace. Section (X0.5)

Use and Power Requirements of the Furnace

The furnace was initially outgassed by raising the temperature slowly over a period of several trials lasting a total of about 30 hours. The pressure was not allowed to exceed 5×10^{-4} torr and was more typically half this value. Some brown deposit was formed on the bell jar during this stage. Having been removed this did not reoccur.

The furnace was used typically at a muffle temperature of 500°C. This temperature could be reached, from cold, in approximately 1 hour with a current of 3 Amperes (∿ 250 watts) for the first 30 minutes and a current of 4 Amperes (∿ 520 watts) for a further 30 minutes.

A current of 1.9 Amperes (∿ 100 watts) would maintain a steady temperature of 500°C. Under these conditions with the base plate of the bell jar cooled with tap water (∿ 10°C) the bell jar temperature was about 35°C. Whilst being pumped [1] the pressure indicated by an ionization gauge was 4×10^{-5} torr or less.

When the power supply was switched off the temperature would fall from 500°C to 250°C in about 3½ hours. No experiments were conducted into more rapid correction cooling of the furnace by admission of an inert gas [2]. If this were done great care would be necessary lest the pyrex bell jar were subject to sudden and large thermal gradients.

The furnace was used at a maximum temperature of about 800°C, (an element current of about 4 Amperes, 520 watts) for fluxless brazing of some small copper and stainless steel components using the copper-silver

---

(1) By oil diffusion pump, effective speed 10 litres s^{-1} and a liquid nitrogen cooled cold finger, effective speed for condensible gases of 1 litre s^{-1}.

(2) For example, argon.

eutectic alloy (melting point 779 ^{o}C). The results were excellent and there was no visible sign of oxidation of the components.

The electrical power supply was from the a.c. mains via autotransformer and ammeter. Typical potential differences applied were about 50 volts (R.M.S.).

Appendix 14

Evacuating of the vacuum apparatus

The whole apparatus (see figure 3) was evacuated to low pressure several times following modifications or mishaps so that a carefully planned routine was developed. The following numerical values are typical.

Rough pumping the apparatus

Baking ovens and heater tapes were placed in position on the whole of sections A and B. If the system had been exposed to the laboratory atmosphere for more than a few hours it was flushed with dry nitrogen (1) from section A towards section C overnight (2). The temperature of sections A and B, with all valves open, was slowly increased to about 30°C. Vapour traps VT_2 and then VT_1 were cooled with liquid nitrogen and the whole system evacuated to about 20 torr with the water jet pump when V_6 and v_5 were closed. The sorption pumps were then used in tandem. Valve v_1 was then opened and sorption pump (3) allowed to pump that part of C between V_6 and v_5. If gauge P_c indicated satisfactory reduction of pressure, V_6 was opened and the whole of A and B pumped. As the pressure came near to its equilibrium value ($\sim 30\times10^{-3}$ torr), V_6, v_1 and v_3 were closed and v_2 opened. If the gauge P_c indicated a further satisfactory reduction in pressure, V_6 was opened again. The ion pump on B was allowed to cool and when the pressure was about 10^{-3} torr V_6 was closed, isolating B and C, and the ion pump on B started. This pump indicated

---

(1) from the natural evaporation of a 25 litre liquid nitrogen dewar

(2) approximately 16 hours. This was sufficient to remove visibly condensed water from vapour trap VT_2 or even cold finger CF_2 after some emergency glass blowing

(3) These pumps were filled with artificial zeolite (or molecular sieve) type 5A manufactured by Union Carbide. See Stern and Di Paulo for characteristics of these materials. The sorption pumps were already evacuated and isolated with their own valves v_1 and v_2 at the end of their reactivation cycle. They were each pre-cooled with liquid nitrogen

the pressure in the system and it was left pumping A and B.

Reduction of pressure to ultra high vacuum

After 24 hours the ion pump on B had reduced the pressure to 0.2×10^{-6} torr with A and B at $20^{o}C$.

The whole of A was then baked to $150^{o}C$ whilst B was at $100^{o}C$ and both sections pumped with the sputter ion pump and liquid helium cold finger on B. This was continued for about 6 hours and the sputter ion pumps on A then allowed to cool. The valve between A and B was then closed and A was pumped with its own ion pumps. Section B was maintained at low pressure acting as guard on the valve between A and B.

The whole of A, was then baked to about $220^{o}C$ for about 36 hours pumped with its own (cold) sputter ion pumps. At the end of the bake, before cooling, the pressure was typically 10^{-6} torr. During cooling the filaments of the titanium sublimation pump were outgassed as were the ion gauges. The pressure achieved at room temperature was 10^{-9} torr, sputter ion pumps only, active.

The titanium sublimation pump was then cooled in liquid nitrogen and the pump "fired". This caused the pressure to fall to about 3×10^{-10} torr. When the liquid helium pump was in operation the pressure (occasionally) further reduced to 2×10^{-10} torr where it remained even if the sputter ion pumps were turned off.

References

Altemose V O 1961 J. Appl. Phys. 32 1309-16

Bassett D W and Robertson A J B 1959 J. Sci. Instrum. 36 321-2

Baule B 1914 Ann. Physik. 44 145-76

Becker J A, Becker E J and Brandes R G 1961 J. Appl. Phys. 32 411-23

Bickerdike R L 1969 private communication

Billing B F 1964 Thermocouples. Institute of Engineering Inspection. Monograph

Blodgett K B and Langmuir I 1932 Phys. Rev. 40 78-104

Blodgett K B and Langmuir I 1934 Rev. Sci. Inst. 5 321-33

Carpenter L G, Humphries D E and Mair W N 1963a Nature 199 164-5

Carpenter L G, Humphries D E and Mair W N 1963b R.A.E. Tech. Note CPM.38

Clark D 1971 private communication

Cochran M E and Irey R K 1972 Adv. Cryogen. Engng. 17 456-61

Dance D F and Duncan C 1972 J. Phys. E 5 10.

Devonshire A F 1937 Proc. R. Soc. A158 269-79

Espe J W 1966 Materials For High Vacuum Technology Volume 1 p 54 (Oxford Pergamon)

Goodman F O 1966 Rarified Gas Dynamics ed. J H De Leeuw (New York: Academic Press) p 366

Goodman F O 1967 Surf. Sci. 7 391-421

Goodman F O 1969 J. Chem. Phys. 50 3855-63

Goodman F O 1971 Surf. Sci. 26 327-62

Goodman F O 1972a Surf. Sci. 30 525-35

Goodman F O 1972b J. Chem. Phys. 56 6082-8

Goodman F O 1973 Private communication - see also p 115(a).

Goodman F O 1974 Prog. Surf. Sci. 5 261-375

Green J W 1968 Design and Construction of Small Vacuum Systems (London: Chapman and Hall)

Hobson J P 1959 Can. J. Phys. 37 300-12

Hobson J P 1973 J. Vac. Sci. and Technol. 10 73-9

Klett D E and Irey R K 1969 Adv. Cryogen. Engng. 14 217-23

Kouptsidis J and Menzel D 1970 Ber. Buns. Ges. Phys. Chem. 74 512-20

Knudsen M 1909 Ann. d. Phys. 28 75-130

Knudsen M 1909 Ann. d. Phys. 28 999-1016

Knudsen M 1911 Ann. d. Phys. 34 593-656

Holland L, Laurenson L and Allen P G W 1961 8th Vacuum Symposium 208-219

Langmuir I 1915 J. Amer. Chem. Soc. 37 417-25

Leck J H 1964 Pressure Measurement in Vacuum Systems (London:
Chapman and Hall)

Logan R M 1969 Surface Sci. 15 387-402

Mair W N 1967 R.A.E. Tech. Report 67024

Mair W N and Viney B W 1970 private communication

Manson J R 1972 J. Chem. Phys. 56 3451-5

Maxwell J C 1860a Phil. Mag. and J. Sci. 19 19-32

Maxwell J C 1860b Phil. Mag. and J. Sci. 20 21-37

Maxwell J C 1879 Phil. Trans. 170 231-56

McCracken G M and Pashley N A 1965 J. Vac. Sci. Technol. 3 96-8

Milne E A 1929 Phil. Mag. 7 273-6

Moran J P, Wachman H Y and Trilling L 1969 Phys. Fluids 12 987-93

Mullard Ltd 1967 Concern Symposium on Modern Vacuum Technology p 78

Norton F J 1957 J Appl Phys 28 34-9

Osborn A B 1964 R.A.E. Tech. Note CPM.69

Pearson S and Wadsworth N J 1963 R.A.E. Tech. Note CPM.12

Redhead P A, Hobson J P and Kornelsen E V 1968 The Physical Basis of
Ultra High Vacuum (London: Chapman and Hall)

Riviere J C 1969 Phys. Bulletin 20 85-90

Rose-Innes A C 1970 Low Temperature Techniques (London: E.U.P.)

Riviere J C 1971 private communication

Roberts J K 1930 Proc. R. Soc. A129 146-61

Roberts J K 1935a Proc. R. Soc. A152 445-63

Roberts J K 1935b Proc. R. Soc. A152 464-77

Roberts J K 1936 Nature 137 659-60

Smithalls C J 1952 Tungsten (London: Chapman and Hall)

Smoluchowski M S 1898 Phil. Mag. and J. Sci. 46 192-206

Soddy F and Berry AF 1910 Proc. R. Soc. 83 254-64

Soddy F and Berry AF 1911 Proc. R. Soc. 84 576-85

Thomas L B 1967 Fundamentals of Gas Surface Interactions ed. Saltsburg H, Smith J N and Rogers M (London: Academic Press) 346-69.

Thomas L B and Brown R E 1950 J. Chem. Phys. 18 1367-72

Wachman H Y 1962 ARS Journal 32 2-12
Wachman H Y 1965 J. Chem Phys. 42 1850-1
Wachman H Y 1966 J. Chem. Phys. 45 1532-8

Waelbroeck F G and Zuckerbrodt P 1958 J. Chem. Phys. 28 523-4

Watt W and Moreton R 1964 R.A.E. Tech. Note CPM.80

Watt W, Moreton R and Carpenter L G 1974 Surface Science 45 238-48

Watts M J 1972 J. Sci. Inst. 5 1044

West L A, Kozak E I and Somorjai G A 1971 J. Vac. Sci. Technol. 8 430-6

Whetten N R and Young J R 1959 Rev. Sci. Inst. 30 472-3

Yamamoto S and Stickney R E 1970 J. Chem. Phys. 53 1594-604

Kaye G W C, Laby T H 1973 Tables of Physical and Chemical Constants 13th edition (London: Longman) p 49

Stern S A and Di Paolo F S 1969 J. Vac. Sci.and Tech. 6 941-50

Thorn R J and Winslow G H 1961 Temperature its Measurement and Control in Science and Industry volume 3 part 1 (New York: Reinhold 1962) p 421-47

Wong H Y 1966 B.J.A.P. 17 1329-37

Carpenter L G and Mair M N 1953 R.A.E. Tech Note Met 174

Sweets D E, Roe R W and Frank R C 1961 J. Chem. Phys. 34 17-22

Bernasek S L and Somorjai G A 1975 Prog.Surf.Sci. 5 377-439

Jones R V 1961 J.Sci. Inst. 38 37-45

Robinson N W 1968 The Physical Principles of U.H.V. (London:Chapman and Hall)

Honig R E 1957 Radio Corporation of America.

Saunders OA 1929 Proc.Phys.Soc. 41 569-575

Wadsworth NJ 1963 RAE. Tech Memo CPM 11

Cyranski P 1970 Vacuum 20 266. abstract 545

Newton SW and O'Niell J. 1966 Vacuum 16 677-80

Trilling L 1967 Fundamentals of Gas Surface Interations. ed Saltzberg. Smith JN and Rogers M (London: Academic Press) pp 392-421

Goodman FO and Wachman HY 1967 J Chem Phys 46 2376-86

Trilling L 1970 Surf.Sci 21 337-65